CHEMICAL REVIEWS

REVIEW

pubs.acs.org/CR

Dendrimers as Encapsulating, Stabilizing, or Directing Agents for Inorganic Nanoparticles

Lyudmila M. Bronstein*,† and Zinaida B. Shifrina‡

†Department of Chemistry, Indiana University, Bloomington, Indiana 47405, United States

‡A.N. Nesmeyanov Institute of Organoelement Compounds of the Russian Academy of Science, Moscow, Russia

CONTENTS

1. INTRODUCTION

Inorganic nanoparticle/dendrimer nanocomposites received considerable attention in the past decade due to their unique properties (catalytic, optical, magnetic, biomedical, electrical, etc.) and a strong promise for future applications, which was reflected in numerous review articles.[1−26] Nowadays, this area is characterized by swift development, and it requires a timely analysis of achievements and trends. In this Review, we will discuss the synthesis and properties of the above nanocomposites, where the inorganic (metal, metal oxide, metal halide) nanoparticle (NP) is either encapsulated by the dendrimer molecule, or surrounded by dendrimers, or is a dendrimer core after attachment of dendrons to its surface. All other kinds of metallodendrimers, that is, bearing metal ions, but not a NP, in the center or periphery, are beyond the scope of this Review.

Dendrimers are complex monodisperse macromolecules with a regular and highly branched three-dimensional architecture

Received: March 7, 2011
Published: June 30, 2011

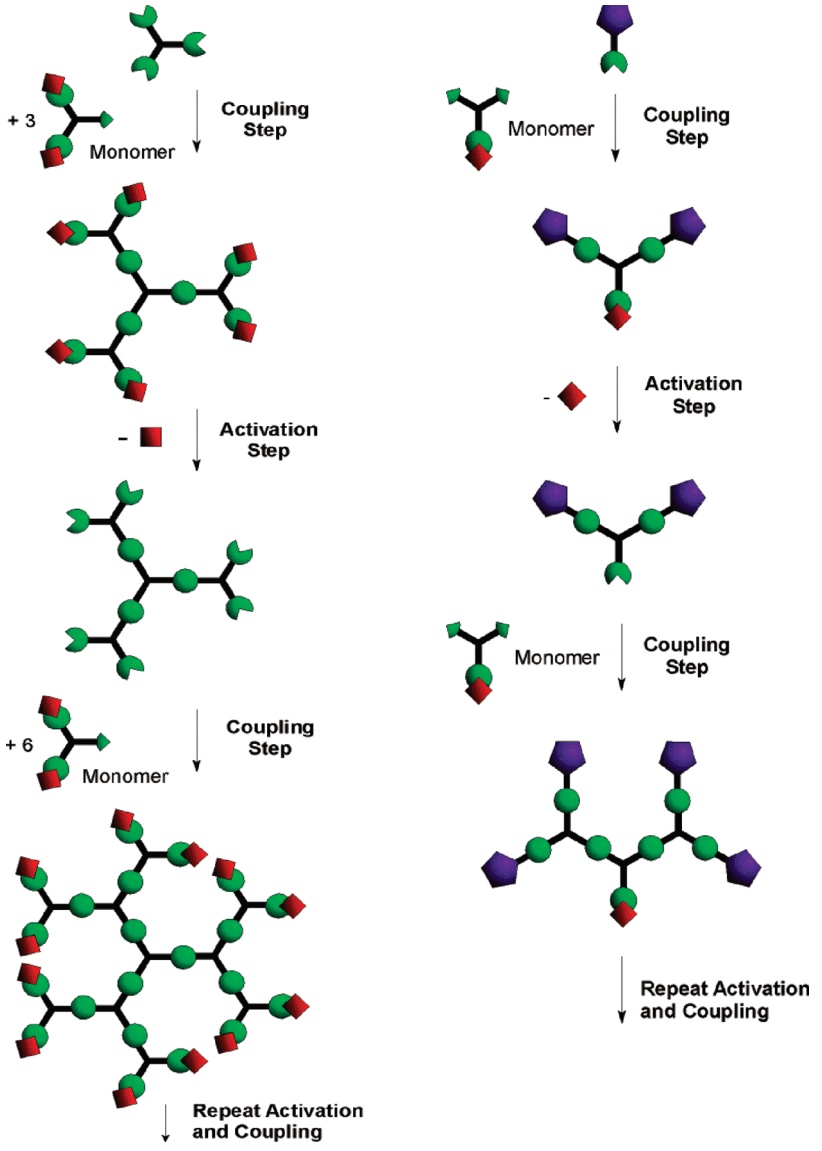

Figure 1. Schematic representation of divergent (left) and convergent (right) methods of dendrimer synthesis. Reprinted with permission from ref 55. Copyright 2001 American Chemical Society.

and well-defined chemical structure.[1,2,4,27−54] Dendrimers are produced in iterative sequences of reaction steps, in which each additional iteration leads to a higher generation dendrimer. The synthesis of dendrimers using a specially designed high yield chemical reactions is one of the best examples of a controlled hierarchical synthesis that allows for a "bottom-up" approach to complex systems.

The construction of dendrimers can be carried out in two major ways: by a divergent approach[1,2] where the molecule grows from the center to the periphery, and a convergent approach (Figure 1),[47,55,56] where the dendrimer molecule is built starting from the periphery fragments. The choice of the divergent or convergent synthetic methods is determined by the available chemical reactions, requirements toward the dendrimer molecules, or the type of the "building blocks" used in the dendrimer construction. The advantage of a divergent approach is easy preparation of dendrimers in large quantities and of high generations, while the major disadvantage is the difficulty to control the dendrimer quality because numerous reaction steps take place at the same time in each growth step. Commercially available dendrimers, such as poly(propyleneimine) (PPI) and poly(amidoamine) (PAMAM), are synthesized by a divergent approach. Oppositely, the convergent approach permits better structural control due to a low number of coupling reactions at each growth step; however, it does not allow syntheses of dendrimers of high generations due to steric hindrances. In addition, the convergent approach provides targeted functionalization of the core and the dendron exterior, allowing for further chemical reactions with high yields and dendritic products of high purity and functional versatility. Examples of commercially available dendrimers synthesized by a convergent method are polyether dendrimers (Fréchet dendrimers). It is noteworthy that the majority of dendrimers can be synthesized by a combination of both methods.

The majority of known dendrimers are synthesized on the basis of covalent bonding as indicated in review articles.[1,2,4,28,44,46,49,51−53,55,57,58] There are also dendrimers obtained by self-assembling of metal ions with high coordination

numbers and multidentate ligands. Such dendrimers were first reported by the Balzani group[59,60] and then developed by a number of other groups. This kind of dendrimer is described in numerous reviews,[3,4,33−36,40,43,61,62] but it is out of the scope of the present Review.

2. METHODS OF THE NANOPARTICLE/DENDRIMER NANOCOMPOSITE FORMATION

NP synthesis in the presence of dendrimers is carried out using procedures similar to those developed for NP formation in the presence of surfactants or polymers. Normally metal NPs are formed from metal salts or complexes by their chemical reduction with $NaBH_4$, $N_2H_4 \times H_2O$, H_2, $LiBH(C_2H_5)_3$, etc.,[63−66] by UV irradiation,[67−69] or by decomposition (thermal, microwave, ultrasound, etc).[70−73] Metal oxide NPs are formed by oxidation of metal compounds at high pH or/and using H_2O_2 or CO_2 as oxidants.[74,75] Semiconductor metal halide NPs (frequently called quantum dots (QDs), due to their unique optical properties determined by quantum confinement) can be obtained by numerous techniques including thermal decomposition of organometallic compounds,[76,77] interaction of metal oxide (e.g., CdO) with elemental S or Se,[78] or interactions of metal cations (e.g., Cd^{2+}, Zn^{2+}, Pb^{2+}, etc.) with halide anions (e.g., S^{2-}, Se^{2-}, Te^{2-}, etc).[79−82] For the NP/dendrimer composites, mainly the last route is employed, unless QDs have been synthesized by well-established solvothermal route with trioctylphosphine oxide (TOPO) as a surfactant, and then dendrimers were attached by a ligand exchange reaction.[83,84]

2.1. Encapsulation of Inorganic Nanoparticles by Dendrimers: Dendrimer-Templated Approach

When dendrimers were first used as nanoreactors for templating metal nanoparticles (NPs), the idea was to stabilize a single NP within a single dendrimer molecule, leading to so-called dendrimer-encapsulated nanoparticles (DENs). This seemed to be especially advantageous because dendrimers are well-defined single macromolecules with cavities between branches so they were destined to be perfect nanoreactors. The idea of using a nanostructured polymer as nanoreactor was actively explored earlier for block copolymer micelle cores;[63,85] however, in the latter case, the exchange of macromolecules between micelles was not completely prevented, unless the core or corona was cross-linked.[86−89] This led to the exchange of metal ions between micelles and thus nonideal nanoreactor conditions. Because a dendrimer is a single molecule ("unimolecular" micelle[31]), no additional cross-linking is needed; however, to prevent the exchange of ions, several conditions should be followed: (i) terminal groups of dendrimers do not complex with metal compounds, thus suppressing stabilization of a single NP with several dendrimer molecules, (ii) terminal groups are charged, thus leading to repulsion between dendrimers, (iii) there are inert tails in the dendrimer exterior, (iv) the dendrimer molecule size (generation) has to be sufficient to encapsulate the nanoparticle formed (the dendrimers of low generations might provide only interdendrimer stabilization of nanoparticles), and/or (v) the reaction conditions are specifically modified (for example, extremely diluted solutions).

2.1.1. Inert Terminal Groups. For the first time, Crooks' group[90] reported formation of copper NPs in G4-OH and G6-OH PAMAM dendrimers as templates. This method was based on complexation of Cu(II) ions with amino groups of the dendrimer interior followed by reduction. The presence of hydroxyl groups in the exterior of dendrimers prevented formation of NPs between dendrimers. It is noteworthy that NP size can be controlled by varying the size of the host dendrimer nanoreactor (a 16-atom Cu NP in the G4 and a 64-atom Cu NP in G6 dendrimers): the larger is the dendrimer, the larger are the NPs. Nearly at the same time, Tomalia's group[91] also reported the synthesis of Cu NPs in the G4-OH PAMAM dendrimer. Copper NPs were chosen as they allowed estimation of NP sizes from the position of the maximum in the UV−vis spectra. Neither paper used transmission electron microscopy (TEM) to accurately evaluate the particle size distribution or X-ray powder diffraction (XRD) to resolve crystallinity; nevertheless, these were pioneering works allowing further vigorous development of this field.

Similar methodology with hydroxyl-terminated PAMAM dendrimers was employed later for syntheses of Au,[92] Pd,[10,93] and Pt[93−96] NPs. An interesting example of DENs was proposed by displacement of Cu_{55} NPs formed in the G6-OH PAMAM dendrimers by an in situ exchange process driven by differences in the electrochemical potentials of the two metals involved.[7,97]

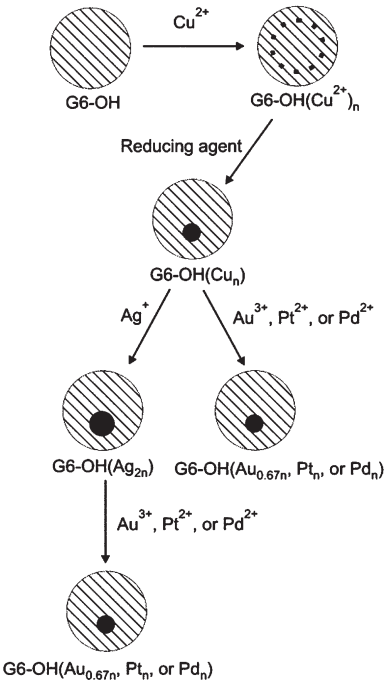

Figure 2. Encapsulation of Cu NPs by G6-OH PAMAM DENs and displacement of copper ions with other metal ions to form metal NPs. Reprinted with permission from ref 7. Copyright 2001 American Chemical Society.

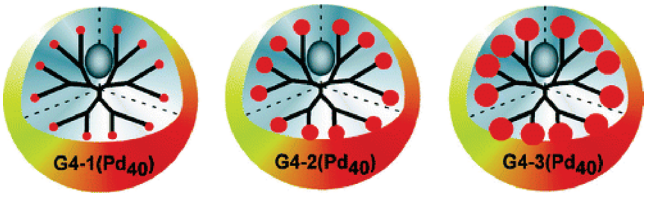

Figure 3. Pd nanoparticles encapsulated within dendrimers functionalized with different-sized end groups: glycidol (1), 2-methyl glycidol (2), and *tert*-butyl glycidyl ether (3). Reprinted with permission from ref 108. Copyright 2005 American Chemical Society.

dx.doi.org/10.1021/cr2000724 |*Chem. Rev.* 2011, 111, 5301–5344

The motivation for this approach was based on the fact that Cu ions are easier sequestered into dendrimers as compared to, for example, Au or Ag ions so the displacement leads to the formation of well-defined Au, Ag, Pt, or Pd NPs. However, the displaced ions, that is, Cu(II), also reside in the dendrimers. In a later paper,[98] the same group identified optimal conditions for the synthesis of monodisperse Au NPs without ion displacement (see Figure 2).

Dendrimer encapsulated bimetallic Pd−Pt,[99,100] Pd−Ru,[101] or Au−Ag[102] alloy NPs were formed when a mixture of the corresponding salts was simultaneously added to the hydroxyl-terminated PAMAM followed by reduction.

Alternatively, Pd−Au[103] or Au−Ag[102] core−shell NPs can be encapsulated by dendrimers using a sequential-loading approach. In the first step, the core particle is formed followed by selective reduction of the shell metal onto a core of the first metal. Using a weak reducing agent for the second step, the reduction can be efficiently catalyzed by the seed of the first metal to ensure the formation of core−shell particles. Another approach to the core−shell NPs is an electrochemical method. Recently, the electrochemical synthesis of Au@Pt (core/shell) NPs encapsulated within the G6-OH PAMAM dendrimer has been reported to give 2 nm NPs.[104] To develop such a catalyst, first, the dendrimer-encapsulated Au NPs comprised of about 147 atoms were synthesized and immobilized on a glassy carbon electrode (GCE). Next, a one-atom-thick shell of Cu was added to the Au core by electrochemical underpotential deposition, and then this shell was replaced with Pt by galvanic exchange, that is, by replacement of a metal with a lower standard electrode potential (Cu) for a metal with a higher standard electrode potential (Pt) from the Pt salt solution. The Au147@Pt NPs were proved to remain encapsulated within their dendrimer templates following electrode immobilization, deposition of Cu, galvanic exchange of the Cu for Pt, and throughout the oxygen reduction reaction. The authors believe that this methodology can be applicable to the synthesis of other core/shell NPs that would otherwise be difficult or impossible to synthesize using traditional complexation and chemical reduction steps.

Particularly small luminescent gold nanodots Au_8 were prepared in the PAMAM G2-OH and G4-OH dendrimers.[105] This was achieved by the addition of a small fraction of gold ions, using only 1 equiv of $NaBH_4$, and removal of large particles. The final solution was absolutely colorless, indicating that gold NP size is below 2 nm, a size for which surface plasmon resonance is not observed.[106] The particle size was, however, not confirmed by HRTEM or any other technique, while in the earlier paper of the same group the size of small (2−8 atom) Ag nanoclusters prepared within both G4-OH and G2-OH PAMAM dendrimers was confirmed by mass spectrometry.[107] We believe that the formation of such small particles is a significant advantage of dendrimers with inert exterior providing a unique opportunity of nanocluster encapsulation, which is hardly available with any other templates or capping molecules.

Besides the hydroxyl groups, a series of glycidol, 2-methyl glycidol, and *tert*-butyl glycidyl ether PAMAM derivatives was employed for Pd NP formation.[108] In all three cases, the NPs were encapsulated by the dendrimers, and the particle sizes were identical (Figure 3).

Terthiophene-terminated G4 PAMAM was used to stabilize Cu, Au, and Pd NPs.[109] This work presented extensive optical studies of dendrimer−NP ensembles and their attachment to graphite; however, the absence of a direct assessment of NP sizes and size distributions[98] or a confirmation of encapsulation with

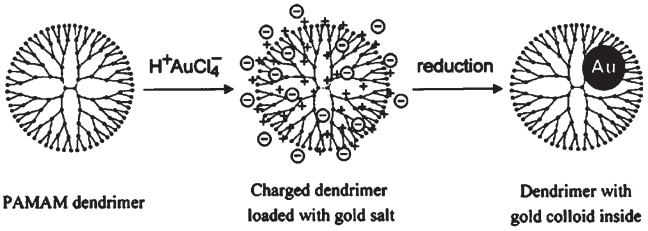

Figure 4. Dendrimer nanotemplating in aqueous solution. In a first step, the dendrimer is loaded with a precursor salt ($H^+AuCl_4^-$), resulting in a charged dendrimer with the precursor as counterions. In a second step, the chemical reduction is performed, which yields a colloid inside the dendrimer. Reprinted with permission from ref 110. Copyright 2000 American Chemical Society.

stained TEM images[110] does not allow for a proof of encapsulation versus surfactant-type stabilization.

Adamantyl-derivatized G4 and G5 PPI dendrimers complexed with β-cyclodextrin (β-CD) behaved as a template (nanoreactor) to form Au- and Pt-based DENs.[111] Imino groups of PPI here were fully protonated, thus providing positively charged groups to interact with negatively charged gold or platinum anions. Another function of charged groups, as is discussed below, is repulsion of similarly charged dendrimers, which decreases the probability of interdendrimer NP stabilization. Thus, here two mechanisms of the dendrimer isolation were employed: bulky terminal groups (adamantyl) and charges to avoid NP stabilization between dendrimers.

Although PAMAM and PPI dendrimers and their derivatives are the most popular dendrimer templates for DENs, other dendrimers were also used for NPs encapsulation. For example, Yamamoto's group designed phenylazomethine dendrimers[112] for encapsulation of catalytic Rh clusters.[113] Astruc's group synthesized "click" dendrimers[114] with intradendritic 1,2,3-triazolyl ligands, which play a key role in the NP encapsulation process at least for generations G1 and G2.[65,115]

However, even inert terminal groups of PAMAM do not necessarily prevent formation of NPs between dendrimers. The example is formation of gold and silver NPs in the presence of PAMAM with terminal sugar groups.[116,117] Probably in this case, sugars do not serve as a protective layer because their alcohol groups are reducing agents for gold ions. TEM images of the resultant NP−dendrimer composites demonstrate a very broad particle size distribution and the presence of large particles, indicating formation of dendrimer particle ensembles with interdendrimer stabilization of NPs (dendrimer stabilized nanoparticles, DSNs).

2.1.2. Charged Groups. When ~50% of the terminal groups of G4-NH_2 PAMAM dendrimers were quaternized using glycidyltrimethylammonium chloride, the positive charges allow repulsion between dendrimers, and thus formation of DENs despite the reacting metal ions, $PdCl_4^{2-}$ and $PtCl_4^{2-}$, are negatively charged and can easily interact with positively charged terminal groups, due to both electrostatic interaction with quaternized groups and hydrogen bonding.[118] Thus, the encapsulation of a NP within a single dendrimer, which is well-documented with TEM (the NPs measure 1.7 nm and the NP size distribution is narrow), is furnished by strong repulsion between dendrimers overcoming the interaction of terminal groups with metal species. Another way to provide such repulsion is selective protonation of only terminal amino groups to provide interdendrimer repulsion, but at the same time, to preserve nonprotonated interior amino-groups as well.[119] This

allowed the preparation of DENs with nearly monodisperse Pt and Pd NPs having mean diameters of 1.4 and 1.5 nm, respectively.[118,119] In both cases, the partial preservation of terminal amino-groups allows the attachment of DENs to surfaces via self-assembled monolayer (SAM) as an adhesion layer of a gold surface.

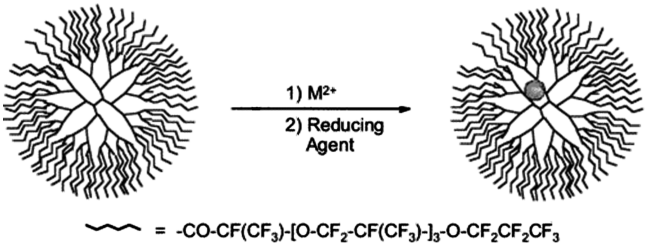

Figure 5. NP formation in the dendrimer with inert tails. Reprinted with permission from ref 122. Copyright 2001 American Chemical Society.

For partially quaternized G4-NH_2 and G6-NH_2 PAMAM dendrimers, it was also discovered that to make highly monodisperse encapsulated Au NPs, a certain ratio of gold ions toward dendrimers should be used, for example, 55 or 140 Au ions per dendrimer.[98] According to ref 120, NPs containing these "magic numbers" of atoms form energetically favorable crystals with closed shells. Indeed, in the case of 100 Au atoms, the NP size distribution was much broader than that of Au_{55} and Au_{140} NPs.

Dendrimers can host more than one NP per dendrimer when the dendrimer size increases as demonstrated in ref 110. In these experiments, amino-terminated PAMAM dendrimers were positively charged due to protonation caused by interaction with $HAuCl_4$ (Figure 4). The degree of charging was determined by the ratio of the $AuCl_4^-$ ions to the end amino groups as 1:1. G2−G4 dendrimers behaved merely like surfactants, when several dendrimer molecules surrounded the forming NP. When G6−G9 PAMAM dendrimers were used, a single gold NP was encapsulated by a dendrimer, yet the NP size increased with increase of dendrimer generation. For the G10 dendrimer,

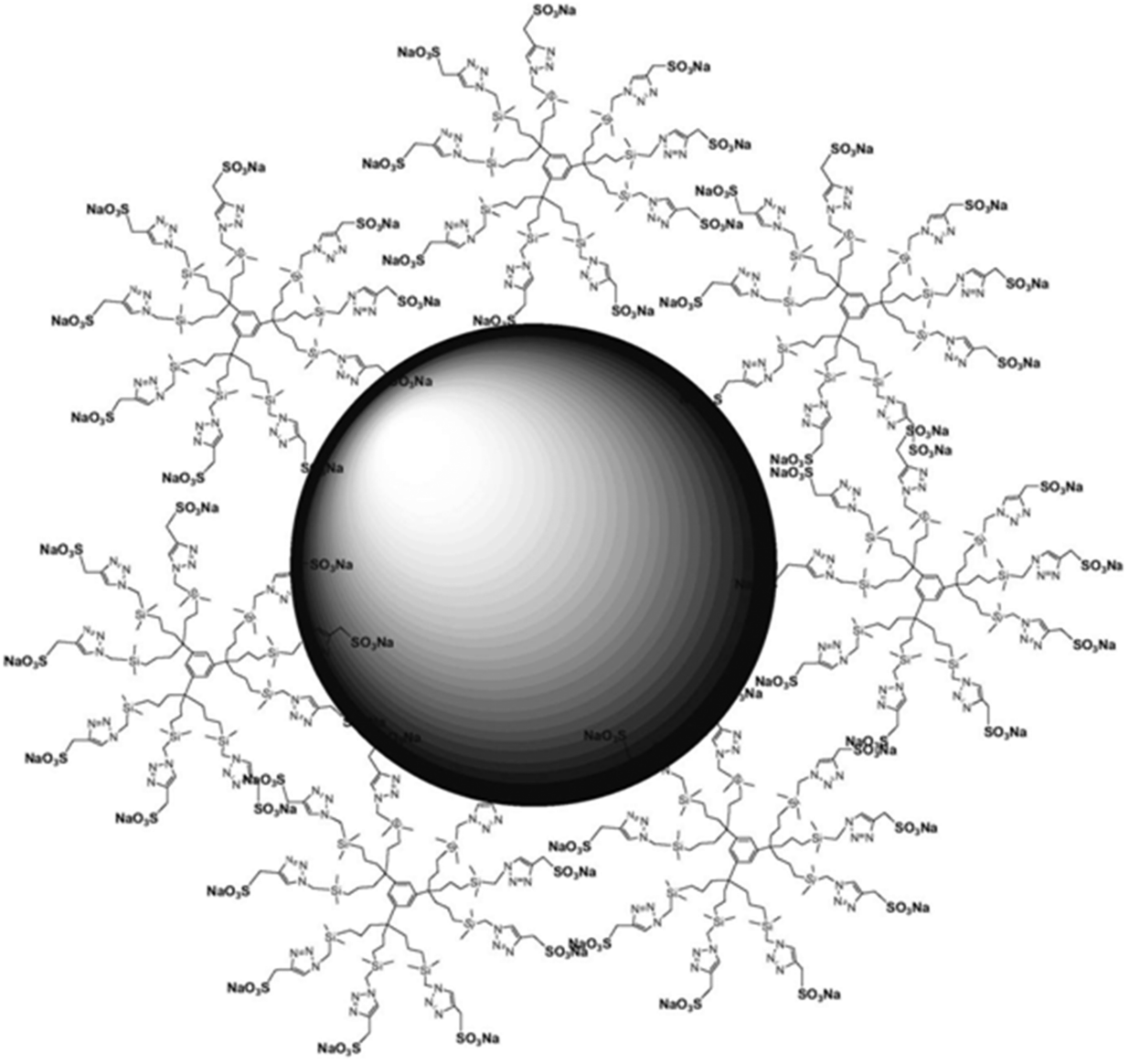

Figure 6. Representation of DSN-G0. Reproduced with permission from ref 134. Copyright 2008 Wiley-VCH Verlag GmbH & Co. KGaA.

dx.doi.org/10.1021/cr2000724 |*Chem. Rev.* 2011, 111, 5301–5344

multiple NPs were formed within one dendrimer molecule due to the more crowded volume inside the dendrimer. This was the first systematic study where such a transition from a single NP to multiple NPs per dendrimer was observed. The authors believe that when a NP grows in a polymeric environment, elastic forces of the surrounding polymer become important along with the free energy of crystal formation and surface tension. The volume of a single gold NP would double with each generation, yet the space available for its formation would decrease. Apparently, for the G10 PAMAM dendrimer, the chain flexibility is not sufficiently high to allow for growth of one NP, while the increased surface to be stabilized for multiple smaller particles is likely to be provided by the G10 dendrimer.

Similarly, charging of amino-terminated PAMAM dendrimers at pH 3 allowed encapsulation of bimetallic PdPt and PdRh NPs.[121]

2.1.3. Inert Tails. Similar to hydroxyl or other noncomplexing groups, inert tails prevent interdendrimer interactions via complexation with metal ions, but also add steric protection to single dendrimers (Figure 5). Pd NPs were formed within PPI dendrimers covalently functionalized with perfluorinated polyether chains on their periphery and used as catalysts in Heck coupling reaction.[122] In ref 122, the role of perfluorinated polyether chains was not discussed beyond stabilization of DEN formation; however, one might expect that in certain reactions these chains might influence a catalytic process by facilitating or preventing penetration of reacting molecules to catalytic sites.

Amine-terminated, sixth-generation PAMAM dendrimers substituted on the periphery with dodecyl functional groups were employed for synthesis of monodisperse Ni NPs with diameters 0.8 and 1.2 nm[123] and bimetallic NiSn NPs with a diameter 1.2 nm.[124] Here, the hydrophobic tails provide steric protection and solubility in organic media (toluene) and prevent interdendrimer ion exchange, leading to DENs with small monodisperse NPs. The fabrication of bimetallic NiSn NPs is especially interesting because this is the first example of DENs with stable bimetallic NPs consisting of two reactive metals, which typically degrade in the presence of O_2 and H_2O. The authors believe the NiSn-based DENs are relevant to Li ion battery technology for use as anodes.

2.2. Formation of Nanoparticles between Dendrimers as Surfactants

The method of the NP/dendrimer nanocomposite formation involving interdendrimer stabilization of NPs (DSNs) is widely spread as it does not require any specific conditions.[125,126] PAMAM and PPI dendrimers with terminal amino,[127,128] thiol,[83] and carboxyl[129] groups along with carbosilane-containing dendrimers[130,131] were used to stabilize the growth of various NPs. The dendrimer molecules behave as surfactants adsorbing on the growing NPs. Normally, this method results in larger and broader distributed NPs as compared to encapsulation by a single dendrimer molecule.

It is noteworthy that even charged dendrimers[110] or dendrimers with inert periphery but of low generations[65,115,132−134] may be unable to encapsulate NPs due to insufficient amounts of functional groups and then behave as surfactants (Figure 6).

The inert polyphenylene periphery of the rigid shape-persistent polyphenylenepyridyl dendrimers of forth generation with interior pyridine groups did not prevent clusterization of 2 nm Pd NPs.[135] Despite the inert periphery, the interdendrimer stabilization is probably reinforced by the rigidity of this dendrimer preventing encapsulation. Recently, CdS QDs with diameters 3.4−3.6 nm have been prepared in the presence of the same dendrimers of third and fourth generations using the high temperature method from CdO and sulfur. This procedure was possible due to the high thermal stability of the polyphenylenepyridyl dendrimers. These DSNs displayed blue-green emission, which does not change with passage of time (no NP aggregation).[136] It is worth noting that in this work for the first time the direct high temperature QD synthesis in the presence of dendrimers (no other surfactants were added) was carried out.

An interesting phenomenon was reported in ref 137. Nanocomposites comprised of gold or silver NPs stabilized or encapsulated by G5-NH_2 PAMAM dendrimer (the former case is more probable taking into account the broad NP size distribution) were subjected to an acetylation reaction to make them more biocompatible. While Au-based nanocomposites remained unchanged when modified with different degrees of acetylation, the Ag-containing ones were found to be sensitive toward acetylation. The size and size distribution of Ag NPs significantly increased with increasing acetylation degree, revealing processes of NP dissolution and growth (similar to Ostwald ripening), which might be caused by changing properties of capping molecules.

The dendrimer generation and some other factors influence the NP formation in the DSN composites. For example, the Au NP size was found to depend on the ratio of the number of amino groups to $HAuCl_4$ and on the number of amino groups in the dendrimer interior, that is, on the generation number.[125,128] The NP size decreased with the increase of the generation number and the amino group concentration, allowing formation of very small particles.[125] The opposite dependence on the generation number has been observed when Au NPs were prepared by Brust−Schiffrin's method in the presence of G0 and G1 oligothiadendrimers.[138] Both the dendrimer generation and the position of the sulfur atoms in the dendritic structure (S6G1 and S9G1) influenced the formation and properties of the nanoparticles. The authors believed that the branches and the nature of the groups connecting to sulfur play an important role in the stability and solubility of the Au NPs, while the thinner shell formed by these dendrimers is an advantage as compared to traditional alkanethiols, a statement that is not clearly explained, however. We think that dendritic structures might allow for higher stability of these NPs, but no comparative data are provided.

Surfactant-type stabilization of NPs by dendrimers is not necessarily created during NP formation. In a number of cases, the NPs are synthesized in the presence of other surfactants, which can be replaced with dendrimers due to stronger chelating groups and/or due to an entropy increase: more surfactant molecules are released when dendrimers are attached (several terminal groups of a single dendrimer can be attached to a NP). For example, CdSe/ZnS QDs stabilized with TOPO were made water-soluble by the exchange of TOPO for ester-terminated PAMAM dendrimers in the presence of an additional surfactant, poloxamer 188 (only 0.1%), for better water solubility.[84] The authors discovered that half-generation PAMAM and especially G4.5 PAMAM provided the best stabilization because more amide and ester functional groups afforded more binding sites toward QDs. In this manner, water-soluble QDs retained the optical properties of the original hydrophobic QDs.

2.3. Coating of NPs with Dendrons

Preparation of nanoparticle-core dendrimers (NCDs) with well-defined dendritic wedges could offer enhanced stability and

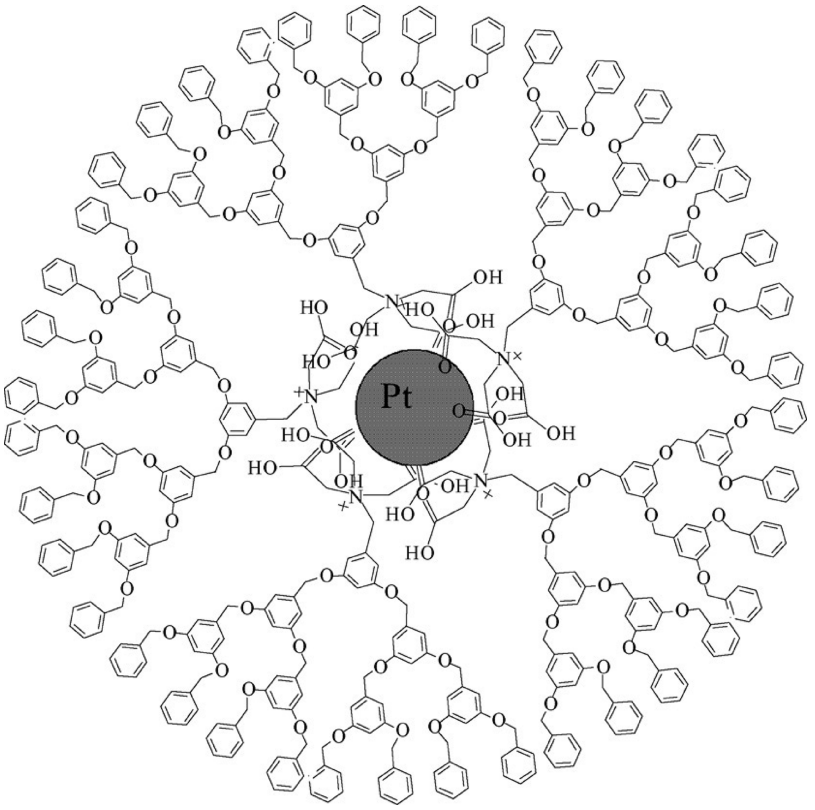

Figure 7. The proposed configuration of Pt-NCD. Reprinted with permission from ref 153. Copyright 2006 Elsevier.

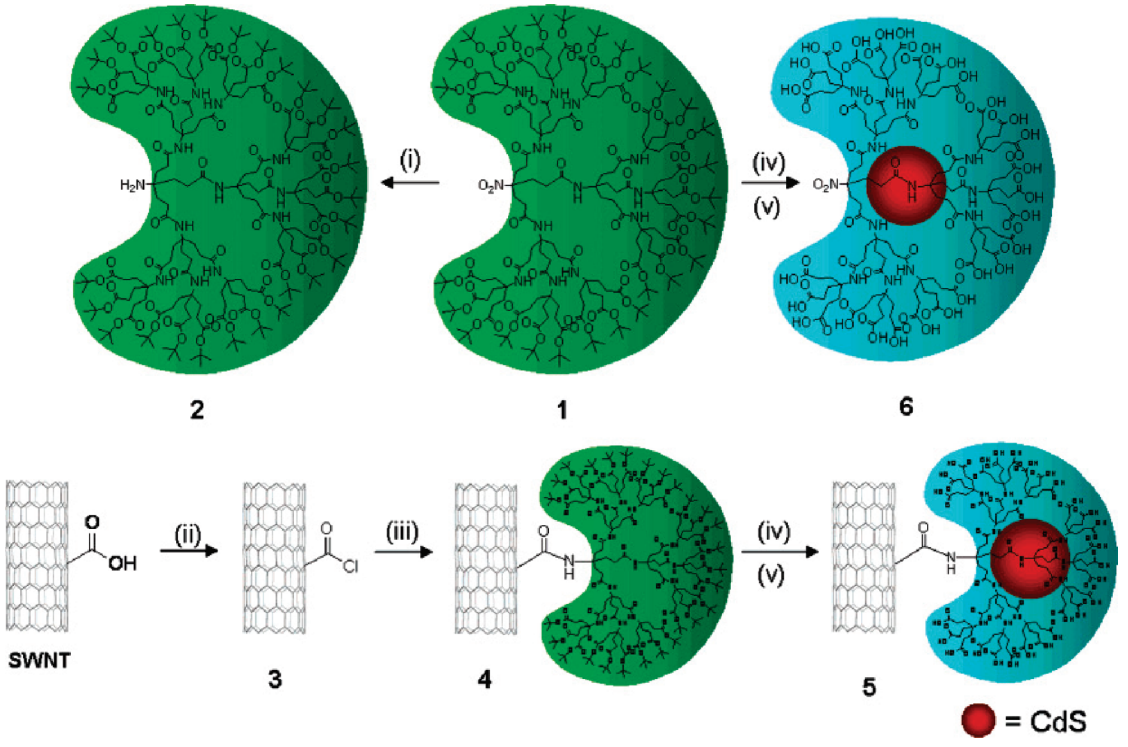

Figure 8. Synthesis of the tethered (**5**) and untethered (**6**) CdS QDs. Reprinted with permission from ref 155. Copyright 2006 American Chemical Society.

various interesting properties.[139−152] Dendrons with coordinating groups in a focal point can be used as ligands forming the NP shell (i) during NP formation, (ii) by secondary stabilization (place exchange reaction), or (iii) by growing dendrons from the

NP surface. Because of steric hindrances, a number of dendrons that might be attached to a NP is lower than that for other surfactants. This can lead to a "non-passivated surface", that is, unoccupied with any ligand, thus making it readily available for participating in catalytic reactions. Although a ligand exchange is a standard way of NP functionalization, the direct synthesis of NPs using dendrons has its advantages. It is believed that a more homogeneous shell is formed than that in the case of ligand exchange. Below we describe the examples of all three scenarios for the NCD formation.

2.3.1. NP Formation in the Presence of Dendrons. Fréchet type[47] polyaryl ether dendrons with different focal groups are commonly used to stabilize NPs. These dendrons are frequently chosen because they are chemically inert, yet only focal groups are capable of coordinating noble metals. Such a dendron with an ammonium chloride focal group containing three carboxyl groups to react with metal NPs was described in ref 153. The Pt/dendrimer nanocomposite was synthesized by reduction of platinic acid, H_2PtCl_6, with aqueous ethanol in the presence of these dendrons, allowing successful stabilization of NPs (Figure 7).

Fullerodendrons, C60(G*n*-COOK) (n = 0.5, 1.5, 2.5), were synthesized by Diels–Alder reaction of C60 with anthracenyl focal PAMAM dendrons, which had potassium carboxylate terminal groups.[154] It is noteworthy that the size and shape of the C60(G*n*-COOK)-passivated silver NPs synthesized by reduction of Ag^+ with $NaBH_4$ were independent of the dendrimer generation number.

The third-generation 1 → 3 C-branched amino-polyester dendrons tethered to single-wall carbon nanotubes ([$(HO_2C)_{27}$-Den]*n*-SWNTs) were used for formation and stabilization of CdS NPs (Figure 8); however, in this case, the focal group serves for the attachment to carbon nanotubes, while the NPs are formed in the interior of a dendron similar to DENs.[155] The NP size was estimated to be 1.4 nm from their optical absorption spectra, and the NPs are clearly seen in TEM images. The authors believe that luminescence, long-term stability (>90 days), and the sizes of quantum dot assemblies with [(HO_2C)27-Den]-*n*-SWNT may be useful for fabricating molecular electronic devices; however, so far no further work has been published demonstrating such developments.

In other work,[156] the PAMAM dendrons with carboxyl periphery and a single hydroxyl focal group were used to attach to the commercial multiwall carbon nanotube (MWCNT) surface followed by coordination with silver ions and reduction with formaldehyde. Silver NPs were well visible on the nanotube surface in TEM images. Unfortunately, this interesting work has not been continued beyond the cited communication.

In ref 157, Fréchet-type G2-modified dendrons functionalized with carbazole fragments were tailored with a phosphonate group at a focal point. These dendrons were used as surfactants for high temperature in situ synthesis of CdSe QDs. Although the authors claim that this is a direct synthesis of NPs in the presence of dendrons, nevertheless, some amounts of surfactants (dodecylamine and trioctylphosphine) were added into the reaction solution for NP stabilization, and no proof is provided in the work that the above surfactants do not stay on the NP surface along with dendrons. The photophysical properties of these nanocomposite are discussed in the section Optical Properties.

Fréchet-type polyaryl ether dendrons with phosphine focal groups were reported in ref 158. Reduction of $Pd(acac)_2$ with hydrogen in the presence of these dendrons led to stabilization of Pd NPs via coordination with phosphine ligands. The NP size

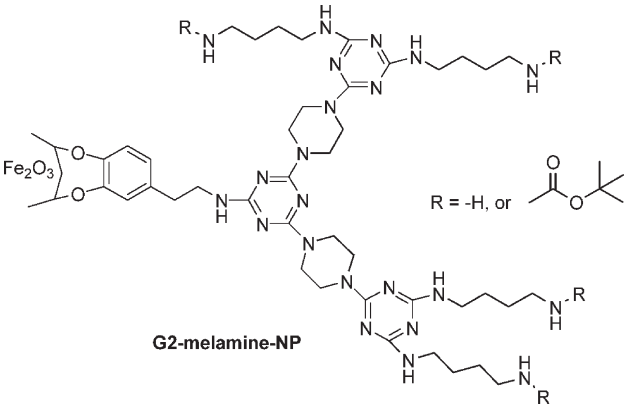

Figure 9. Maghemite nanoparticles protected with a shell of melamine dendrons. Reprinted with permission from ref 164. Copyright 2006 American Chemical Society.

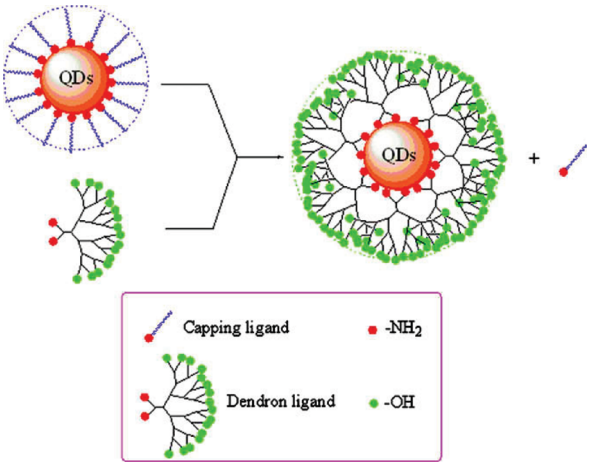

Figure 10. Schematic illustration of the formation of the core–shell CdSe/ZnS quantum dots by using bidentate dendron ligands. Reprinted with permission from ref 167. Copyright 2009 Elsevier.

ranged from 5.0 ± 0.4 to 4.6 ± 0.5 to 3.2 ± 0.5 nm, decreasing with the increase of the generation of the dendritic ligands. The authors believe that this should be attributed to the improvement of the stabilizing ability of higher generation dendrons as surfactants; however, we believe the difference in the NP size for the G1 and G2 dendrons is low, so more dendron generations should be studied to make the above conclusions.

Not surprisingly, the Fréchet-type dendrons with thiol focal groups were employed for gold NP stabilization; however, no NP size dependence on the generation number was observed.[159,160] In the same way, Au NPs stabilized with G1–G3 dendrons containing 4-pyridone focal groups[150] were synthesized using the Brust–Shiffrin method.[161] The average NP size depended on the generation number and increased with the increase of the latter. This was explained by the fact that the higher is the dendron generation, the greater is the steric requirement of the focal metal-binding moiety, and therefore the more room there is for gold atoms to agglomerate. This sounds reasonable but is conflicting with the paper discussed above,[158] where the opposite trend was observed for the same Fréchet type G1–G3 dendrons.

We believe that the coordination ability of phosphine functionality toward the Pd NP surface is greater than that of pyridone

dx.doi.org/10.1021/cr2000724 |*Chem. Rev.* 2011, 111, 5301–5344

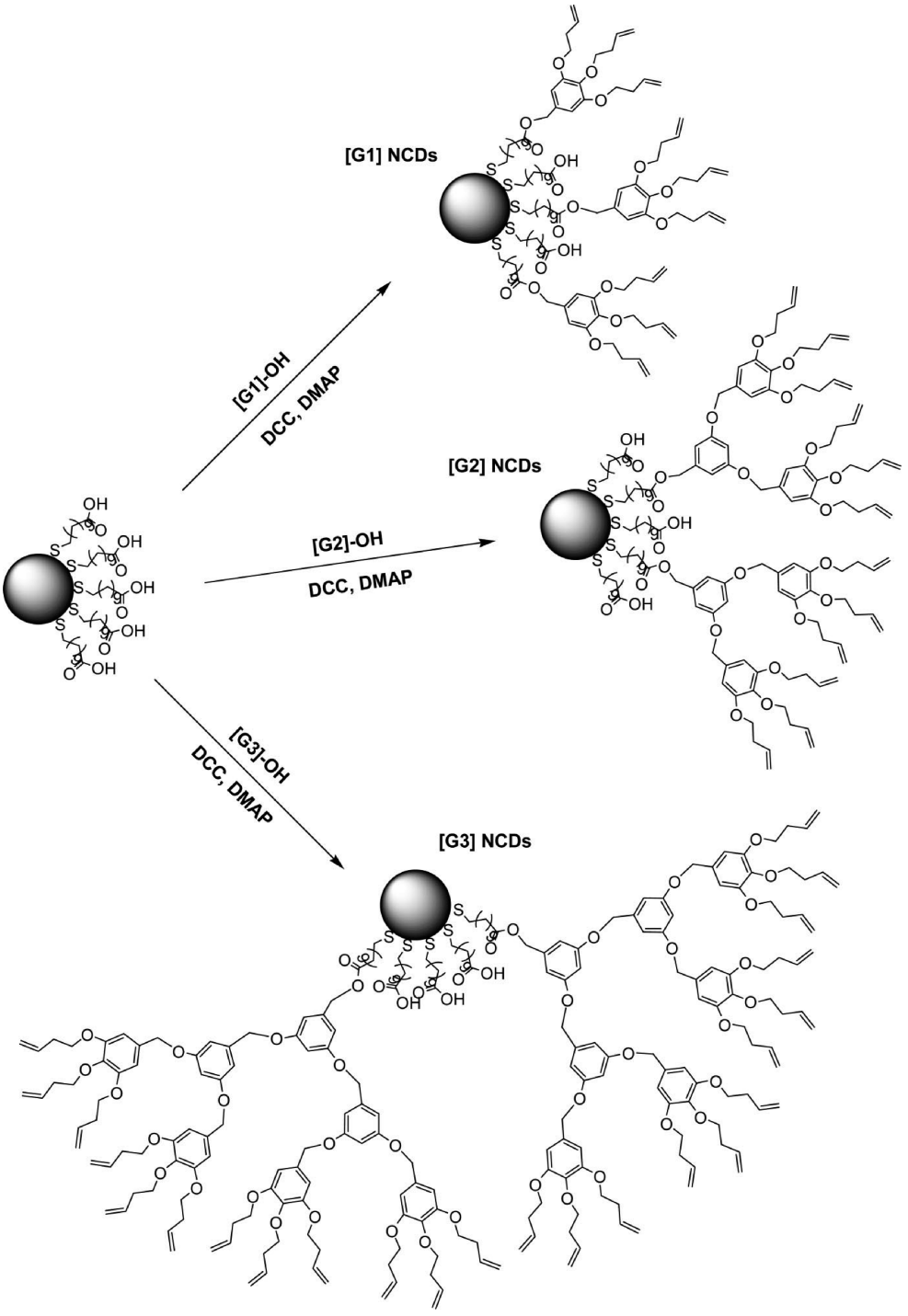

Figure 11. General synthesis of [Gn] NCDs by the ester coupling reaction. Reprinted with permission from ref 151. Copyright 2008 American Chemical Society.

toward the Au NP surface. On the other hand, the thiol group/Au surface interaction is most favorable as a covalent bond is formed, but in ref 159 no clear NP size dependence on the generation number was observed for the dendrons with a thiol focal group. We believe that the steric hindrance exerted by dendrons of higher generations (at least in the range G1−G3) is not a dominant factor, while the nature of metal NPs and the bonding strength of the focal functionality toward the NP surface control the NP formation.

2.3.2. Ligand Exchange for Dendrons. PAMAM dendrons with thiol focal groups were also used for NP stabilization via a ligand exchange reaction. The dendrons with carboxyl or hydroxyl periphery and thiols in a focal point stabilized prefabricated Au NPs and CdSe/CdS QDs after ligand exchange with surfactants used in the NP syntheses.[162]

The Fe_3O_4 nanocrystals modified with poly(ethyelene glycol) (PEG)-terminated organic dendrons containing a new bonding group, hydroxamic acid, in a focal point were successfully

dx.doi.org/10.1021/cr2000724 |*Chem. Rev.* 2011, 111, 5301–5344

obtained through a surface ligand displacement reaction without any changes in the size and size distribution of nanocrystals.[163] The PEG terminal groups provided stable colloidal solutions in a broad spectrum of organic solvents and in water. The authors demonstrated superior stability of the PEG-dendron/Fe_3O_4 nanocomposites against acid etching and thermal treatment, making these NPs appealing in numerous magnetic applications involving harsh conditions.

The G1−G3 Simanek-type melamine dendrons have been synthesized using the multistep approach for a dendron synthesis. The Fe_2O_3/dendron nanocomposites have been formed using a ligand exchange reaction on the NP surface between oleic acid and the melamine dendron containing two hydroxyl groups (from a dopamine moiety) in a focal point (Figure 9). Depending on the terminal groups of the dendron, the magnetic NPs were either water-soluble (in the case of polar groups) or soluble in THF, chloroform, and other organic solvents in the case of nonpolar groups.[164]

Reference 165 describes the synthesis of CdSe and Au NPs stabilized by oligothiophene dendrons using two different methods. In the case of QDs, composite CdSe/dendron NPs were formed via a ligand exchange of TOPO for a thiophene dendron. In the case of Au NPs, the latter were directly formed in the presence of dendrons with long alkyl tails in a focal point. The authors studied the influence of the alkyl chain length and dendron size on the NP size and the efficiency of the electron transfer (see details in the section "Optical Properties").

The ligand exchange was also used for formation of composite Au NPs with polyphenylazomethyne dendrons, containing thiol focal groups.[166] Octanethiolate has been replaced by dendrons of first, second, and third generations. The composite NPs were prone to complexation with various cations (Fe^{3+}, Sn^{2+}, Au^{3+}) due to imine groups of the dendrons, which led to the formation of large spherical NP aggregates, thus allowing control over nanocomposite characteristics.

In ref 167, the authors reported the water-soluble dendron-functionalized CdSe/ZnS core−shell QDs synthesized through a ligand exchange process from octadecylamine-stabilized (ODA) NPs. The dendron had two primary amine anchoring groups at its focal point and hydroxyl groups as its terminal functionalities. The amine anchoring groups served as bidentate ligands for the QDs, while hydroxyl groups enhanced water solubility of the dendron nanocrystals (Figure 10).

It is noteworthy, however, that the characterization of the NPs in this work is confusing. The authors observed a significant increase of the NP diameter after coating with dendrons from 6.3 to 15.8 nm. Their interpretation of this event was that the NP size has to increase because a dendron is added on top of the NP coated with ODA. In fact, dendrons are supposed to replace the ODA molecules, and thus no NP increase is expected. The observed NP size increase is most likely due to partial aggregation of NPs in water, which in turn is due to incomplete replacement of ODA with dendrons.

The above two most popular methods for the NCD syntheses are not free from disadvantages. For example, the direct method using a modified Brust−Schiffrin's reaction with thiol- or disulfide dendrons[144−149,168−170] requires a large excess of dendrons and provides rather poor process control. The indirect method using ligand exchange reaction suffers from a low exchange rate.[145] One more disadvantage is that the synthesis of thiol- or disulfide-functionalized dendrons usually requires additional organic reactions and steps. These disadvantages can be overcome by growing dendrons from a NP surface.

2.3.3. Dendron Growth from the NP Core. In ref 151, the authors introduced a method in which the synthesis of monolayer-protected NPs is followed by building the dendrimer architecture on the NP surface leading to NCDs with a controlled core particle size, different dendron generations, and dendron ligand density. The convergent synthesis of NCDs was accomplished by the ester coupling reaction of 11-mercaptoundecanoic acid-functionalized gold nanoparticles with hydroxyl functionalized dendrons of different generations (Figure 11). The authors claim that, as compared to the direct method, their approach allows one to maintain an intact average core size for NCDs with different numbers of interior layers (generations) and dendritic wedge densities. Because the authors controlled the number of terminal COOH groups on the NP surface, further control of the number of dendrons attached was achievable.

In a very similar procedure,[152] unreacted carboxyl groups on the NP surface were allowed to react with ferrocene−methanol, leading to redox-active NP/dendron nanocomposites. It is worth mentioning, however, that the dendron growth from a NP must be compatible with the NP, and this is often a problem due to side reactions, difficulty to separate encapsulated reactants, etc.

An alternative method was reported in ref 171 for the synthesis of G0−G3 PAMAM dendrons directly on the surface of Fe_3O_4 NPs coated with SiO_2 shell. This approach differs from those described above because the dendron growth was carried out directly on a solid support and was going on from the center to periphery; that is, it was carried out by a divergent method. After the dendron formation, the NPs became more stable and better soluble in organic solvents.

2.4. Directing the NP Placement or Self-Assembling with Dendrimers toward 2D and 3D Structures

Formation of two- (2D) and three-dimensional (3D) structures can occur by self-assembling of NP/dendrimer(dendron) composite particles or individual components on surfaces or in a third dimension. The other option is placing these composite particles within prefabricated 2D/3D structures as templates. There are several methods to attach NP/dendrimer composites on the surfaces or within prefabricated structures. They are (i) layer-by-layer (LbL) deposition of oppositely charged layers due to electrostatic interactions, (ii) noncovalent interactions of dendrimer terminal groups on surfaces, (iii) covalent attachment of terminal groups of dendrimers on surfaces (for example, thiol groups on a gold surface), and more complex cases when several forces are involved.

2.4.1. Two-Dimensional Structures. Two-dimensional arrays of DENs, DSNs, or NCDs are much more common than 3D structures as they require only the ability of the former species to interact with the surface in some way and form a monolayer.[172,173] These monolayer films are rarely well-ordered. However, when DENs (for example, Pt-DENs formed by G4-OH PAMAM) were deposited on the prokaryotic surface-layer (S-layer) proteins as biomacromolecular templates, the results were remarkable (Figure 12).[174] The authors demonstrated highly periodic topochemical properties of these 2D films. This can be a new, effective pathway for creating patterned arrays of Pt nanoparticles with potential technological applications.

LbL deposition has been actively used for the formation of composite films,[175−177] capsules,[178,179] etc., after pioneering work by Moehwald and Decher.[180] Normally, it results in 3D structures (see the next section), but when only a few layers are deposited, it leads to very thin films that are rather 2D architectures. The example of the LbL approach to form ultrathin film

matrix based on G2 PAMAM and pyromellitic dianhydride in supercritical CO_2 was described in ref 181. Pt NPs were formed within this matrix to use for nonvolatile memory. The dendrimer in the film structure is used to control nanoparticle size and to improve NP distribution. The retention capability and the memory effect were demonstrated by a metal−insulator semiconductor device, which was fabricated using the NP-containing thin film as the insulating layer.

Recently, spontaneous formation of 2D nanonecklaces by self-assembling the composite G7 PAMAM dendrimers/HgTe QDs has been reported (Figure 13).[81] Although the dendrimers employed bear NH_2 terminal groups, the authors had no doubts regarding formation of DENs based on very detailed FTIR studies. The distance between QDs in nanonecklaces (which was much smaller than that afforded by the DEN structure) demonstrated interpenetration of dendrimers in necklaces. As a result, close packing of the QDs led to electronic coupling. The large optical absorption cross section allowed one to predict that such strongly coupled systems could serve as a platform for enhanced light absorption centers in photovoltaic devices. The authors believed that tailoring of the hydrogen-bonding network between neighboring dendrimers in self-assembled structures may allow for rational design of 2D nanostructures with well-defined geometry, but no other examples except necklaces were presented in that work.[81]

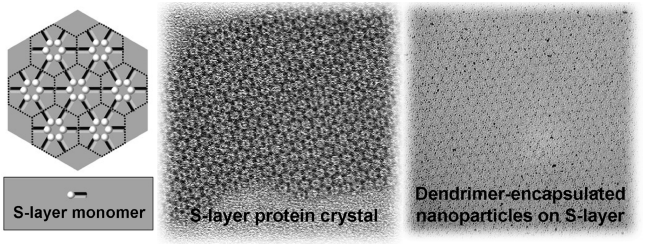

Figure 12. Structure of the hexagonally packed intermediate (HPI) S-layer (p6 symmetry) (left), TEM images of native HPI S-layer protein lattices (center), and DENs on S-layer (right). Reprinted with permission from ref 174. Copyright 2006 American Chemical Society.

The example of adsorption by $\pi-\pi$ stacking (noncovalent interactions) was explored in ref 109, where PAMAM dendrimers modified with thiophene groups containing hydrophobic tails, G4(3T6C), and stabilizing Au and Pd NPs were immobilized on highly ordered pyrolytic graphite substrate (HOPG). Hydrophobicity of both the substrate and the dendrimers allowed regular spread of DENs on the HOPG surface.

Covalent bonding was used to adhere a NP/dendrimer layer on the surface of polymer substrates (polydimethylsiloxane or polyethyleneterephthalate) after a plasma treatment with maleic anhydride.[182] The latter resulted in covalent attachment of the G3 and G4 PAMAM dendrimers preloaded with a gold compound via interaction of their amino groups. Further UV irradiation via a mask resulted in chosen patterns of Au NPs stabilized by dendrimers on a polymer template.

2.4.2. Three-Dimensional Structures. Multilayers based on PAMAM dendrimers with Au NPs as positively charged layers and poly(sodium 4-styrenesulfonate) (PSS) as the negatively charged ones have been described in ref 183. Although the authors schematically presented dendrimer/Au NP composite as DENs, the Au NP sizes in the range 5−20 nm (for the G5 PAMAM

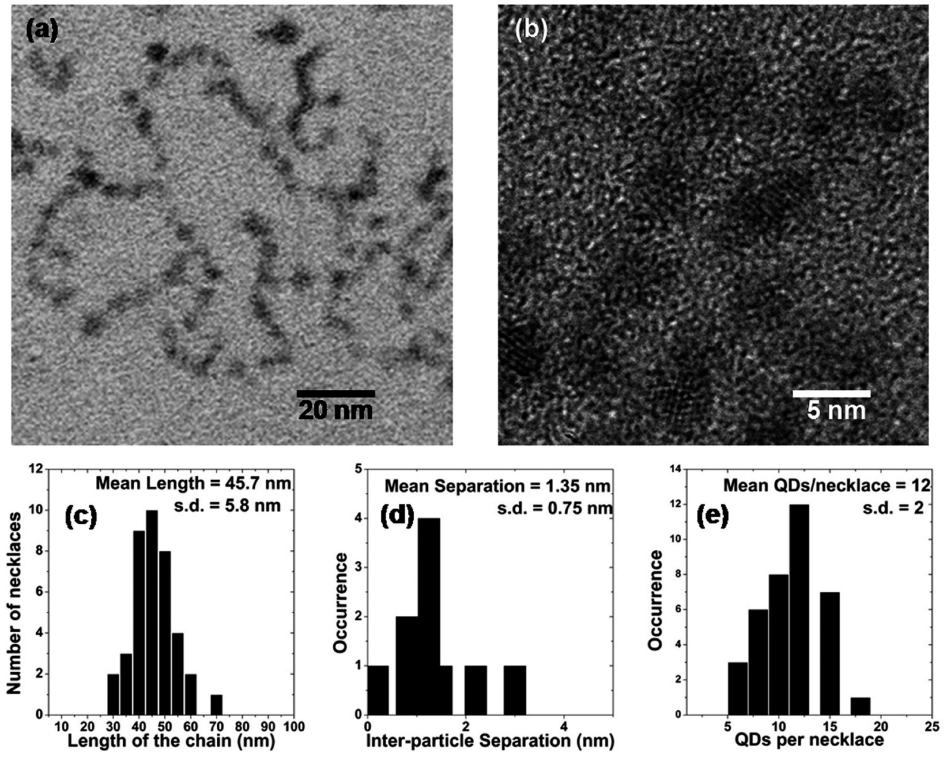

Figure 13. (a) TEM image of HgTe nanonecklaces formed by keeping G7 dendrimer-encapsulated nanoparticles in the dark at 10 °C. These results are typical for samples stored for at least 3 weeks. (b) High-resolution TEM image showing interparticle spacing typical of HgTe nanonecklaces. (c−e) Histograms showing the chain length distribution (c), mean separation between QDs (d), and number of QDs per necklace (e). Reprinted with permission from ref 81. Copyright 2010 American Chemical Society.

dx.doi.org/10.1021/cr2000724 |*Chem. Rev.* 2011, 111, 5301–5344

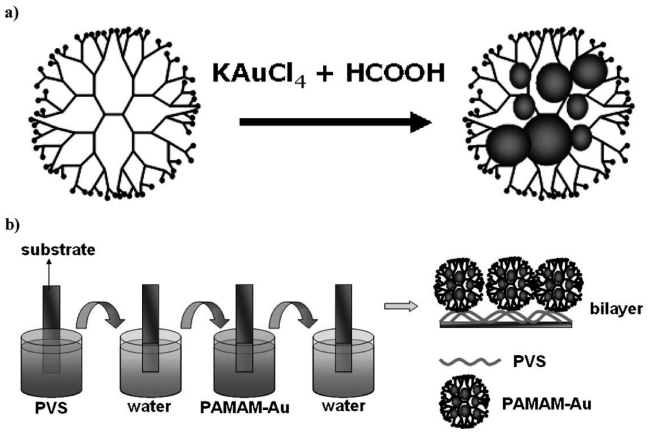

Figure 14. Schematic fabrication of LbL films comprising PVS and PAMAM-Au. (a) Formation of PAMAM-Au. (b) Sequential deposition of LbL multilayers by immersing the substrates alternately into PVS and PAMAM-Au solutions for 5 min. Before each deposition step, the excess of nonadsorbed molecules was removed by immersing the substrate in water. Reproduced with permission from ref 184. Copyright 2007 Wiley-VCH Verlag GmbH & Co. KGaA.

dendrimers) are indicative of NP stabilization by dendrimers as surfactants, that is, DSNs. Using AFM, the authors concluded that the nanoclusters are arrayed with high uniformity at the nanometer scale within PSS/gold-dendrimer nanocomposite film.

The LbL self-assembly process showed its importance in fabrication of devices for electrochemical applications, in particular, in those cases where control at the molecular level is needed. In ref 184, the authors demonstrated a structure based on electroactive nanostructured membranes with ITO-PVS/PAMAM-Au LbL electrodes (PVS stands for poly(vinylsulfonate) and ITO stands for indium tin oxide), in which a redox mediator (Me) is electrodeposited around the Au nanoparticles to form an ITO-PVS/PAMAM-Au@Me system (Figure 14). As redox mediators the authors used Co, Fe, Ni, and Cu hexacyanoferrates.[184,185] The three-bilayer ITO-PVS/PAMAM-Au@Me system was characterized by cyclic voltammetry and impedance spectroscopy. The hexacyanoferrate-modified electrodes showed electrocatalytic activity toward hydrogen peroxide reduction, thus demonstrating that this approach can be used in biosensors and nanodevices, where a redox mediator is required.

Three-dimensional structures based on silica and Au-NP containing DSNs were reported in ref 186. Here, PAMAM dendrimers are used as a multifunctional framework, serving as a surfactant for NP synthesis and a template for condensing silica under ambient conditions. Although the authors showed in Figure 15 that the Au NP is encapsulated by a dendrimer, the comparison of the NP and dendrimer sizes clearly demonstrates that DSNs are formed. Nevertheless, this approach seems to be promising for the preparation of composite nanospheres. The authors also used an alternative route for encapsulation, that is, electrostatic interactions between the positively charged surface amines of the dendrimer and a negatively charged surface of QDs.[186] This resulted in luminescent silica nanospheres.

Interesting uniform C/Co nanorods with unique cross sections, Co/C core/shell nanospheres, and MWCNT were synthesized in high yield by solid-state thermolysis of polyphenylene dendrimer/Co complexes under different heating procedures (Figure 16).[72] The authors envisioned unique catalytic, electronic, and magnetic

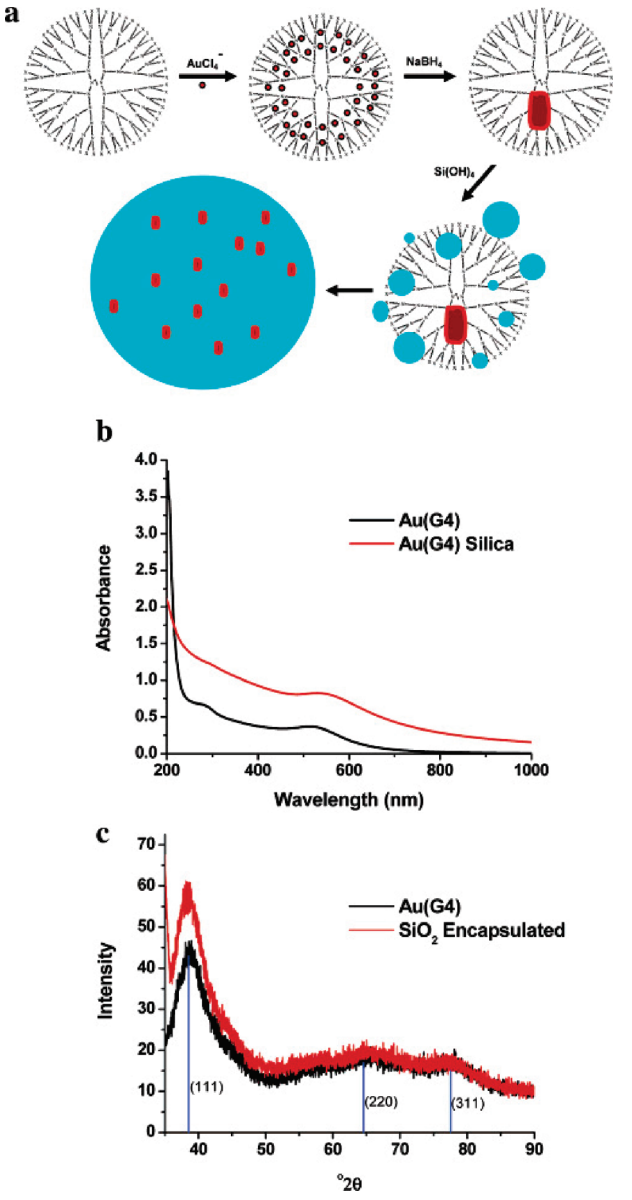

Figure 15. Nanoparticle encapsulation. (a) Schematic diagram of the synthesis of silica encapsulation of dendrimer-supported Au(0) nanoparticles; (b) UV−vis analysis of the Au(0) nanoparticles and composite material; and (c) XRD analysis of the Au(0) nanoparticles and composite material. Reprinted with permission from ref 186. Copyright 2004 American Chemical Society.

behavior of these materials, but, unfortunately, no properties of these materials were ever measured.

Unusual nanocomposites have been prepared using simple chemical reactions of monofunctional Au NPs and PAMAM dendrimers. The 2.8 nm Au NPs modified by a single carboxyl group on the NP surface were synthesized as described elsewhere.[187−189] In the presence of di-isopropylcarbodiimide, the carboxyl group forms amide bonds with a peripheral amine group of the dendrimers. TEM of the conjugates showed formation of 10−13 nm clusters consisting of 4−10 NPs in each cluster (Figure 17). In addition, smaller clusters and larger aggregates were also observed. This work demonstrated the possibility of a "bottom-up" approach to form ensembles of

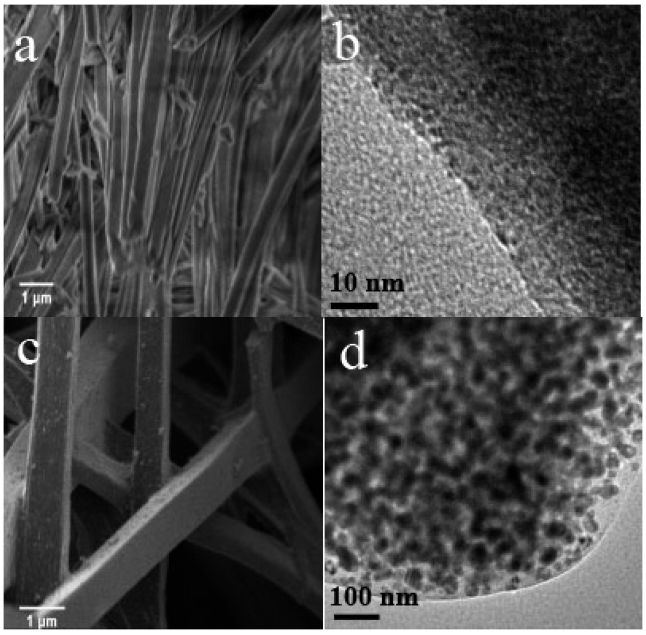

Figure 16. SEM (a,c) and TEM (b,d) images of the obtained carbon/Co materials from dendrimer/Co complexes: (a,b) heating at 130 °C for 2 h (2.2 °C/min from room temperature); (c,d) further heating at 800 °C for 8 h (5.6 °C/min from 130 °C). Reproduced with permission from ref 72. Copyright 2005 Wiley-VCH Verlag GmbH & Co. KGaA.

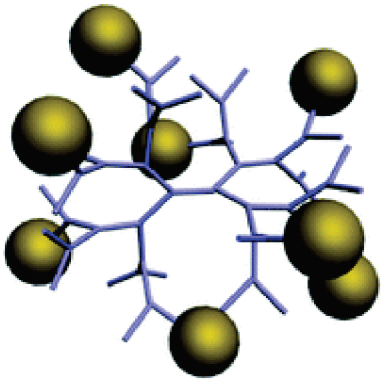

Figure 17. Gold nanoparticle−dendrimer conjugate clusters prepared by a covalent coupling of monofunctional gold nanoparticles with a G5-NH_2 PAMAM dendrimer. Reproduced with permission from ref 190. Copyright 2006 Royal Society of Chemistry.

covalently linked conjugates;[190] however, no control over cluster size was demonstrated.

Three-dimensional materials have been prepared by encapsulation of 1 nm Rh and Pt NPs in G4 PAMAM dendrimers immobilized in the pores of mesoporous silica SBA-15.[191] Here, two possible types of interactions allowing attachment of DENs onto SBA-15 should be considered: electrostatic interaction and hydrogen bonding between dendrimer and silica.[192] Indeed, because the loading was carried out at pH 5, while the isoelectric point (point of zero charge) of silica material is ~2, the PAMAM dendrimer at this pH is positively charged,[192] while the surface of SBA-15 silica is negatively charged. Thus, electrostatic interaction is one of the driving forces of a 3D nanocomposite formation. At the same time, because the PAMAM dendrimer is terminated with 64 hydroxyl groups, multiple hydrogen bonds with hydroxyl groups on the surface of SBA-15 silica can be an additional strong factor.[192] The catalytic properties of these and other analogous materials are discussed in the section Catalytic Properties.

The template approach can be even more complicated, but it may result in well-ordered 3D structures. The example of such approach was reported in ref 193. The strategy suggested in that work includes three major steps: top-down nanoimprint lithography (NIL) for the fabrication of patterned polymer templates, then bottom-up supramolecular LbL assembly of multilayered adamantyl-functionalized dendrimers and approximately 3 nm CD-functionalized Au NPs, and finally a lift-off process (Figure 18). The authors also explored supramolecular recognition properties of the 3D structures to examine the potential of the supramolecular LbL structures in encapsulating external guest molecules and NPs.

Recently, unusual ordered 3D rice-shaped architectures (RSAs) have been reported in ref 194 using polyphenylene-dendrimer-templated strategy (Figure 19). Surprisingly, both CuO NPs and rice-shaped ensembles had analogous monocrystalline structure, which became possible due to sharing a common crystallographic orientation. As a result, CuO NPs gradually self-organized, protected and cross-linked by the G2 dendrimer molecules with terminal carboxyl groups. The authors proved that cross-linking due to bonds between Cu^{2+} and COO^- ions is crucial for rice shape structures, while the dendrimer provided a rigid spacing between NPs. In the following article, the authors studied the high-energy electron beam of the transmission electron microscope for in situ modification of RSAs.[195] The electron beam-modified RSAs retained their rice shape, while the primary CuO NPs were converted to the Cu_2O NPs with an increased size. Detailed investigation demonstrated that such a modification process consists of two stages, involving the arrangement of the primary CuO NPs and then their transformation.

3. CHARACTERIZATION TECHNIQUES FOR NP/DENDRIMER (DENDRON) COMPOSITES

To characterize NPs, dendrimers (dendrons), DENs, DSNs, NCDs, 2D and 3D structures, and the composition−structure−function relationships, generally a combination of characterization techniques should be employed as a single method does not allow an accurate description of complicated systems. We feel that it is important to clarify what information can be obtained by a researcher when using particular techniques and how to approach solving structural puzzles. In some cases, when no references on techniques are available to describe NP/dendrimer(dendron) nanocomposites, we will use references for other NP-based materials to make a point.

3.1. NP (Dendrimer, DEN, DSN, NCD) Shape, Size, and Size Distribution

3.1.1. Transmission Electron Microscopy (TEM). TEM is the most widely used method for characterization of the shape, size, and size distribution of NPs by observing and processing TEM images.[65,81,124,196−199] However, to allow meaningful quantitative data, hundreds of NPs have to be processed. One should also take into consideration if any aggregation is observed on a TEM grid. It can be a secondary aggregation on the surface, which may not reflect the condition of the sample in solution.[197] TEM allows great visualization of NPs, but even when several hundreds of NPs are processed from TEM images, it is still a small fraction of the sample (see below on solution techniques).

Because of the electronically rich environment of NPs, they can be seen even in complex composite materials.[200−203] In ref 200, the

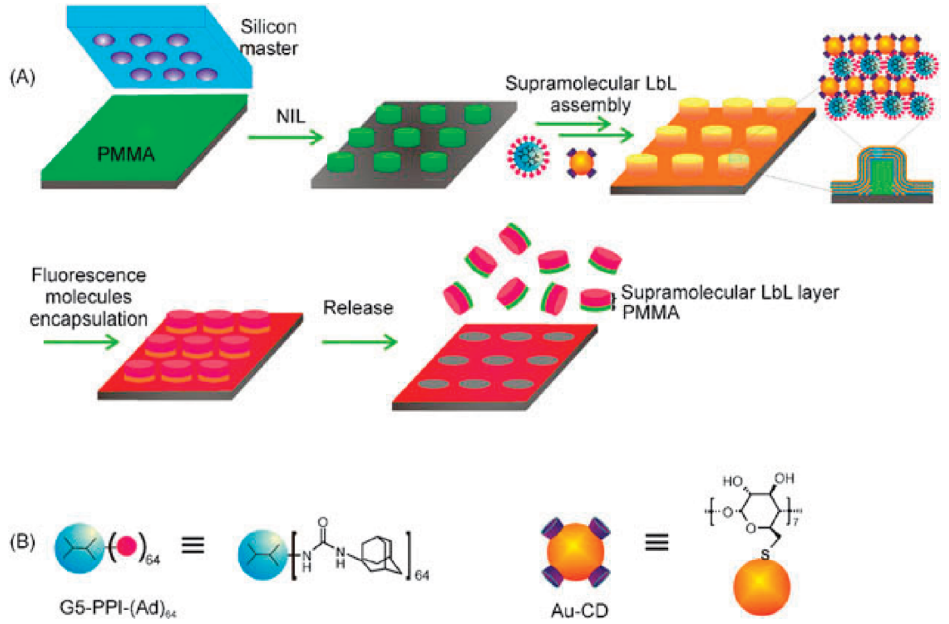

Figure 18. (A) 3D hybrid structures prepared by three key steps: (i) NIL fabrication of a polymer template, (ii) supramolecular LbL assembly of multilayered Ad dendrimers and Au-CD nanoparticles on the pattern, and (iii) a lift-off process. Fluorescent molecules can be encapsulated within the structures to form discrete fluorescent hybrid objects. (B) The chemical structures of adamantyl-terminated poly(propylene imine) dendrimers of generation 5 (Ad dendrimers) and Au-CD nanoparticles. Reproduced with permission from ref 193. Copyright 2009 Royal Society of Chemistry.

MWCNTs were covalently modified with G4-NH_2 PAMAM dendrimers. By simply tuning the metal ion-to-dendrimer terminal amine ratio, Au NPs with different sizes from 3 to 11 nm were in situ synthesized and deposited on the surface of CNT/G4-PAMAM, as confirmed by TEM (Figure 20). Moreover, Ag, Cu, and Pt NPs, as well as Ag@Au, bimetallic NPs were synthesized and visualized. Clearly, in this case, based on NP sizes no DENs were formed (no encapsulation), although the authors erroneously use this term.

3.1.2. Atomic Force Microscopy (AFM). AFM provides the vertical height measurements of NPs that complement the lateral measurements from TEM.[173] The use of AFM to measure particle size raises a number of other questions,[173] including specimen preparation and sample purification. Specimens for AFM are usually prepared by soaking a mica, gold, or HOPG surface in the sample and then rinsing. Drop casting or spin coating the sample on the surface can be also used.[109,192,204−208] A number of studies demonstrated that dendrimers are extensively deformed from their globular shape when they are neat, in contact with a surface presenting a flat disk.[204,205,209,210] However, despite the flattening of the dendrimer on the mica surface, it is possible to observe a growing dendrimer size upon increasing the dendrimer generation (Figure 21).[173] In refs 173,211, the authors thoroughly investigated the behavior of PAMAM dendrimers and PAMAM-Pt NPs by AFM. They believe the flatness of the "empty" dendrimer can be attributed to the considerable flexibility of a dendrimer molecule, a molecular collapse of which on the surface is due to water removal and sufficient dendrimer−mica attraction. In all cases, the AFM mean heights for PAMAM-Pt samples deposited on mica were greater than the corresponding values for "empty" PAMAM, thus allowing one to distinguish between "empty" and Pt NP-containing PAMAM, although no single dendrimer molecule could be observed. AFM also allows observation of aggregation by arrested precipitation of PAMAM-mediated templating of Pt nanoparticles. The authors[211,212] reported the conditions when this aggregation is minimized.

3.1.3. Scanning Tunneling Microscopy. Scanning tunneling microscopy (STM) is known to provide the highest spatial resolution in real space imaging of materials, and its applications are most common among conductive and semiconductive systems. As such, this method can offer limited information on nonconductive dendrimers. These systems present high-energy barriers and, thus, little tunneling probability. Efforts to lower the barriers included incorporation of more conductive functionalities such as metal porphyrins and phenyl rings[46,213] as well as implementation of metal nanoparticles displaying single-electron tunneling.[214]

For example, STM allowed visualization of unusual petal-like dendritic structures as scaffolds to realize a wheel-like or spherical arrangement of multiple zinc porphyrin (P) units (DP_m, where m is 6, 12, and 24),[213] which are capable of ligating multiple molecules of bipyridine compounds having 1−3 fullerene (F) units (Py_2F_n, where n is 1−3) (Figure 22).

3.1.4. Solution Techniques. There are several solution techniques allowing one to determine the NP size, shape, and size distribution in a natural NP environment of a whole sample consisting of hundreds of thousands of particles.

Dynamic light scattering (DLS) is a common technique to obtain a NP size in solution if the NP diameter exceeds 1 nm. The determination of the diffusion coefficient of the NPs in solution gives access to the hydrodynamic radius of a corresponding sphere and the polydispersity of the colloidal solution. This radius is an intensity-weighted mean value. A correct conversion to a number or volume-weighted mean values requires the knowledge of the complex refractive index. However, it is worth noting that for NP/dendrimer (dendron) composite particles, only the final composite particles and their aggregates can be characterized.[82,215−217]

Small-angle scattering methods such as small-angle X-ray and neutron scattering (SAXS and SANS, respectively) are powerful techniques to obtain information on shapes and sizes of NPs.[110,218−221] Groehn and co-workers reported the SANS

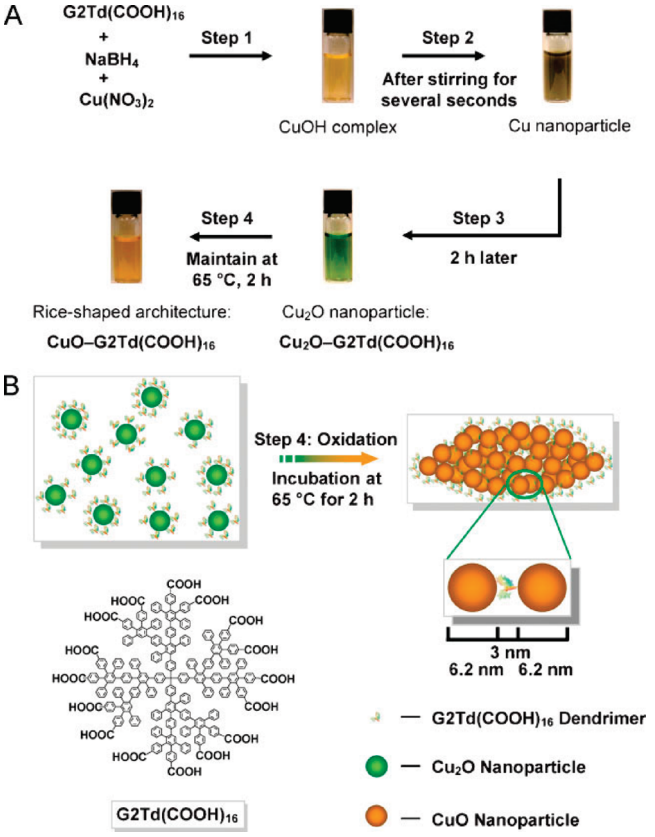

Figure 19. Schematic illustration of (A) the synthesis of CuO-G2 Td(COOH)$_{16}$ RSAs, and (B) formation of CuO-G2 Td(COOH)$_{16}$ RSAs in step 4. Inset: Molecular structure of G2 Td(COOH)$_{16}$. The change in solution color at each reaction step is shown in (A). Reproduced with permission from ref 194. Copyright 2010 Wiley-VCH Verlag GmbH & Co. KGaA.

and SAXS profiles for Au NPs templated by PAMAM dendrimers of generations from 2 to 10 in aqueous solutions.[110] SANS and SAXS showed that the gold particles are formed inside the dendrimer and located offset from the center.

The use of a combined time-resolved method of SAXS and SANS techniques in situ allowed the authors of ref 222 to explore both the association process of the neat G1-NH_2 PAMAM dendrimers interacting with $Pd(OAc)_2$ and the reduction of Pd ions into Pd atoms along with self-assembling into Pd NPs. This sophistication has been possible due to modern advances of SAXS and SANS applied in situ (Figure 23).

SAXS was used to quantify the interparticle spacing for Au NPs functionalized with a carboxylic acid monolayer and assembled with excess of PAMAM dendrimers,[223] and to characterize gold, platinum, and copper NPs formed within dendrimers dispersed within the polymer networks.[224]

The latest developments of SAXS data processing techniques applied to numerous NP/polymer composites and polymers[225−229] demonstrate the wealth of information that can be obtained from SAXS data, thus opening new opportunities of materials characterization beyond those already employed for NP/dendrimer composites.

3.2. Inorganic NP Structure and Composition

3.2.1. X-ray Powder Diffraction. X-ray powder diffraction (XRD) is commonly used to determine the crystal structure of

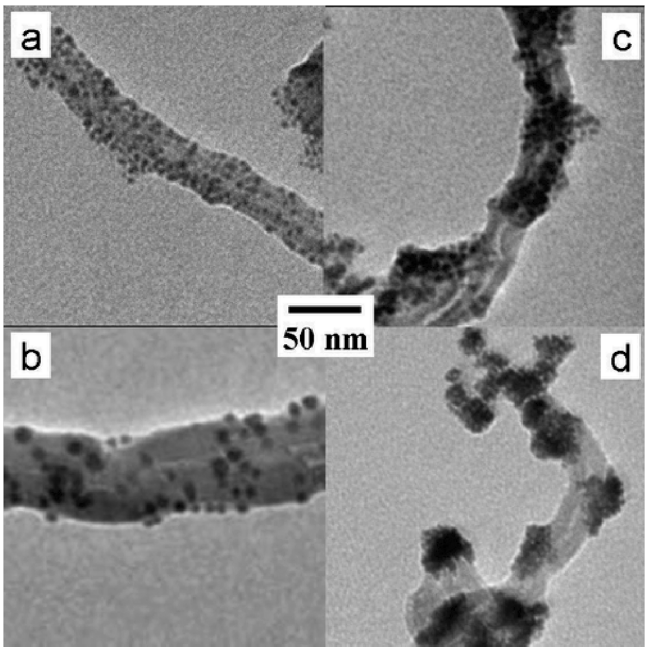

Figure 20. TEM images of CNT/dendrimer/NPs: (a) Au; (b) Ag; (c) Cu; (d) Pt. Reprinted with permission from ref 200. Copyright 2007 American Chemical Society.

NPs.[194,230−232] By comparing the positions and intensity of the experimental and reference peaks (from bulk materials), one can establish the crystal structure of NPs, although for NPs, more complicated structures can be formed than for bulk materials.

In refs 232−234, the atomic-scale three-dimensional structure of dendrimer encapsulated Au, Pt, and Cu NPs was determined using high energy XRD techniques and reverse Monte Carlo simulations. A relatively new method of XRD analysis, the atomic pair distribution function (PDF) analysis, has been used previously to determine 3D atomic structures of nanosized materials.[232] In the PDF analysis, structural data are obtained from both Bragg and diffuse features of the XRD pattern. It was observed that Pt NPs in DENs are more ordered than those stabilized by long-chain alkanes in similar environmental conditions.[234] It was also determined that dry NPs show more structural coherence than do NPs in solution.

Crystal size is estimated from the line broadening of the XRD spectra by the Scherrer equation.[235] It is noteworthy that crystallite sizes are not necessarily equal to NP sizes, if the NPs are not single crystals.

Although very frequently XRD diffraction is the method of choice, due to line broadening some structures that are well distinguishable in bulk cannot be resolved for small NPs. The typical examples are magnetite (F_3O_4) and maghemite (γ-Fe_2O_3) NPs. Their XRD profiles are so similar that more methods should be employed to find out which structure is formed. Here, high resolution TEM (HRTEM) can be a useful technique along with Raman spectroscopy (Figure 24) and, in some cases, FTIR spectroscopy.[236−238]

Information similar to that from XRD can be obtained from selected area electron diffraction (SAED), which is normally combined with TEM.[82,239−241]

3.2.2. High Resolution TEM. With further development of instrumentation, high resolution TEM (HRTEM) became quite a common technique, which is employed for assessment of

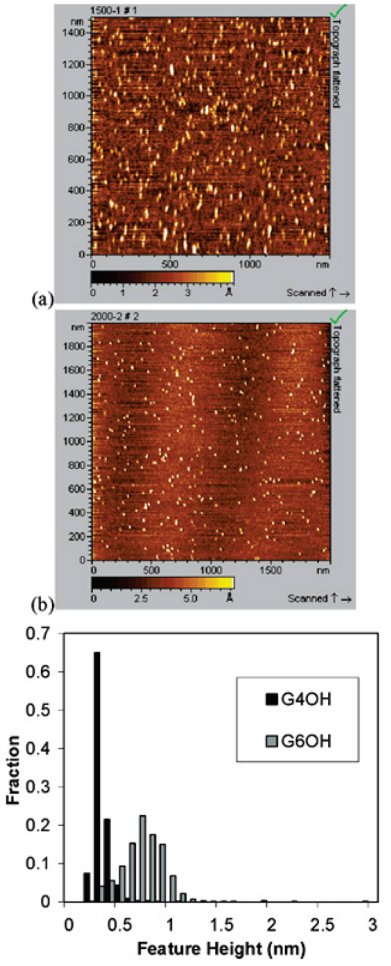

Figure 21. AFM topography images and corresponding feature height distributions for G4OH (a) and G6OH (b) on mica. The bottom panel shows the feature height distribution compiled from multiple images. Reprinted with permission from ref 173. Copyright 2005 American Chemical Society.

inorganic phases. It gives access to the atomic arrangement in NPs and allows getting information on lattice vacancies and defects, lattice fringes, glide planes, or screw axes along with surface atomic arrangement of crystalline nanoparticles (Figure 25).[65,201,242−244]

Furthermore, HRTEM allows one to determine the structure of bimetallic nanoparticles due to differences in lattices.[245,246] The most reliable results regarding complex NP composition and structure can be obtained when HRTEM is combined with SAED and energy dispersive X-ray spectroscopy (EDS) (see below) of the same particles. Fast Fourier transform (FFT) of HRTEM images gives information on whether the NP is a single crystal or not. HRTEM has been also used for structural characterization of layered materials including NPs and dendrimers.[247] One should however be careful to avoid overinterpreting the HRTEM images because measuring lattice spacing can be inaccurate due to positioning of a crystal.

3.2.3. Energy Dispersive X-ray Spectroscopy. Energy dispersive X-ray spectroscopy (EDS) provides information on elemental composition of materials. Sometimes, it is called energy dispersive X-ray analysis (EDX).[248] This method can be used for characterization of the structure of bimetallic nanoparticles in

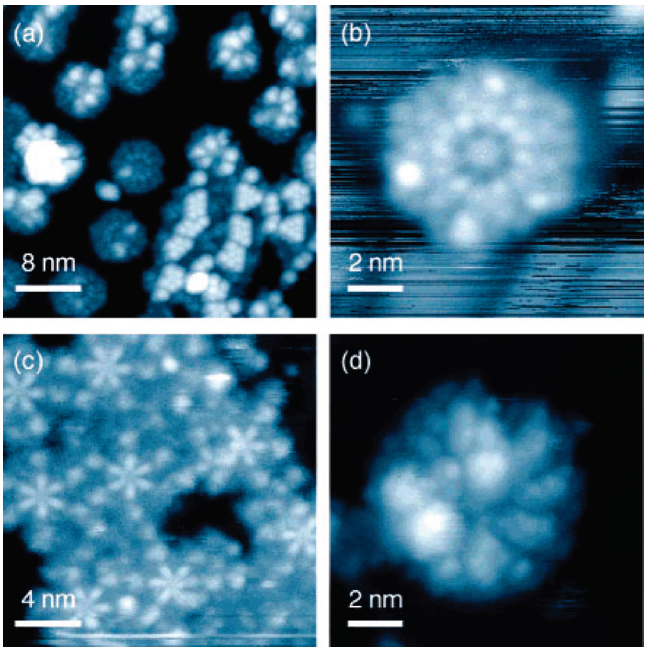

Figure 22. Ultra high vacuum STM micrographs of (a,b) DP12 in the presence of 6 equiv of Py_2F_3, (c) DP6 in the presence of 3 equiv of Py_2F_1, and (d) DP24 in the presence of 12 equiv of Py_2F_1, on a Au(111) surface at a liquid nitrogen temperature. Conditions: (a) *I*, 1 pA; *Vs*, +3 V; (b) *I*, 1 pA; *Vs*, +2 V; (c) *I*, 2 pA; *Vs*, +4.5 V; (d) *I*, 1 pA; *Vs*, +2 V. Reprinted with permission from ref 213. Copyright 2006 American Chemical Society.

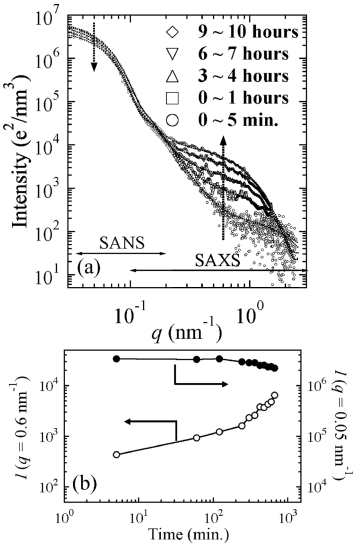

Figure 23. (a) Time evolution of combined SAS (SANS plus SAXS) profiles during the reduction process. (b) Time change in the scattered intensity at q = 0.05 and 0.6 nm^{-1}. Reprinted with permission from ref 222. Copyright 2007 American Chemical Society.

dendrimers using single-particle analysis.[99−102,248−251] For example, EDS analysis was used for the rod-shaped and spherical Ag−Cu nanoclusters[248] and allowed the authors to detect both silver and copper elements in nanoclusters (the heavy elements are easily detectable by EDS), but the line intensity of elements in the EDS analysis of the rod-shaped Ag−Cu nanoclusters was different from that of the spherical ones. The atomic

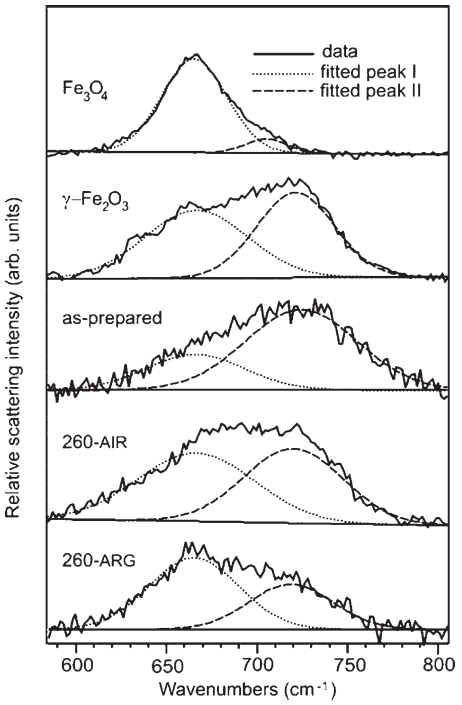

Figure 24. Raman spectra in the 585−805 cm^{-1} region for commercial γ-Fe_2O_3 and Fe_3O_4 samples and FeO_x aerogel samples treated under various temperature/atmosphere conditions. For all samples other than Fe_3O_4, the spectra were deconvoluted into a band at 665−667 cm^{-1} (peak I) and a band at 720−725 cm^{-1} (peak II) by curve-fitting analysis. Reprinted with permission from ref 236. Copyright 2004 American Chemical Society.

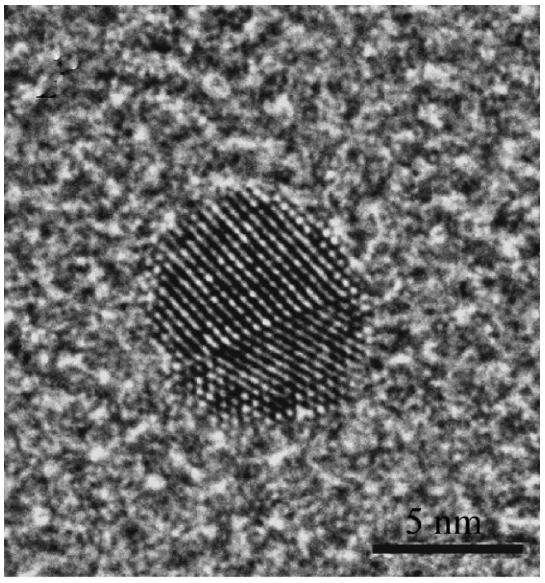

Figure 25. HRTEM image of gold NPs stabilized with "click" poly(ethylene glycol) dendrimers shows the cubic crystalline structure of the Au NPs. Reprinted with permission from ref 65. Copyright 2010 American Chemical Society.

percentages of silver and copper of the rod-shaped nanoclusters were 63% and 37%, respectively, in agreement with the expected values. This indicated that the Ag−Cu bimetallic nanoclusters prepared with $NaBH_4$ reduction were Ag−Cu alloy nanoclusters. In contrast, the atomic percentages of silver and copper of the spherical nanoclusters were 21% and 79%, respectively, indicating that the surface of nanoparticles was made of Cu^0.

The EDS analysis of several PdPt[99] individual particles allowed constructing a particle composition distribution. This work is important as it gives a quantitative sense as to how much control exists over particle composition.

When EDS is combined with scanning TEM (STEM), it is possible to carry out mapping the composite material and determining the distribution of NPs in a matrix.[252]

3.2.4. X-ray Photoelectron Spectroscopy. For estimating the elemental composition and electronic states of elements contributing to composite materials, X-ray photoelectron spectroscopy (XPS) can be employed. If for bulk metal samples, XPS allows only surface analysis (3−5 nm depth), for small nanoparticles encapsulated by dendrimers, this is in fact a bulk analysis. However, the XPS data of NPs in DENs, DSNs, NCDs, and other inorganic/organic materials should be evaluated with care because of possible charging of the NPs in nonconductive environment (artifact), which leads to the appearance of higher oxidation states than those in real samples.[253,254] This might be a cause of inconsistency of the XPS data of Pt-DENs reported by several research groups.[94,119,255]

Indeed, Zhao et al.[94] observed that the Pt $4f_{7/2}$ peak appeared at 71.3 eV for dendrimer encapsulated Pt_{60} NPs, which indicated complete reduction of Pt(II) to Pt(0). Ye et al.[119] observed the Pt $4f_{7/2}$ peak at 73.0 eV for dendrimer encapsulated Pt_{30} NPs. The higher binding energy of Pt_{30} NPs than that of bulk Pt(0) was attributed to quantum size effect and adsorption of dendritic ligands; however, the 2 eV difference can hardly be explained only by these two effects. Ozturk et al.[255] observed Pt $4f_{7/2}$ peaks at 74.6 eV for dendrimer encapsulated Pt_{40} NPs deposited as a thick layer. The authors explained the higher binding energy by charging of the DEN films, while they did not exclude the incomplete reduction of the Pt(II) species as well. In ref 191, the authors attempted to clarify the above discrepancies examining the dendrimer encapsulated Pt_{20} and Pt_{40} NPs using XPS. They also observed higher Pt $4f_{7/2}$ binding energy (73.5 eV) of Pt_{20} NPs than that of metallic Pt and concluded that this is due to unreduced Pt^{2+}. The major Pt $4f_{7/2}$ peak also had a small shoulder at 71.2 eV, which was attributed to metallic Pt. Therefore, only ~7% of total Pt was metallic, which agreed with a previous study where an alternative method, extended X-ray absorption fine structure (EXAFS), showed that Pt remained oxidized even after exposure to a strong reducing agent, $NaBH_4$.[256] Similar behavior was observed for the dendrimer encapsulated Pt_{40}. In the case of DEN-Rh,[191] 56% of the Rh atoms were found to be metallic, while the remaining 44% were oxidized. The authors suggested that this was due to incomplete reduction of $RhCl_3$ during the synthesis with formation of complexes with internal functional groups of the dendrimer. In general, to figure out whether high binding energies are due to charging or incomplete reduction, the combination of XPS with EXAFS seems to be most reasonable.

3.2.5. X-ray Absorption Spectroscopy. X-ray absorption spectroscopy (XAS) is an extensively used technique for determining the local geometric and/or electronic structure of materials. XAS includes two methods: extended X-ray absorption fine structure (EXAFS) and X-ray absorption near edge structure (XANES). The EXAFS spectra are shown as plots of the absorption coefficient of a given material versus energy (normally in a 500−1000 eV range before an adsorption edge

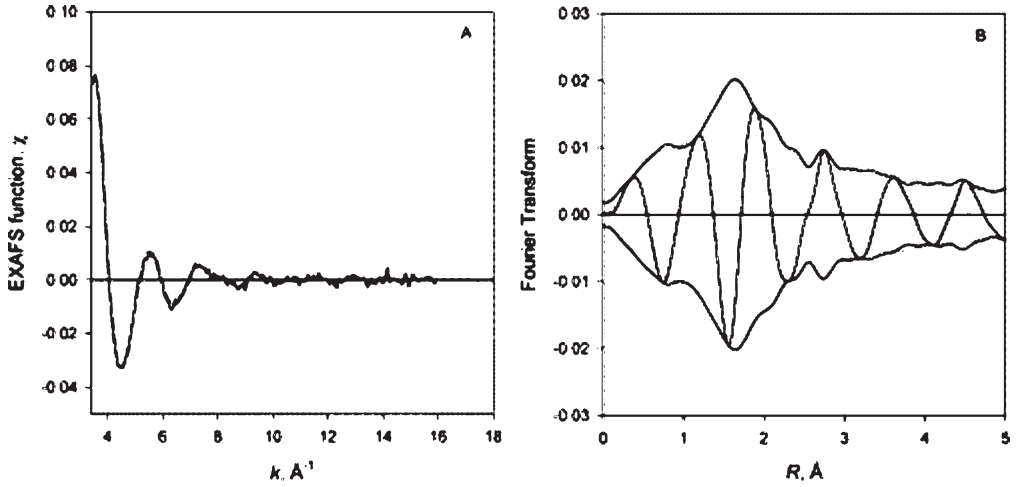

Figure 26. Results of EXAFS analysis characterizing G4OH−$(Pt^{4+})_{40}$ complexes treated with $NaBH_4$ in an aqueous solution: (A) experimental EXAFS (χ) function (solid line) and sum of the calculated contributions (dashed line); (B) imaginary part and magnitude of uncorrected Fourier transform (k^0 weighted, Δk = 3.5−15.0 $Å^{-1}$) of experimental EXAFS data (solid line) and sum of the calculated contributions (dotted line). Reprinted with permission from ref 256. Copyright 2006 American Chemical Society.

of an element in the sample). The XANES data indicate the absorption peaks due to the photoabsorption cross-section in XAS.

Monometallic Nanoparticles. The development of EXAFS has provided a powerful tool for clarifying the local atomic arrangements and electronic effects of small metal clusters in supported metal catalysts as well as in colloidal metal catalysts. Using EXAFS, the possible structure of bimetallic nanoparticles was estimated via calculating the number of surrounding atoms of each absorbing metal element.[257] In ref 256, precise structural characterization of Pt-PAMAM dendrimer nanocomposites was achieved for the first time using EXAFS and XANES spectroscopy. In particular, the authors were able to characterize and understand on a molecular level the various steps of the preparation of supported Pt/γ-Al_2O_3 catalysts via G4-OH dendrimers as templates. The results indicated that strong interaction of $[PtCl_3(H_2O)_3]^+$ and $[PtCl_2(H_2O)_2]$ (partially hydrolyzed $PtCl_6^{2-}$ and $PtCl_4^{2-}$ ions) with amine and/or amide groups in the interior of the G4OH dendrimer led to transfer of electron density from the dendrimer to platinum and to the replacement of Cl^- ions in the coordination sphere of Pt^{n+} by functional groups of the dendrimer, indicating that the dendrimer plays role of a ligand. Contrary to previous observations for different Pt−dendrimer systems,[14,211,212,258−260] the authors did not observe formation of NPs in solution when $NaBH_4$ was used as reducing agent (Figure 26).[256] This is a very surprising result contradicting numerous previous studies on Pt NP formation in various polymers, but no explanation has been given in that paper. When reduction of G4OH-$(Pt^{4+})_{40}$ was performed with H_2, the formation of Pt dimers or extremely small clusters incorporating on average no more than four platinum atoms was observed. These clusters remained strongly bonded to the dendrimer. Formation of ~1 nm NPs was observed only after deposition of the above DENs on a γ-Al_2O_3 surface and subsequent drying, presumably because the solvent removal leads to the collapse of the dendrimer branches and clustering of the Pt species. The obvious advantage of EXAFS and XANES methods is the possibility of identifying subnanometer size clusters, which would be rather "invisible" for many other techniques.

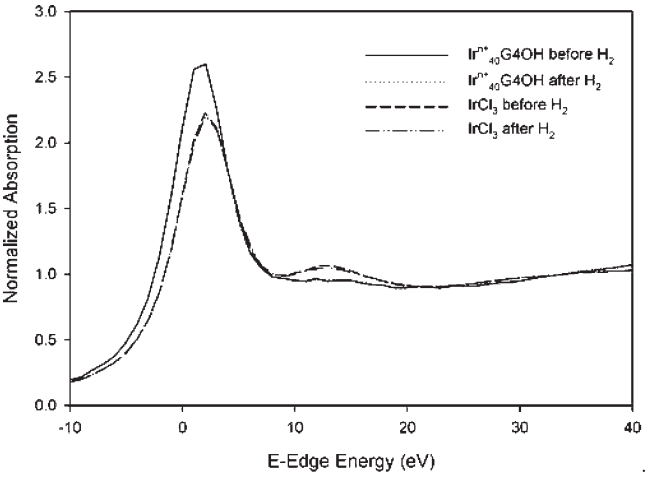

Figure 27. Ir L_{III}-edge XANES spectra for $(Ir^{3+})_{40}$G4OH complex and $IrCl_3$ aqueous solutions before and after reduction with H_2. Reprinted with permission from ref 261. Copyright 2008 American Chemical Society.

The preparation of Ir/Al_2O_3 catalysts from dendrimer metal precursors was investigated using XANES measurements at several stages of the synthetic process.[261] The spectra obtained in the liquid phase showed that the Ir^{3+} ions (from $IrCl_3$) and dendrimer functional groups formed complexes that were stable even after reducing with $NaBH_4$ or H_2 in solution. The absence of Ir−Ir contributions demonstrated that NPs were not formed in these conditions. Only after treatment of the species deposited onto Al_2O_3 support at elevated temperature with O_2/H_2 or H_2 were the Ir NPs formed (Figure 27).

The authors of ref 262 reported a study of Cu(II)−PPI dendrimer complexes with a diaminobutane core by EXAFS and XANES spectroscopy. The EXAFS and XANES spectra of these complexes at the copper K-edge allowed assessment of the geometry of the dendrimer end-group complex with the Cu ion and parameters such as bond distances, coordination numbers, and nature of the ligands contributing to the copper coordination

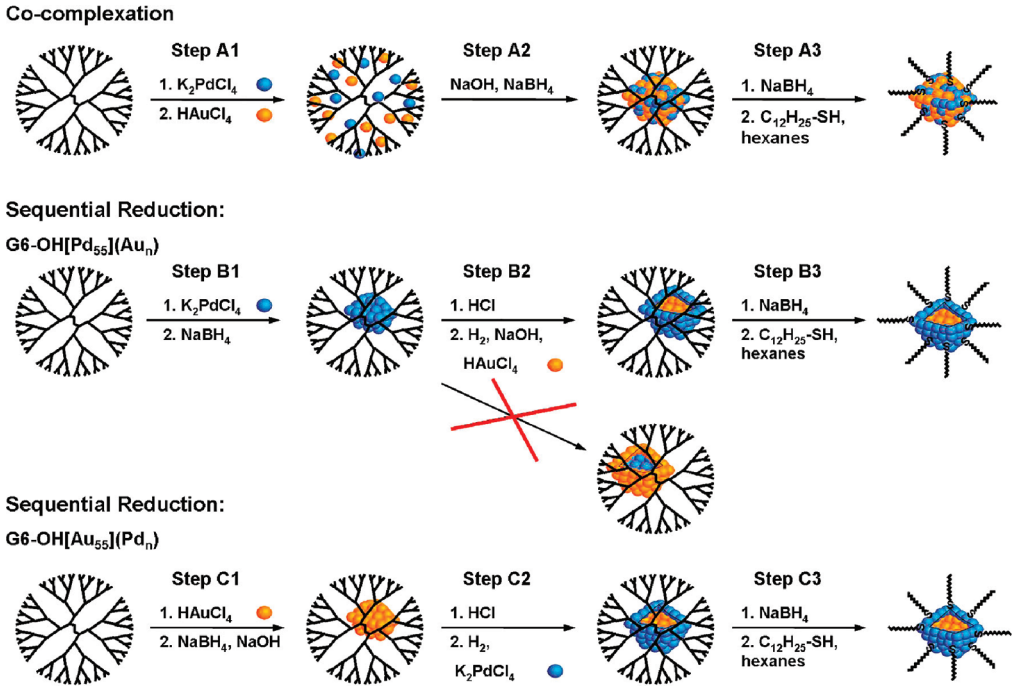

Figure 28. Schematic representation of the formation of PdAu bimetallic nanoparticles in the case of cocomplexation (A) and sequential reduction (B,C). Reprinted with permission from ref 263. Copyright 2010 American Chemical Society.

sphere. The evidence of nanocluster formation upon reduction with $NaBH_4$ was demonstrated in the XANES data by a shift of the K-edge threshold of 1.4 eV. The EXAFS results indicate a decrease in the size of the clusters with increasing dendrimer generation (in agreement with the TEM results) and adsorption of dendrimers on Cu NPs.

Bimetallic Nanoparticles. Recently, Weir et all.[263] reported EXAFS analysis of core−shell PdAu DENs prepared in the PAMAM dendrimer by two different ways: sequential reduction of Pd ions on gold core and vice versa. Surprisingly, due to inversion of two metals in one case, and no inversion in the other, both methods resulted in the identical core−shell structure. Indeed, in the case B (Figure 28) when Au is reduced onto 55-atom Pd DEN cores, Au migrates into the core, while Pd resides on the surface (inversion of two metals). However, when Pd is reduced onto a 55-atom Au core, no inversion takes place (Figure 28C).

The EXAFS analysis performed by the same group on bimetallic PdAu DENs prepared by cocomplexation of metal ions with dendrimers followed by reduction demonstrated that the PdAu DENs are quasi-random alloys regardless of their relative elemental composition.[264] The same scenario was demonstrated for PdCu bimetallic NPs prepared by cocomplexation of the corresponding ions to interior functional groups of a G6-OH PAMAM dendrimer template followed by chemical reduction to yield DENs.[265]

3.3. Dendrimer−Metal Interactions, NP Presence, and More

3.3.1. UV−Vis Spectroscopy. UV−vis spectroscopy is often used for various purposes in DEN and DSN formation, in particular, for in situ observation of coordination between metal ions and dendrimer functional groups. Numerous publications include UV−vis spectroscopy studies of interactions with metal ions or NP formation. This generates a huge amount of references, the comprehensive discussion of which is not possible here. In this section, we will cite only those references that, in our opinion, are typical and demonstrate the usefulness of the method.

In a number of references on DEN preparation, the Crooks group[7,90,93,94,97,119,126,266] used UV−vis analysis to evaluate coordination of different metal ions with amino groups of PAMAM dendrimers and to propose the ion reduction scenario. Astruc's group reported complexation of 1,2,3-triazolylferrocenyl and 1,2,3-triazolylsulphonate dendrimers with Pd(II) by interaction with the triazole ligands using UV−vis spectroscopy.[115,132−134] The changes in UV−vis spectrum of K_2PdCl_4 upon addition of the dendrimer have been attributed to coordination of Pd(II) to triazole ligands in the dendrimer. UV−vis spectroscopy was successfully used to follow the extraction of Au NPs out of DENs to regenerate templates.[92]

UV−vis spectroscopy is even more crucial for analysis of semiconductor nanocrystals also known as QDs. The optical absorbance of QDs is mainly characterized by a band gap between the valence band and the conduction electron band, which is a function of the QD size, called a size quantization effect.[267,268] The method of HWHM (half-width at half-maximum to the longer wavelength side of the first absorption peak) is employed for estimation of QD size and size distribution from UV−vis data.[269−272] For Au NPs with the size exceeding 2−3 nm, the plasmon adsorption band in UV−vis spectra is a key tool to characterize NP size and shape and for applications in imaging.[12,273]

3.3.2. Fourier Transform Infrared Spectroscopy. Fourier Transform infrared (FTIR) spectroscopy is extensively used for dendrimer characterization[274] and for monitoring complexation of dendrimer functional groups with metal species or NPs.[81,194,217,275] Normally either a shift of characteristic bands or their disappearance from the FTIR spectra are observed upon complexation[275] or adsorption on NP surface.[81,194,217] For example, in ref 194, the FTIR spectrum of a composite material showed two characteristic bands at 1617 and 1384 cm^{-1} due to the formation of $Cu^{2+} \rightarrow COO^-$

dx.doi.org/10.1021/cr2000724 |*Chem. Rev.* 2011, 111, 5301–5344

coordination bonds both upon complexation and when CuO NPs were fully dissolved. The latter case revealed the importance of cross-linking through coordination of Cu ions for retaining the rice-shaped architecture of CuO−dendrimer nanocomposites.

3.3.3. Thermogravimetric Analysis. Recently thermogravimetric analysis (TGA) has been actively used to determine the amount of dendrimers or dendrons grafted on a NP surface.[140,143,169,231,248,276−281] Using TGA it was found, for example, that the number of branching units connected to the Au core decreased with the increase of the generation number of the dendritic wedge: this number changed from 2.18/nm^2 for G2 to 0.27/nm^2 for G5.[170] In the case of mixed ligands, the multiple steps in the TGA graph can be observed, which result from different types of ligands.[151] Similarly, TGA can be used to determine a fraction of several components in a nanocomposite if the components decompose at different temperatures (carbon nanotubes and dendrimers).[282]

3.3.4. Nuclear Magnetic Resonance Spectroscopy. For NP/dendrimer (dendron) nanocomposites, nuclear magnetic resonance spectroscopy (NMR) can be used to characterize grafted dendrons or dendrimers only if NPs are sufficiently small (∼2−3 nm).[169] When NP size increases, line broadening occurs, preventing such studies even for nonmagnetic NPs. There are a few exceptions, however, when NP/dendrimer (dendron) nanocomposites were successfully characterized by NMR without significant line broadening even for larger particles (for example, ∼23 nm Ag NPs coated with amine-terminated G5 PAMAM dendrimers),[283] which can be explained by weak adsorption of these ligands on the NP surface. Even for small NPs, however, there are differences in the NMR spectra of free and coordinated ligands due to loss of mobility of the groups adjacent to the NP surface and the Knight-shift effect associated with many metals.[284]

Recently, the Pd NP size was determined using high-resolution proton NMR.[285] The Pd NPs measured in this work contained 55, 147, 200, or 250 atoms (with NP diameters from 1.0 to 1.7 nm) and were encapsulated within G6-OH PAMAM dendrimers. Analysis of the NMR data revealed that signals arising from the innermost protons of G6-OH(Pd$_n$) decrease significantly as the size of the encapsulated NPs increase. A correlation between this decrease in the integral value and the theoretical number of Pd atoms in the NP allowed elucidation of the size of Pd DENs by ^{1}H NMR spectroscopy. NMR pulse-field gradient spin−echo experiments showed that G6-OH dendrimers with and without Pd NPs have identical hydrodynamic radii, revealing the absence of dendrimer/nanoparticle aggregates. The detailed analysis of 1D and 2D NMR spectra of dendrimers with and without NPs for the G4-OH(Pd$_{55}$) nanocomposite based on the behavior of innermost methylenes in comparison with terminal groups[286] unambiguously demonstrated that single NPs were encapsulated within individual dendrimers.

In addition, ^{1}H and ^{13}C NMR spectroscopy along with matrix-assisted laser desorption/ionization time-of-flight mass spectrometry (MALDI-TOF) and size exclusion chromatography are traditionally used to characterize dendrimers and dendrons similar to any other organic molecules,[65,287] but considering the conventional aspect of this characterization, we will abstain from giving exhaustive citations here.

4. MORPHOLOGY−PROPERTY RELATIONSHIP OF NP/DENDRIMER (DENDRON) NANOCOMPOSITES

The properties of NP/dendrimer composites are mainly determined by the properties of NPs, although the dendrimer functional groups or dendrimer−NP arrangement can create new properties and influence the existent NP properties.

Nowadays, the major prospective applications of NP/dendrimer composites are in catalysis, biomedical research, or for electronic devices. The catalytic applications are mainly determined by properties of various mono- and bimetallic NPs, while the dendrimer role is templating or stabilization of NPs, which, in turn, controls the NP size and morphology. There are a few examples when a dendrimer generation (size) puts a limitation on the accessibility of the active centers for reacting molecules due to a different size cavity in the dendrimer, thus creating size selectivity for a catalytic reaction. A similar effect was demonstrated for mesoporous catalysts with reactants of different sizes.[288] The biomedical applications become possible due to biocompatibility of many NP/dendrimer composites and their optical, magnetic, and sensor properties. All of these aspects will be discussed in the following sections. First, we will discuss general optical, magnetic, and sensor properties followed by implementation of these properties in the biomedical field. We will also discuss catalytic, electronic, and other applications of NP/dendrimer composites.

4.1. Optical Properties

Luminescent properties of QDs formed in PAMAM-COOH dendrimers of generations 3.5 and 4 were first reported in the literature in 1998.[129] From the absorption edge, the particle size was estimated in the range 2.4−4.2 nm depending on pH and solvent, although TEM displayed aggregation of NPs. Despite this aggregation, blue luminescence was stable, thus indicating good stabilization of CdS NPs with dendrimers. Moreover, the films cast of the luminescent solutions retained the optoelectronic properties of their parent solutions. In the similar composite based on PAMAM-NH$_2$, the CdS/dendrimer NPs displayed polarized emission with the anisotropy rising progressively from 340 to 420 nm excitation, reaching a maximal value in excess of 0.3.[127] The luminescent properties were also observed for CdS NPs stabilized by other dendrimers, that is, PPI.[289]

The CdS QDs with diameters of 1.3, 1.8, and 2.3 nm giving a rise to emission at 320, 470, and 510 nm were formed in the PAMAM G4-OH, G6-OH, and G8-OH dendrimers, respectively.[79] Here, the nanocomposite particles possessed all of the advantages of QD-based luminescent probes, such as high quantum yield, good photostability, and color tunability, but the synthetic conditions of their preparation were much milder than those reported for organometallic precursors. In this work,[79] metal halide NPs were prepared by a simple ion exchange reaction.

Dendrimers or dendrons can be also used for stabilization of luminescent QDs synthesized in the presence of other capping molecules. This place-exchange reaction may lead to the solubility change of NPs or the nanocomposite properties. Dendrons with eight peripheral hydroxyl groups and two carboxyl groups at the focal point were effectively used for stabilization of core−shell CdSe/CdS NPs by replacing alkylamine by dendrons, leading to water solubility.[290] These nanocomposite particles were considerably more luminescent than the similar NPs stabilized with regular thiols and as stable as the latter. The dendron stabilized CdSe/ZnS core−shell nanocrystals discussed in section 2.3.2 exhibited the same fluorescence and absorption spectra after dissolution in water as the ODA-CdSe/ZnS core−shell nanocrystals dissolved in organic solvents such as chloroform.[167] However, the quantum yield (10%) of the dendron nanocrystals in the aqueous solution has dropped by 75% as compared to the initial nanocrystals (40% quantum yield)

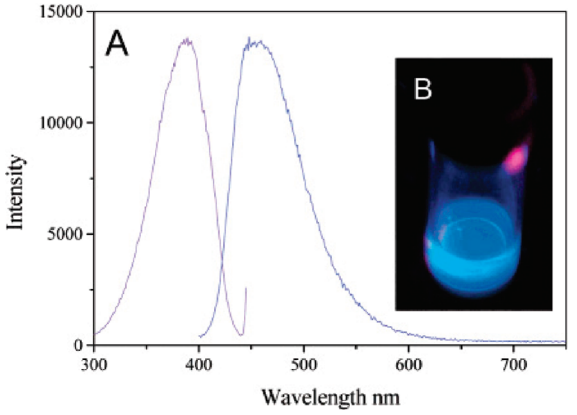

Figure 29. (A) Excitation and emission spectra of G4-OH PAMAM encapsulated gold nanodots at room temperature. (B) Emission from Au nanodots under long-wavelength UV lamp irradiation (366 nm). Reprinted with permission from ref 105. Copyright 2003 American Chemical Society.

in chloroform solution. The decrease of photoluminescence intensity is a common phenomenon during QD water solubilization, especially by using ligand-exchange methods.[291]

Strong blue emission was observed for water-soluble, monodisperse (narrow emitting band) Au_8 nanodots encapsulated and stabilized by PAMAM G2-OH or G4-OH (Figure 29).[105] No difference was observed between both dendrimers. These nanocomposite particles exhibited a fluorescence quantum yield of 41 ± 5%, which was more than a 100-fold improvement over other gold nanoclusters reported earlier.[292,293] Strong blue luminescence centered at about 2.8 eV photon energy was also observed for Au nanoclusters encapsulated within 1.5 generation sodium carboxylate-(G1.5-COONa-)-terminated PAMAM.[294] The photoluminescence from dendrimer-encapsulated Au nanoclusters with a diameter less than 1.0 nm was attributed to the new visible optical transition that results from the change of electronic structure due to quantum confinement. Here, the authors, however, assumed that the nanocluster size is below or equal to 1 nm because they could not see NPs in the TEM images, which is a questionable size characterization.

The observations of blue luminescence of small Au nanoclusters generated a great deal of excitement among scientists. However, later it was demonstrated that simple oxidation of G4-OH, G2-OH, and even G0-OH PAMAM dendrimers using $(NH_4)_2S_2O_8$ allowed similar luminescence with a high quantum yield.[295] The authors concluded that this blue luminescence originated from oxidized OH-terminated PAMAM dendrimers, and the luminescence observed in ref 105 was due to oxidation with Au(III) and unrelated to Au_8 nanoclusters. However, in the later papers,[296−299] the correlation of the gold cluster size and its emission was clearly demonstrated, thus suggesting that gold clusters are of paramount importance in displaying luminescence. The authors[299] concluded that the observed protoplasmic fluorescence arises from intraband transitions of the free electrons that smoothly link atomic and NP limits in condensed-phase Au nanoclusters (Figure 30).

Strong blue luminescence was also reported in ref 128 for large crystalline Au NPs in the size range 7−15.4 nm stabilized by amine-terminated PAMAM of different generations. The authors compared these samples with the commercial Au NPs with 5 and 100 nm in diameter, displaying no luminescence, and concluded that the luminescence is provided only in the presence of the dendrimer, but did not analyze the possibility of the formation of small gold clusters along with large NPs. They recognized the oxidation of the PAMAM dendrimers but did not analyze what could be the source of luminescence: in our opinion, the 7−15.4 nm NPs are not luminescent.

As was well documented in ref 300 the luminescence did not come from silver (4 nm) or gold (1.8 nm) NPs encapsulated by G4-OH or G2-OH PAMAM dendrimers or short amine-rich peptides, but only from 2 to 8 atom nanoclusters formed in these matrices. Because of comparison of two stabilizing molecules, that paper allowed one to rule out the importance of solely dendrimers for this kind of luminescence with gold or silver subnanometer clusters. In addition, in the absence of large NPs providing a plasmon band, the dendrimers and peptides encapsulating small Ag nanoclusters produced scaffold-specific single molecule Stokes and anti-Stokes Raman scattering. The strong single molecule vibrational signatures were enhanced by the Ag_n transitions in nanoparticle-free samples and could not arise from plasmon enhancement.

Luminescence of NP/dendrimer composites can originate from the dendrimer- or dendron-containing component and can be enhanced or partially quenched by the particles. Specially designed dendron grafted phenyleneethynylenes showed strong blue luminescence (here, dendritic structures are used to improve solubility),[301,302] which, however, was significantly decreased for an α,ω-sulfur-terminated oligomer.[302] When this oligomer was combined with ∼2 nm Au NPs (not luminescent but electroconductive) via the ligand exchange reaction, the composite film exhibited enhanced luminescence, revealing synergy, although NPs themselves are not luminescent.

Alternatively, luminescence of specifically designed dendrimers can be quenched by metal NPs. For example, fluorescence of PAMAM dendrons assigned to both anthracenyl and PAMAM dendron moieties (PAMAM dendrons containing carboxylate terminals and fullerene and anthracenyl groups in focal points) was quenched by comparatively large silver NPs (7−10 nm).[154] This indicated the excitation energy transfer to NPs. SWNTs can also partially quench luminescence of QDs templated by amide-ester dendrons as reported in ref 155 (Figure 31).

Interesting effects can be expected when both components, dendron-containing polymer and QDs, are luminescent. Placing a small amount of phenyl-tailored CdS NPs into the dendritic structure of copolyfluorene allowed the authors to substantially improve the efficiency of the polymer photoemission, as well as the purity of the emitted light.[303] The authors believed that the enhancements in photo- and electroluminescence were due to the decrease in the concentration of interpolymer excimers through which energy transfer occurred from the excited polymer chains to their neighboring ground-state polymer chains; that is, the CdS NPs caused an increase in the interpolymer chain distance, thus the enhancement here was unrelated to the luminescence of QDs.

Unlike the above case, CdSe NPs stabilized by thiol-terminated thiophene dendron ligands with alkyl spacers exhibited energy transfer and photoinduced charge transfer interactions between the semiconductor and conjugated ligands.[165,304] The authors believed this nanocomposite to be the best for certain devices such as bulk-heterojunction photovoltaic cells in which the separation of charge upon photoexcitation is required for high efficiency. To prove that, the authors fabricated one-layer photovoltaic devices, which showed a power conversion efficiency of 0.29% (Figure 32).[304,305] For CdSe NPs prepared in the

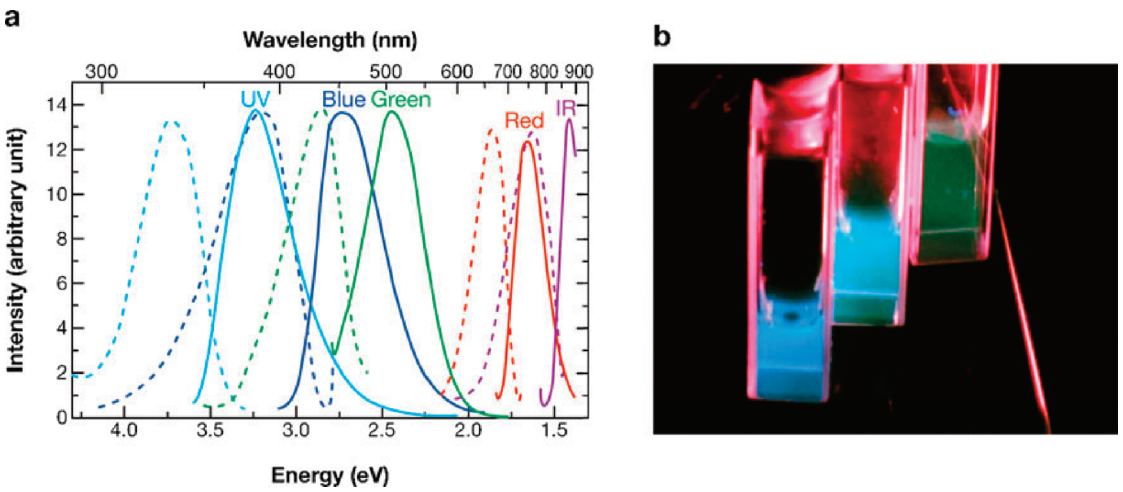

Figure 30. (a) Excitation (dashed) and emission (solid) spectra of different gold nanoclusters. Emission from the longest wavelength sample was limited by the detector response. Excitation and emission maxima shift to longer wavelength with increasing initial Au concentration, suggesting that increasing nanocluster size leads to lower energy emission. (b) Emission from the three shortest wavelength emitting gold nanocluster solutions (from left to right) under long-wavelength UV lamp irradiation (366 nm). The leftmost solution appears slightly bluer, but similar in color to Au_8 (center)[105] due to the color sensitivity of the human eye. Green emission appears weaker due to inefficient excitation at 366 nm. Reprinted with permission from ref 299. Copyright 2004 American Physical Society.

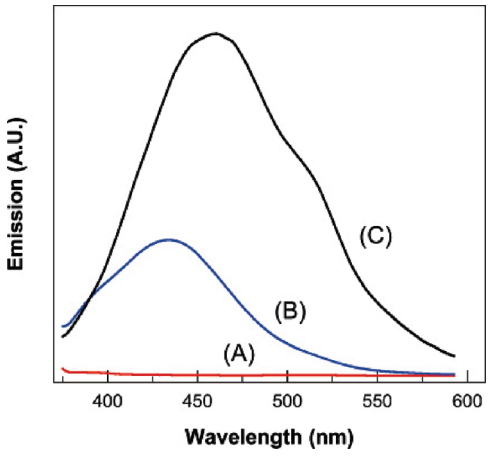

Figure 31. Photoluminescence spectrum for [$(HO_2C)n$-SWNT] (A); CdS/Den-SWNT hybrid (B); and CdS/dendron hybrid (C). Reprinted with permission from ref 155. Copyright 2006 American Chemical Society.

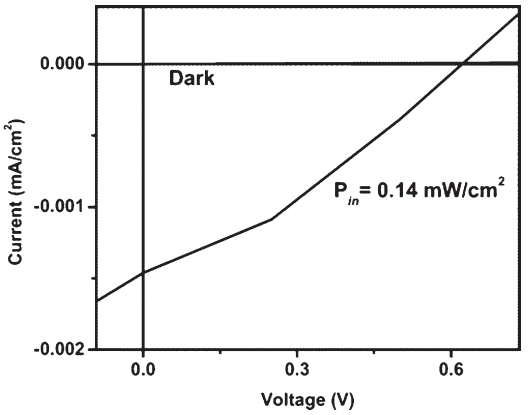

Figure 32. Current density versus voltage for a dendron/CdSe device in the dark and under 0.14 mW/cm^2 illumination. Reprinted with permission from ref 304. Copyright 2004 American Chemical Society.

presence of dendrons with the donor carbazole peripheral groups, the energy transfer properties from the latter to the acceptor CdSe NPs were also observed. Thus, overlap of the fluorescence of the carbazole with the absorbance of the CdSe NP resulted in an enhanced fluorescence with concentration through Förster resonance energy transfer.[157]

Nonlinear optical (NLO) properties were studied for nanocomposites based on Au NPs and G5 PAMAM with different terminal groups including a chromophore (dansyl).[306] The results of fluorescence quenching measurements indicated that there is a strong interaction between dansyl chromophores attached to the dendrimer and the NPs. This further demonstrated that the mechanism of NLO effect is mainly due to light scattering of the metal NP assisted by increased aggregation of the particles in some of the templates. The same group showed that the nanocomposite of Au NPs and G2 PAMAM dendrimers functionalized with more hydrophilic lissamine rhodamine B displayed enhanced third-order NLO effects.[307] The authors suggested that the mechanism for the enhanced optical nonlinearity is related to local field enhancement. The understanding of the mechanism is very important in the control of the distance and the dipole orientation between the dye and metal and applications of these composites in photonics and biophotonics.

4.2. Magnetic Properties

In this section, we will consider general magnetic properties of the composites containing magnetic NPs, while their biomedical applications (both in vitro and in vivo) will be discussed in the section Imaging and Biomedical Properties. One of the most promising applications of water-soluble magnetic NPs is magnetic resonance imaging (MRI). MRI is a powerful tool for studying biological processes (cancer metastases or inflammations) and diagnostics of various diseases. Among other MRI enhancement contrast agents, superparamagnetic iron oxide NPs are found to be

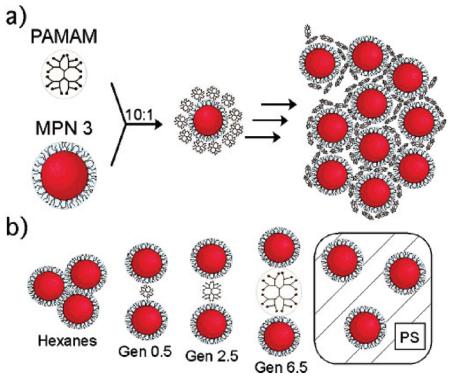

Figure 33. (a) Schematic depiction of dendrimer-mediated nanoparticle assembly. (b) Increase in average interparticle spacing upon assembly with PAMAM dendrimers, as well as hexane and polystyrene controls. Reprinted with permission from ref 311. Copyright 2005 American Chemical Society.

most promising candidates both due to biodegradability[308,309] and due to their efficiency in marking cells.

Maghemite (γ-Fe_2O_3) NPs in water prepared first by reacting of Fe(II) ions with carboxyl-terminated G-4.5 PAMAM dendrimers followed by oxidative hydrolysis with $(CH_3)_3NO$ were studied as MRI contrast agents.[310] The NPs with a mean diameter of 8.5 nm were broadly distributed and prone to formation of aggregates, but the latter were stable in water, displayed superparamagnetic properties, and demonstrated a strong effect on T1 and T2 relaxation of solvent water protons, making them candidates as MRI contrast agents. However, this work with dendrimers was not continued, while the authors focused on other stabilizing agents.

Strongly aggregated NP/dendrimer composites based on dendrimers with a trimesyl core and Co NPs with mean diameters between 4.5 and 8.9 nm and broad NP size distribution showed superparamagnetic behavior and MRI enhancement effect.[276] We believe, however, that strong aggregation of NPs and moderate relaxivities (especially for aggregated NPs) with a low r^2/r^1 ratio make these materials not promising as MRI contrast agents.

Core−shell maghemite/melamine dendron (Simanek) NPs (their synthesis is described in section 2.3) were selectively dissolved in neutral water or various organic media depending on the terminal groups of the dendritic shells.[164] In the case of terminal phosphine groups, the composite NPs were employed as soluble matrices for supporting magnetically recoverable homogeneous Pd catalysts in organic solvents (Suzuki cross-coupling reactions). On the other hand, water-soluble NPs coated with three generations of melamine dendrons were studied as MRI contrast agents and demonstrated strong transverse relaxivities with generation-specific values; that is, these values depended on a distance between NPs. The authors considered these switchable NPs as effective platforms for fundamental studies of the relationships between a given NP property, the NP medium, and the observed MR behavior; however, to the best of our knowledge, no further papers have been published so far on this kind of NPs.

Dendrimers can be also used for the formation of well-defined 3D magnetic nanocomposites. As an example, cationic superparamagnetic iron oxide NPs were assembled with anionic PAMAM dendrimers of different generations into nanocomposites. These nanocomposites were characterized by a different

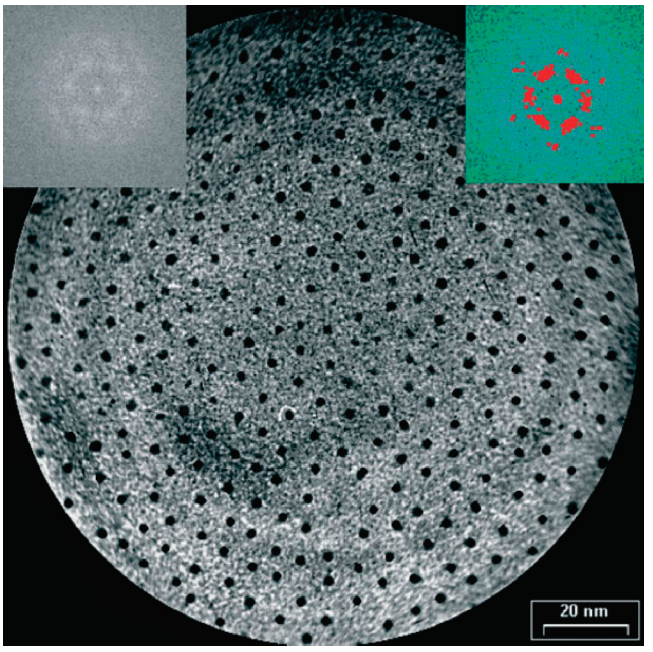

Figure 34. TEM microscopy image of dodecanthiol and G2 dendron-coated NPs drop-cast on a carbon-coated microgrid. The upper left inset is the FFT of the image. The upper right inset is the FFT after digital processing for better clarity. Reproduced with permission from ref 315. Copyright 2007 Wiley-VCH Verlag GmbH & Co. KGaA.

distance between NPs, which was consistent with a generation number (Figure 33).[311] The dendrimer-mediated assembly of magnetic particles was shown to directly alter their collective behavior. The dependence of blocking temperature on interparticle spacing was found to deviate from a theoretical model and to indicate a much more dramatic interdependence at close interparticle spacing, whith a weaker correlation at larger spacings. The authors established that a relatively modest increase in interparticle spacing leads to practically independent NPs within a dense assembly.

Magnetic Ni_{55} and Ni_{147} NPs were prepared in PAMAM dendrimers modified with dodecyl tails.[123] They were stable under air due to hydrophobicity of the dendrimers and organic media, as suggested by the authors. These DENs exhibited ferromagnetic behavior at a temperature below 200 K; however, it would be incorrect to call them ferromagnetic, because at room temperature they displayed superparamagnetic behavior. Superparamagnetic Fe NPs were prepared in a similar way, but they were unstable under air.[312] G5-OH PAMAM dendrimers were used for stabilization of 3 nm bimetallic NiAu NPs displaying superparamagnetic properties. Although NPs were prepared in water, they were destabilized by perchlorate used in the synthesis and needed to be extracted into toluene by decanethiol after the reduction step,[313] thus this method is not efficient.

The simple procedure for the aqueous synthesis of the 3.5 nm monodisperse CoPt NPs in the presence of G6-OH PAMAM has been described in ref 314. The as-made CoPt NPs had disordered fcc structure and were superparamagnetic. The NPs became ferromagnetic after annealing at elevated temperatures (up to 700 °C), but there was no proof that NP aggregation is prevented. After annealing, particles were not characterized.

Unique ferromagnetic mesomorphic materials consisting of nonmagnetic and nonmesomorphic components were reported

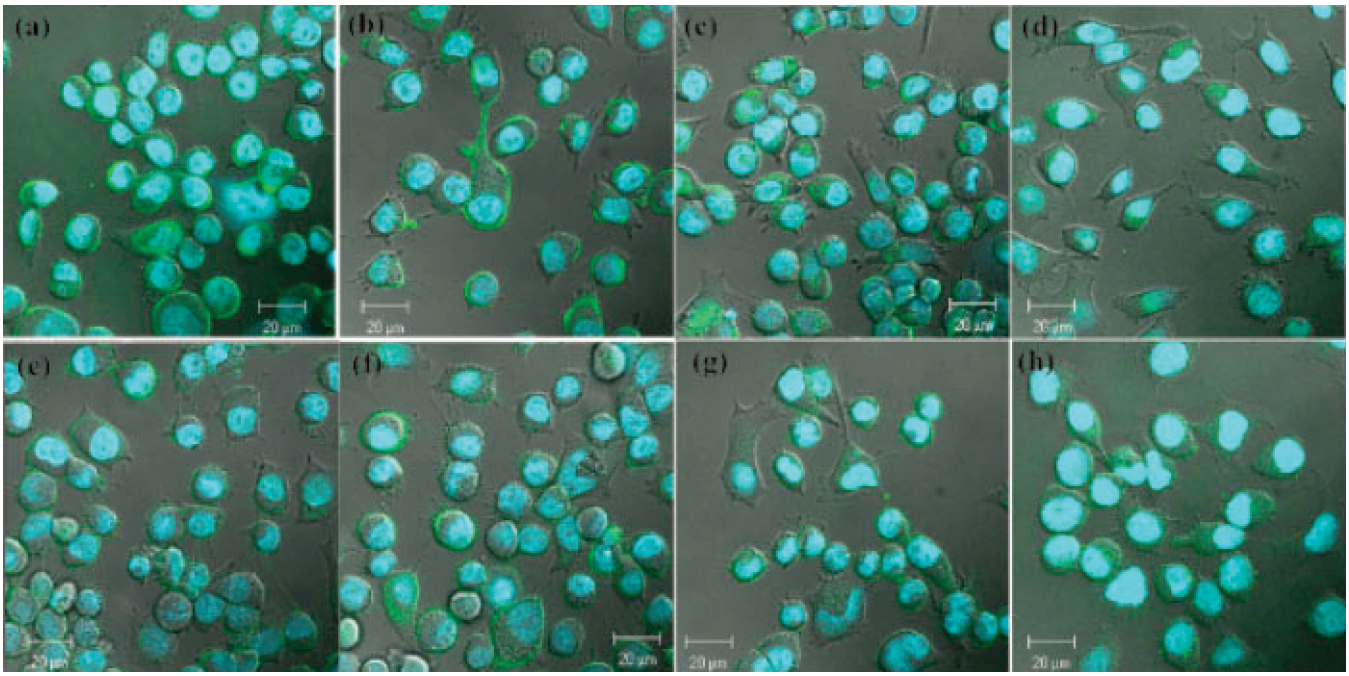

Figure 35. Laser confocal microscopy images of KB cells treated with the G5-NHAc-FI-FA dendrimers at 1 h (a), 2 h (b), 6 h (c), and 24 h (d) and KB cells treated with [(Au0)51.2-G5-NHAc-FI-FA] DSNs at 1 h (e), 2 h (f), 6 h (g), and 24 h (h). Reproduced with permission from ref 325. Copyright 2009 Wiley-VCH Verlag GmbH & Co. KGaA.

in ref 315. These materials were formed by self-assembling of 2.1 nm Au NPs, the protective shell of which consisted of both dodecanethiols and G2 dendrons containing long alkyl tails. Although the capping molecules were not mesomorphic, the NPs self-assembled either as a thermotropic cubic mesophase in bulk or as a 2D hexagonal lattice on surfaces (Figure 34). The system demonstrated ferromagnetic behavior between 1.8 and 400 K in bulk. It is proposed that well-defined organization in the material leads to organization of spins and thus collective magnetic properties, although, at present, the exact origin of these magnetic properties is still debated.

4.3. Imaging and Biomedical Properties

Recent studies demonstrated that dendrimers can be modified with targeting ligands, drugs, Gd(III) ions, or fluorescent molecules for targeted tumor imaging and therapeutics.[316−320] In this Review, however, we will discuss only the literature where inorganic NP/dendrimer (dendron) nanocomposites are employed.

Molecular imaging always requires accumulation of contrast agent in the target site, often achieved most efficiently by steering NPs containing contrast agent into the target.[321] If the NP itself can be a contrast agent due to producing a corresponding signal (fluorescent, magnetic, electronic), this signal will be especially strong due to concentration of atoms or molecules in a small NP volume, while the NP can easily penetrate cells or migrate into a tissue. NPs in the range 20−30 nm are easily taken up into cells via endocytotic vesicles, which are typically 40−60 nm in diameter. NPs larger than 150 nm will not enter the cells by endocytosis and will be at the upper limit for passage through caveolae; they will be phagocytosed by macrophages and therefore routed via the reticulo-endothelial system to lymph nodes and the spleen. This suggests that NPs for molecular imaging should be in a size range 20−150 nm.[321] In the majority of cases, the inorganic NP/dendrimer (dendron) nanocomposite particles measure 20−40 nm, thus being suitable for imaging or drug delivery applications.

For multimodal imaging and cancer therapy, dendrimers have been assembled onto magnetic iron oxide NPs for magnetic resonance imaging of tumors,[322−324] or used to encapsulate or to attach to Au NPs for subsequent cancer cell targeting and imaging.[75,325−327] The CdSe/ZnS QDs stabilized by ester-terminated PAMAM dendrimers in the presence of poloxamer 188 (only 0.1%) (see section 2.2)[84] were able to penetrate HeLa cells and were found in the cytoplasm, indicating that these bioprobes can be useful for tracking cells and intracellular processes.

One of the first papers devoted to imaging in vitro and in vivo using nanocomposites based on PAMAM dendrimers and Au NPs (5−25 nm) was published in 2002.[327] Because of high electron contrast of Au NPs, the authors used TEM to observe the internalization of pDNA/dendrimer complexes. Positively charged gold/PAMAM nanocomposites used as DNA carriers were capable of gene transfection to cancer cells with efficiencies similar to that of their host dendrimer.

In ref 75, the authors demonstrated that nanocomposites based on Au NPs and G5-NH_2 PAMAM dendrimers can be covalently linked with folic acid (FA) and fluorescein isothiocyanate (FI) through reaction with the PAMAM terminal amines. Such functionalized nanocomposites are stable, biocompatible, and can be used for specific targeting and imaging of cancer cells. In vitro studies showed that the FA- and FI-modified nanocomposite particles can specifically bind to KB cells (a human epithelial carcinoma cell line) that overexpress high-affinity folate receptors, and they are mainly internalized into lysosomes of target cells within 2 h. As was verified by confocal microscopy studies (Figure 35), no difference in specific internalization into cancer cell was observed for both dendrimers with and without Au NP.[325] The authors believe that the above nanocomposites may serve as a general platform for cancer

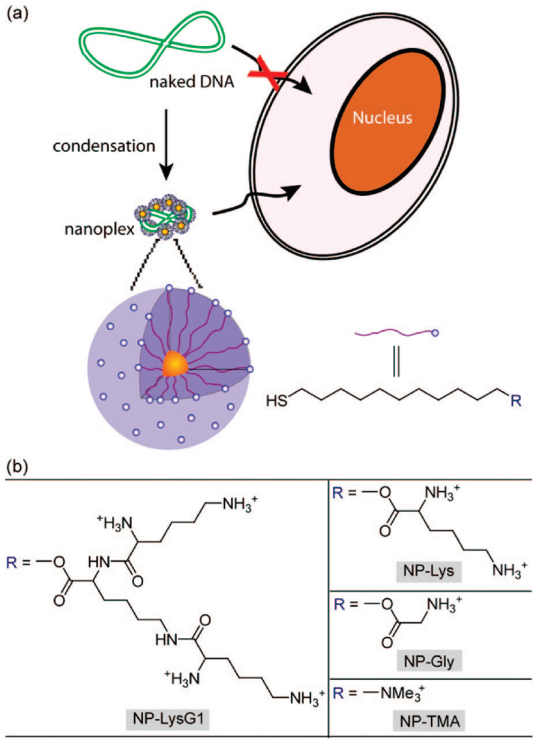

Figure 36. (a) Schematic illustration of the monolayer protected gold nanoparticles used as transfection vectors in this study; (b) chemical structures of headgroups presented on the surface of the nanoparticles. Reprinted with permission from ref 330. Copyright 2008 American Chemical Society.

imaging and therapeutics. In the later paper from the same group, the Au/PAMAM nanocomposites functionalized with FI and Arg-Gly-Asp (RGD) peptide were studied by in vitro targeting efficacy to integrin receptor expressing cells using flow cytometry, confocal microscopy, and ICP-MS.[328] The authors demonstrated the specific activity of these bioprobes toward binding to integrin receptor expressing cells, while the cells without this receptor did not bind to the bioprobes.

A completely different approach was used in ref 329 where plasmid DNA was tethered to Au NPs with a diameter of about 100 nm via cationic polylysine dendrimers and then the behavior of such complexes was studied in a cell culture medium. The authors observed flocculation of the carrier (which is not surprising for such large particles) and decreased release of surface tethered DNA as compared to water. The authors emphasized that this decreased detachment of DNA along with the carrier flocculation should inhibit endocytosis, thus making internalization impossible. This study also accentuated the importance of using biologically relevant liquids for in vitro studies before carrying them out in vivo.

Efficient gene delivery vectors have been designed using ligand exchange reaction on the surface of Au NPs for lysine dendron functionality.[330] These composite NPs formed particularly compact complexes with DNA and afforded highly efficient gene delivery without any observed cytotoxicity (Figure 36). NPs based on the first generation lysine dendrons were 28-fold more efficient in reporter gene expression compared to polylysine. These NP complexes were also responsive to intracellular glutathione levels, providing an instrument for controlled release and expression of DNA.

The partial thiolation of G4 PAMAM dendrimers made them good ligands for CdSe/ZnSe NPs, allowing replacement of

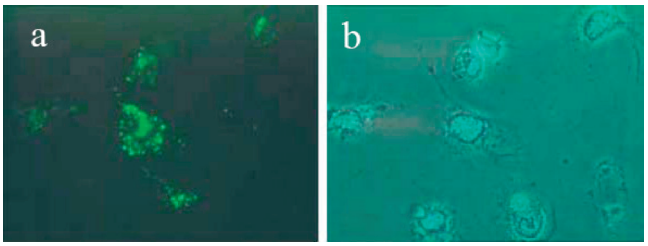

Figure 37. Confocal fluorescence (a) and visible (b) images of live NT2 cells incubated with dendrimer-coated CdSe/ZnSe nanoparticles. Reproduced with permission from ref 83. Copyright 2006 Royal Society of Chemistry.

TOPO ligands on the NP surface.[83] Dendrimer-protected NPs showed high stability in solution and good, stable fluorescence properties. The authors demonstrated that these composite NPs easily penetrate cancer cells (teratocarcinoma NT2) in a buffer solution and can transport other molecules (for example, S100A4 protein) across the cell wall and thus can be considered as promising fluorescent transfection agents (Figure 37).

In a similar fashion, TOPO molecules on the surface of prefabricated CdSe/ZnS NPs were first replaced by pyridine; the latter was further substituted by triantennary, galactoside-capped gallamide dendritic anchor with thiolate focal group, synthesized using click chemistry (Figure 38).[331] This nanohybrid became water-soluble with intact morphology of the NP core. The nanohybrid could be easily delivered inside HeLa, kidney, and metastatic lung cancer cells with differential rates as was confirmed by confocal microscopy. The transmembrane efficiency increased with increasing density profile of asialoprotein receptors on cellular surface, revealing a receptor-mediated endocytosis. It was also demonstrated that cancer cells that are undergoing active mitosis also tended to efficiently uptake the nanohybrids and remained sustainable in serum-containing medium for several days.

Dendrimer encapsulated Ag and Au nanoparticles are widely used for photothermal therapy of cancer.[332,333] The technique is based on irradiation in visible, far-red, and near-IR region of plasmon-band-containing NPs that convert absorbed light to thermal energy, destroying cells. Usually targeting is required to be specific for cancer cells, although studies on nontargeted composite NPs were also reported. Au NPs of 2 nm in diameter encapsulated by G4 PAMAM dendrimers with PEG grafts at all chain ends demonstrated the heat-generating ability comparable to that of widely used Au NPs with ca. 11 nm diameter under visible light irradiation (Figure 39).[334] Recently, the same group carried out a study to enhance photothermal properties of the Au NP-incorporated PEG-attached dendrimers by step-by-step growing of larger Au NPs in the same dendrimers.[199] The photoinduced-heat generation capability of the Au DENs increased as the Au NPs grew. These dendrimers with Au NPs exhibited strong cytotoxicity against HeLa cells under visible light irradiation. The authors claimed that the observed excellent colloidal stability, high heat-generating ability, and their biocompatible surface validate a potential for the PEG-modified dendrimers encapsulating Au NPs as a promising tool for photothermal therapy and imaging. We believe, however, that necessity to use visible light limits this application to surface cancers because visible light cannot penetrate tissue. Recently, it was demonstrated that "smart" aggregation of Au NPs induced by a pH change after NPs entered cells shifts the absorption to

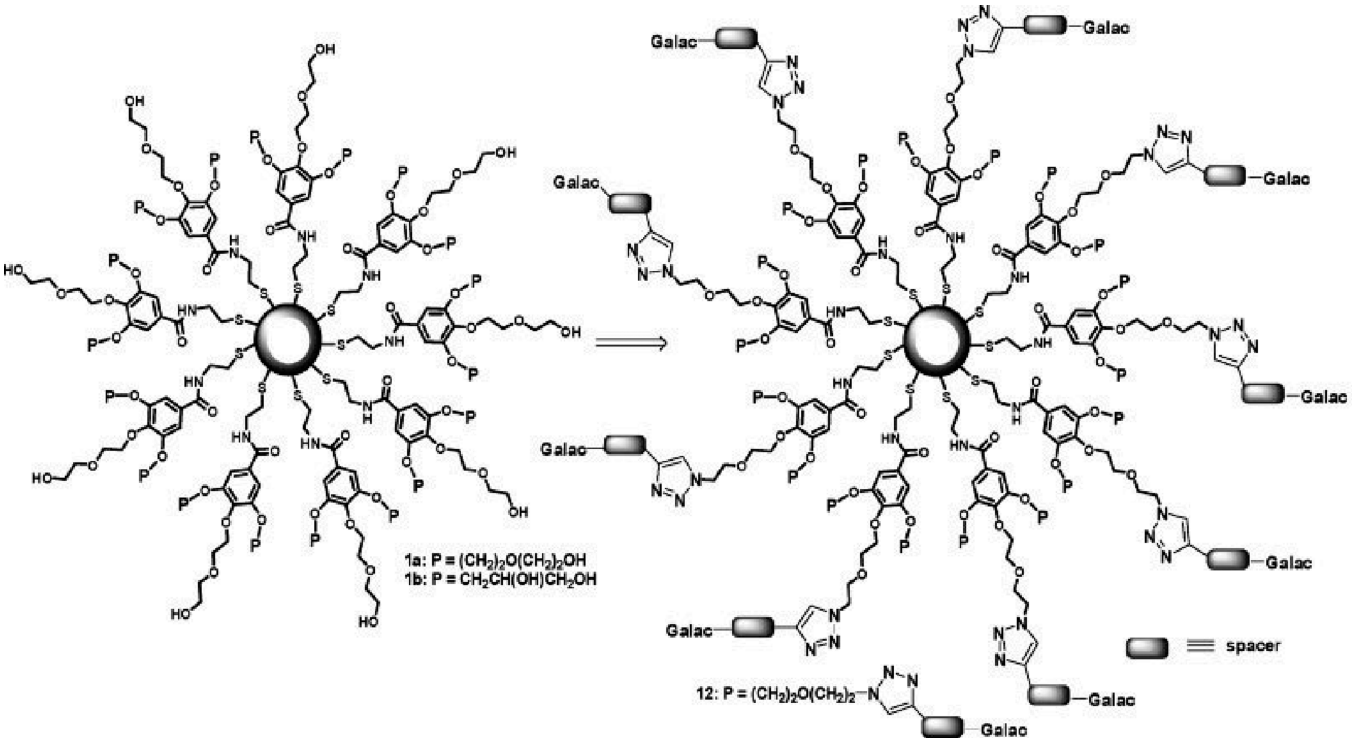

Figure 38. Synthetic design of triantennary galactoside-capped nanohybrid from the gallamide-tethered tripodal nanohybrid **1a**. Reproduced with permission from ref 331. Copyright 2008 Wiley-VCH Verlag GmbH & Co. KGaA.

far-red and near-IR, thus allowing using far-red and near-IR light penetrating the tissue.[335] Similarly, gold nanorods coated with dendrimers can be used for the same purpose with near-IR laser irradiation.[336]

Au NPs can be a potential X-ray computed tomography (CT) contrast agent. In ref 337, Au NPs were stabilized by the PEG-attached dendrimers to provide biocompatibility and tested as CT contrast agents. Because enhancement of X-ray attenuation is crucial for the in vivo application, it was achieved by the growth of the Au NP in the PEGylated dendrimer using a seeding procedure. The contrast sensitivity of these Au NPs in CT was measured, and the in vivo imaging was carried out by using the Au NP-encapsulated PEGylated dendrimer in comparison with a commercial contrast agent, iopamidol. Both contrast agents were injected into mice, and CT images were obtained at different times. The Au NP-loaded PEGylated dendrimer achieved blood pool imaging, which was greater than that for a commercial agent. Even though iopamidol was excreted rapidly, the PEGylated dendrimer carrying the grown Au NP was accumulated in the liver (Figure 40). Because of phototoxicity of these Au NPs, they can serve as a potential CT contrast agent with photothermal properties.

The dependence of cellular transfection on the NP surface characteristics was demonstrated in ref 281. In this work, amine- and ester-terminated PAMAM dendrimers were used to functionalize hybrid fluorescein-doped magnetic mesoporous silica NPs to evaluate the effect of surface functionality on cellular uptake by glioma cells using fluorescence. The results demonstrated that both NP samples with terminal amine and methyl acrylate functionalities showed no severe cytotoxicity and could easily be internalized into 9 L glioma cells, although transfection was faster and more efficient for PAMAM-NH_2. Moreover, FI was

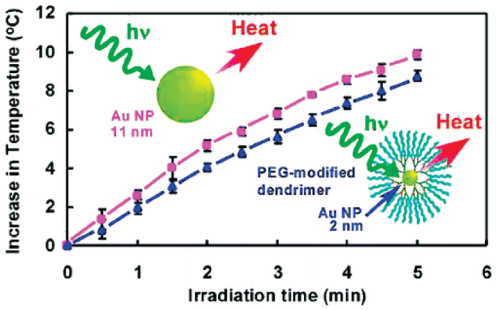

Figure 39. Schematic representation of photothermal action of PAMAM encapsulated 2 nm Au NPs. Reprinted with permission from ref 334. Copyright 2007 American Chemical Society.

also used as a model drug to evaluate the drug release rates of these drug delivery systems. However, similar to many earlier works, magnetic properties of these NPs were not explored.

Magnetic NPs receive increased attention due to their use as MRI contrast agents and magnetic bioprobes for tracking various delivery vehicles (see section 4.3). For example, in ref 338, magnetite NPs synthesized by standard precipitation at high pH and modified with aminosilane have been used for growth of PAMAM dendrons from the NP surface. These NCDs demonstrated an increased ability to absorb streptavidin, serving as targeting molecules for biotin. Moreover, the higher is the dendron generation, the higher is the amount of the streptavidin absorbed. The amount of biotin specifically binding to streptavidin, however, first increased upon the increase of a generation number from G0 to G3 and then decreased. The authors concluded that this effect can be assigned to steric hindrances in large dendrons. However, considering the very broad size distribution of magnetite NPs, the

dx.doi.org/10.1021/cr2000724 |*Chem. Rev.* 2011, 111, 5301–5344

conclusions on the influence of a dendron size seem to be unreliable. It is also surprising that magnetic properties of NPs with dendrons of different generations were not explored. The same NPs have been used to study absorption of bovine serum albumin (BSA).[339] The authors demonstrated that dendron-coated NPs absorb BSA better than those with only aminosilane coating. It was also determined that the interaction with BSA depends on the NP surface group and pH.[340] In a more recent paper from the same group, 8 nm NPs modified with PAMAM dendrons were mixed with antisense surviving oligodeoxynucleotide.[341] The composites based on G5 dendrons exhibited the highest efficiency for cellular transfection and inhibition of the cancer cell growth, while the NPs coated solely with dendrons did not behave the same way. Surprisingly, however, magnetic properties of NPs were not explored in this series of papers.

Superparamagnetic Fe_3O_4 NPs prepared by standard coprecipitation in aqueous solutions and modified with G3-COOH PAMAM due to electrostatic assembly were conjugated with FA molecules in an attempt to achieve specific targeted imaging of tumor cells that overexpress FA receptors using dendrimer-stabilized Fe_3O_4 NPs.[322] The intracellular uptake of dendrimer-stabilized Fe_3O_4 NPs was tested in vitro using KB cells that overexpress FA receptors. The authors believed that carboxyl-terminated PAMAM dendrimer stabilized Fe_3O_4 NPs could be taken up by KB cells regardless of the repelling force between the negatively charged cells and the negatively charged particles. However, an excess of carboxylic groups prevented specificity of binding. In the following work, positively charged Fe_3O_4 NPs were created using a bilayer composed of poly(sodium 4-styrenesulfonate) (PSS) and FA- and FI-functionalized G5 PAMAM dendrimers (G5·NH_2-FI-FA) through electrostatic LbL assembly, followed by an acetylation reaction to neutralize the remaining surface amine groups of G5 dendrimers.[324] Flow cytometry, confocal microscopy, TEM, and MR imaging studies verified that Fe_3O_4/PSS/G5·NHAc-FI-FA NPs specifically bind to cancer cells overexpressing FA receptors (FAR). The NPs lacking the surface FA moieties did not exhibit binding to the cancer cells, suggesting that the binding was mediated by the FAR. For in vivo applications, the authors[323] increased the shell stability using a thicker shell formed by five LbL assembly of oppositely charged polymers followed by the deposition of G5·NH2-FI-FA in the outer layer and the shell cross-linking. The fabricated NPs were water-soluble, stable, and biocompatible. MRI studies showed that these NPs can specifically target tumor cells that overexpress FAR and a FAR-expressing tumor model with a volume as small as 0.60 ± 0.15 cm^3, respectively, both in vitro and in vivo (Figure 41). This approach can be used for the detection of various biological systems using MRI.

Normally iron oxide NPs prepared by low temperature procedures are quite polydisperse and prone to aggregation. This was overcome by using well-defined magnetite NPs prepared by a high-temperature organometallic route.[342] These NPs were transferred from organic medium to water using G5 PAMAM dendrimers functionalized with ~102 acetamide groups and modified with 6-TAMRA fluorescent dye and FA molecules (DC-SPIONs). The simultaneous control by confocal microscopy (registration of fluorescence) and X-ray fluorescence (registration of Fe content) allowed the authors to demonstrate and quantify that dendrimer-coated NPs were successfully internalized into KB cancer cells in vitro (Figure 42). The dendrimer-coated magnetite NPs exhibited exceptional stability versus aggregation in water. After drying, they could be easily resuspended in water and could thus be stored in lyophilized form and dispersed as needed.

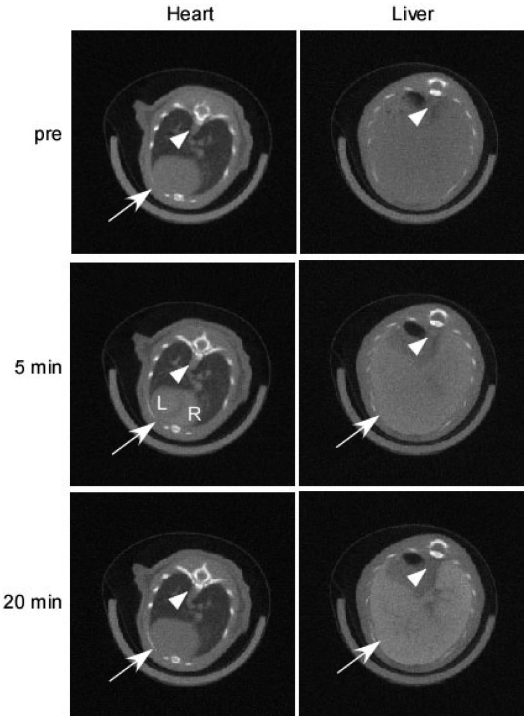

Figure 40. In vivo imaging of mice injected with the Au NP-loaded dendrimer before and after 5 and 20 min. Arrows indicate heart or liver, and arrowheads indicate aorta. Reprinted with permission from ref 337. Copyright 2010 IOP Science.

Superparamagnetic iron oxide NPs have been shown to be efficient MRI contrast agents (see section 4.3), but to furnish high sensitivity in MRI, the cells should be labeled with high amounts of NPs. This can be challenging for nonphagocytic cancer cells. This challenge was overcome in the work[287] where iron oxide NPs were coated with novel cell-penetrating polyester dendron with peripheral guanidines via Click reaction of azide functionalized NPs and alkyne-modified dendrons. In GL261 mouse glioma cells, the dendritic guanidine-coated NPs provided significantly enhanced uptake in comparison with NPs having no dendrons or dendrons with hydroxyl or amine peripheries. Although it was found that the NPs functionalized with dendritic guanidines exhibit rather greater toxicity than those functionalized with dendrons containing hydroxyl or amine terminal groups, they were still relatively nontoxic at the low concentrations required for labeling. The authors believed this work represented the first successful example of the transport of a biologically relevant NP cargo by a dendritic guanidine transporter, which realized the promise of providing improved labeling of cells with such NPs for improved sensitivity in cellular MRI.

It is noteworthy that the future use of various NP/dendrimer composites in biomedical applications strongly depends on the toxicity of these materials, which are determined by both NP and dendrimer toxicity. If the latter should be considered on the case-by-case basis, the NP toxicity is more commonly studied. To date, it is well established that iron oxide NPs are mostly benign because they are easily degraded in vivo, while Au NP toxicity is size dependent.[343,344] For example, 1.4 nm Au NPs were found to cause cell death, while 3.7 nm NPs were benign, although they penetrated the

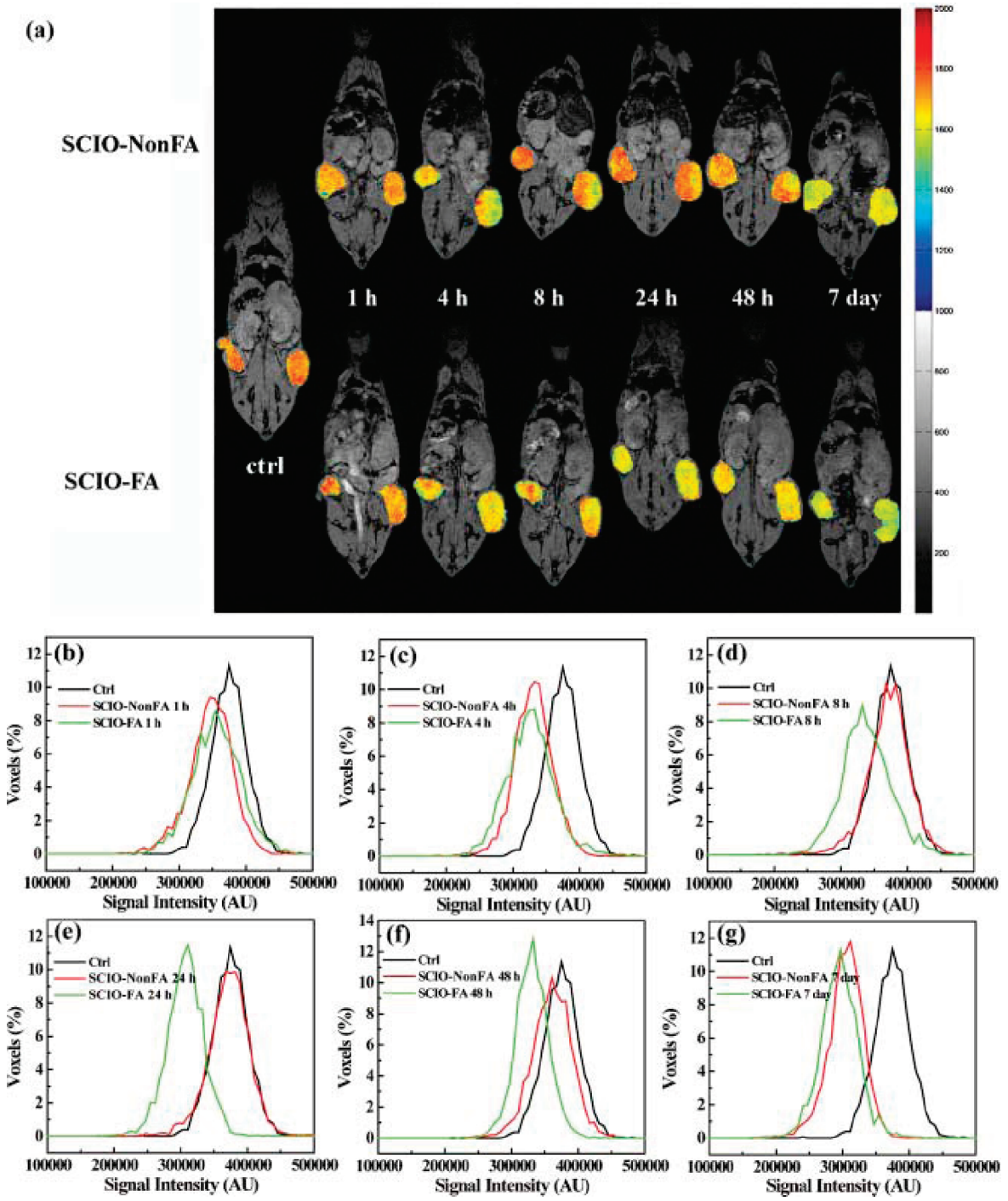

Figure 41. In vivo MR imaging of tumor. In vivo color maps (a) of T2-weighted MR images of mice implanted with cancer cell line KB cells, at different time points after injection of SCIO-NonFA and SCIO-FA NPs, respectively. (SCIO stands for shell-cross-linked iron oxide.) The color bar (from red to blue) indicates the MR signal intensity changes from high to low. Comparison of statistically normalized histograms of the voxel intensities (whole tumor) from targeted SCIO-FA (green histogram) and nontargeted SCIO-NonFA (red histogram) NPs at the time points of 1 h (b), 4 h (c), 8 h (d), 24 h (e), 48 h (f), and 7 days (g). Reproduced with permission from ref 323.Copyright 2008 Wiley-VCH Verlag GmbH & Co. KGaA.

nucleus of cells.[345,346] As for QDs, the data on their toxicity are controversial.[344] Many authors believe that when the NPs are stable and clearance from the body is efficient, the toxicity is minimal, while others think that, due to small sizes, all QDs are toxic.[344,347] Because of this controversy, one needs to be careful when in vivo applications of QDs are concerned.

4.4. Sensing Properties

Generally, sensing properties of NP/dendrimer (dendron) nanocomposites are based on the change of an optical or electrical response when an analyte is adsorbed on the composite NP. The major advantage of dendrimer-based nanocomposites as sensors is control over nanoparticle formation and rich chemistry of functional groups.

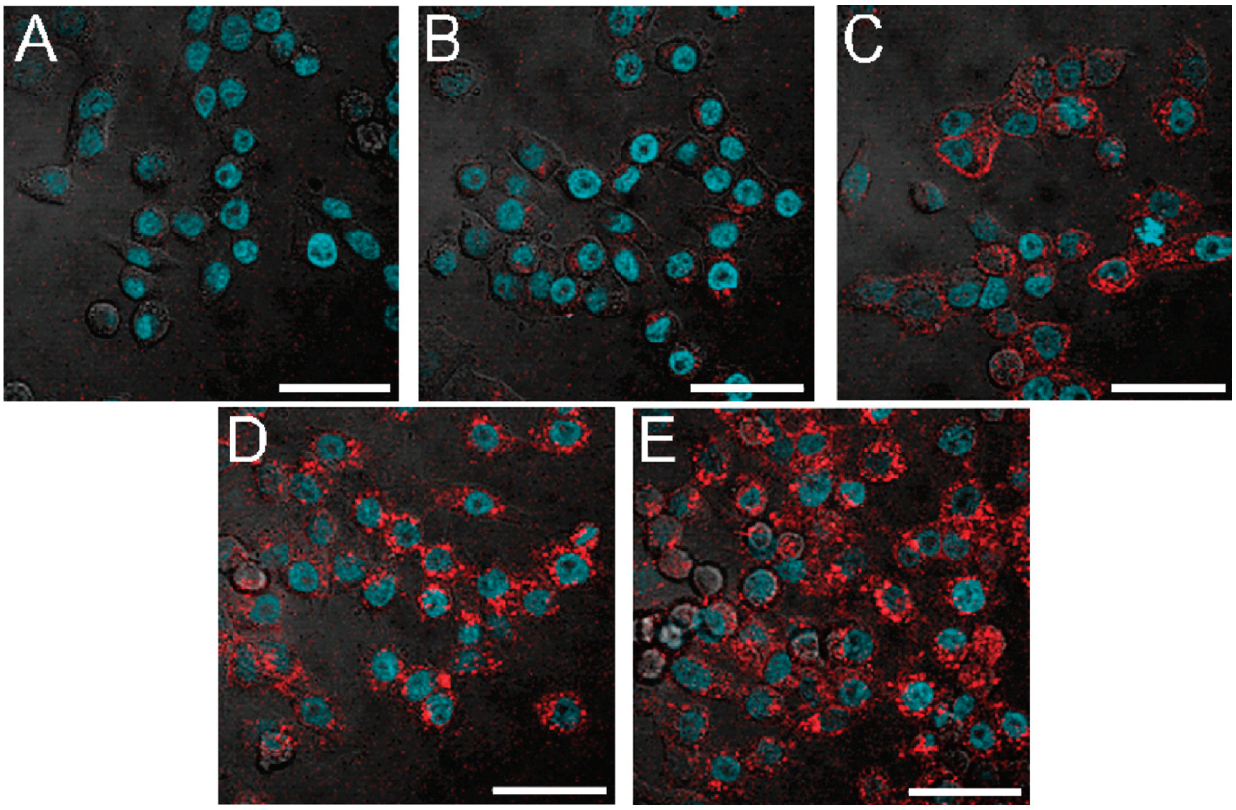

Figure 42. Confocal microscopy images of five experimental conditions demonstrating internalization of DC-SPIONs; scale bars are 40 μm. The slices shown are all from the center of the cells (4 μm from bottom of ~8 μm tall cells). All images are for KB cells after 1 h incubation at 37 °C. Nuclei are visible in blue due to DAPI staining; red fluorescence comes from the 6-TAMRA dye conjugated to neat dendrimers and dendrimers on the surface of DC-SPIONs. The phosphate buffered saline control for KB-FAR+ (A) shows only background fluorescence, and the KB-FAR+ blocked sample (B) exhibits a signal just slightly above this background. Whereas the signal for neat G5-Ac(102)-FA(5)-6T(3) with KB-FAR+ (C) is largely concentrated on the cell exteriors, the fluorescence for 50 nM (D) and 100 nM (E) DC-SPIONs is clearly intracellular and appears in clusters, correlating well with the XRF microscopy data for iron. Reprinted with permission from ref 342. Copyright 2008 American Chemical Society.

For the first time, Au NPs functionalized with dendrons containing redox-active ferrocenyl groups (amidoferrocenyl or silylferrocenyl) were developed in 2001 by Astruc's group.[348] These NPs selectively recognized the $H_2PO_4^-$ and adenosine-5′-triphosphate (ATP^{2-}) anions and could be used to titrate these anions even in the presence of other anions such as Cl^- and HSO_4^- due to the shift of the CV wave.[145] The authors believed that recognition took place due to a positive dendritic effect; that is, the shift of the ferrocenyl redox potential, when anions were introduced, increased with the increase of the dendron generation. Attachment of dendrons to the gold core resulted in clusterization of a large number of peripheral ferrocenyl groups, which, in turn, led to the formation of narrow channels that facilitated the appearance of microcavities at the dendritic surface for a tighter supramolecular interaction with the anion. The advantage of silylferrocenyl system over the amidoferrocenyl one was in fully reversible oxidation, and thus electrodes modified with dendronized NPs could be used multiple times after a simple rinsing with methylene chloride. Redox-active gold NCDs were also synthesized by another group[152] via formation of dendrons with terminal ferrocenyl groups on the Au NP surface; however, this work rather resembled a series of works from Astruc's group.

Vapor-sensitive thin films prepared by LbL self-assembly of Au NPs and PAMAM and PPI dendrimers with terminal aminogroups or polyphenylene (PPh) dendrimers with disulfide groups demonstrated selective sorption of analyte molecules such as toluene, 1-propanol, and water. The film response was estimated as a film resistance. The chemical selectivity of this response was controlled by the solubility properties of the dendrimers used.[349−351] For example, with a decrease of hydrophobicity (PPh > PPI > PAMAM), the sensitivity to toluene vapor decreased, while the relative response to 1-propanol and water vapor increased. Using PPI dendrimers, the same authors discovered that with increasing the dendrimer generation, the film resistivity increased exponentially, indicating that the dendrimer size controls separation between neighboring NPs and thus the tunneling for charge transport.[352] This behavior was explained by the different sorption sites in dendrimers for the different analytes used.

An ultrasensitive method for detecting and quantifying a biomarker has been developed by the authors of ref 353 using Au NPs stabilized by IgG (immunoglobulin) and dendrimers with terminal ferrocenyl groups without using DNA or enzymatic amplification (Figure 43). The ultrasensitive detection was achieved by signal amplification combined with noise reduction. The signal was amplified both by the catalytic reduction of *p*-nitrophenol by Au NP catalyst labels and by the chemical reduction of *p*-quinoimine by $NaBH_4$. The noise was reduced by employing an ITO electrode modified with a ferrocenyl-tethered dendrimer and a hydrophilic immunosensing layer. This immunosensing test allowed detection in a wide range of concentrations that makes it appealing for practical applications.

dx.doi.org/10.1021/cr2000724 |*Chem. Rev.* 2011, 111, 5301–5344

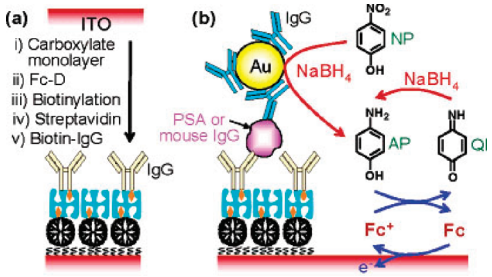

Figure 43. (a) Schematic representation of the preparation of an immunosensing layer. (b) Schematic view of electrochemical detection of mouse IgG or PSA (prostate specific antigen). Reprinted with permission from ref 353. Copyright 2006 American Chemical Society.

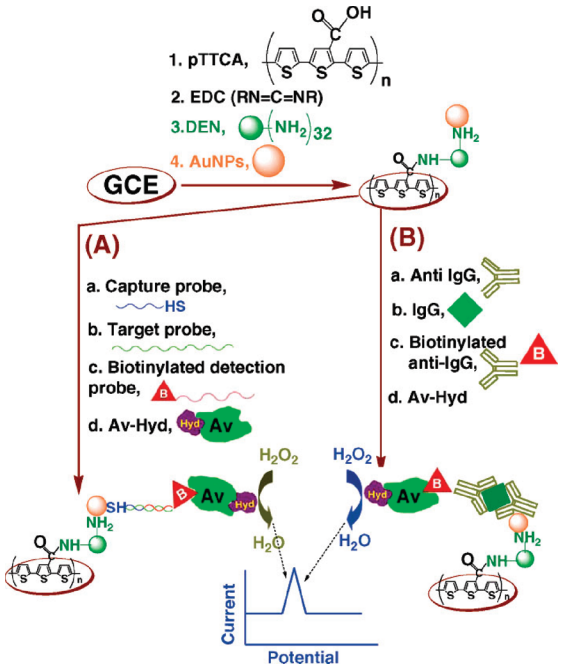

Figure 44. Schematic diagram of the pTTCA/DSN/AuNP/biomolecules-linked avidin−hydrazine assembly for (A) DNA and (B) protein sensors, which are based on the electrocatalytic activity of hydrazine. Reprinted with permission from ref 355. Copyright 2007 American Chemical Society.

Later, the same group reported highly sensitive DNA sensor based on Au NPs, magnetic granules, and similarly modified ITO electrodes.[354] Significant signal amplification and low background current allowed one to achieve a low DNA detection limit of 1 fM.

Another simple method of the signal amplification was developed for DNA and protein detection using two processes: (i) electrocatalytic reduction of hydrogen peroxide to water using the derivative of avidin and hydrazine and (ii) ensemble of conducting polymer, poly-5,2′,5′,2″-terthyophene-3′-carbonic acid (pTTCA), and PAMAM dendrimer with Au NPs, where the analyte molecules (DNA and proteins) were adsorbed (Figure 44).[355] This method allowed detection of DNA and proteins up to 450 aM (2700 DNA molecules per 10 μL of the sample) and 4 fg/mL, respectively. The simplicity of the constructing, easy detection, high sensitivity, and good reproducibility

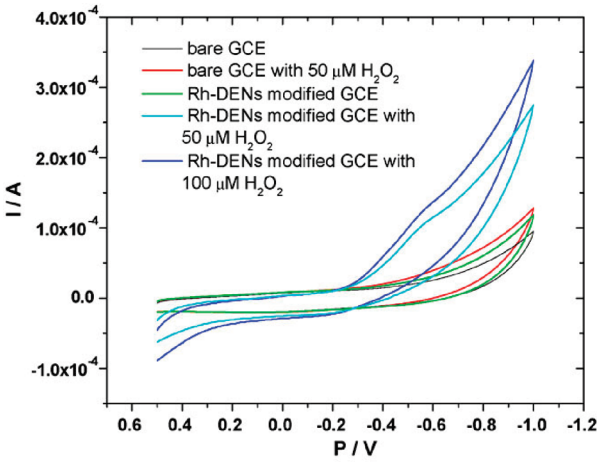

Figure 45. Cyclic voltammograms (CVs) of the different electrodes recorded in phosphate buffer pH 7.0 with a scan rate of 50 mV s^{-1}. Reprinted with permission from ref 358. Copyright 2009 Elsevier.

make this method promising for fabrication of practical devices for diagnostics of infections, identification of genetic mutations, and solving forensics problems. In later work from the same authors, the detection ability of the similar systems was further improved.[356]

In ref 357, dendrimer-encapsulated silver NPs were reported as a promising novel electrochemical label for sensitive immunosensors. Silver/dendrimer nanocomposites were synthesized from G5-G7 hydroxyl-terminated ethylenediamine-core-type PAMAM dendrimers. The G7 Ag/dendrimer nanocomposite synthesized in 2000 M excess of silver (1/4 ratio of tertiary amine/Ag^+) was found to be the most suitable candidate for the label development. The authors believed that the potential advantages of the proposed electrochemical label were (i) long-term stability due to dendrimer-assisted stabilization of NPs, (ii) well-defined functional groups for conjugation, (iii) a narrow NP size distribution, and (iv) a possibility of multiplex assays by using multiple metal NPs or alloy NPs. However, no real measurements of sensing activity have been carried out.

Sensors for hydrogen peroxide detection have been developed from 2 nm rhodium NPs, stabilized by a dendrimer, based on *N,N*-bis-succinimide.[358] The authors immobilized the nanocomposite Rh/dendrimer particles on GCE and studied their electrocatalytic activity toward hydrogen peroxide. Dependence of a cathode current in stationary conditions at −0.3 V was linear toward hydrogen peroxide concentration in the range 8−30 μM with a low detection limit, which allows one to use this nanocomposite as a sensor (Figure 45).

Glucose biosensors play an important role for measuring blood glucose levels especially because type II diabetes is becoming a plague of the 21st century. Despite numerous existing methods and devices, novel glucose biosensors with improved sensitivity toward glucose are being developed to satisfy the growing demand. In this vein, MWCNTs with grafted PAMAM dendrimers containing encapsulated Pt NPs have been used for fabricating modified enzyme electrodes for glucose biosensor applications.[201] This was possible due to electric contact between NPs, nanotubes, and an electrode. The response time and detection limit of this biosensor was determined to be 5 s and 2.5 mM, respectively. Analogous nanocomposite but with added protonated polyaniline (PANI) on the MWCNT surface allowed significant improvement of the glucose detection limit

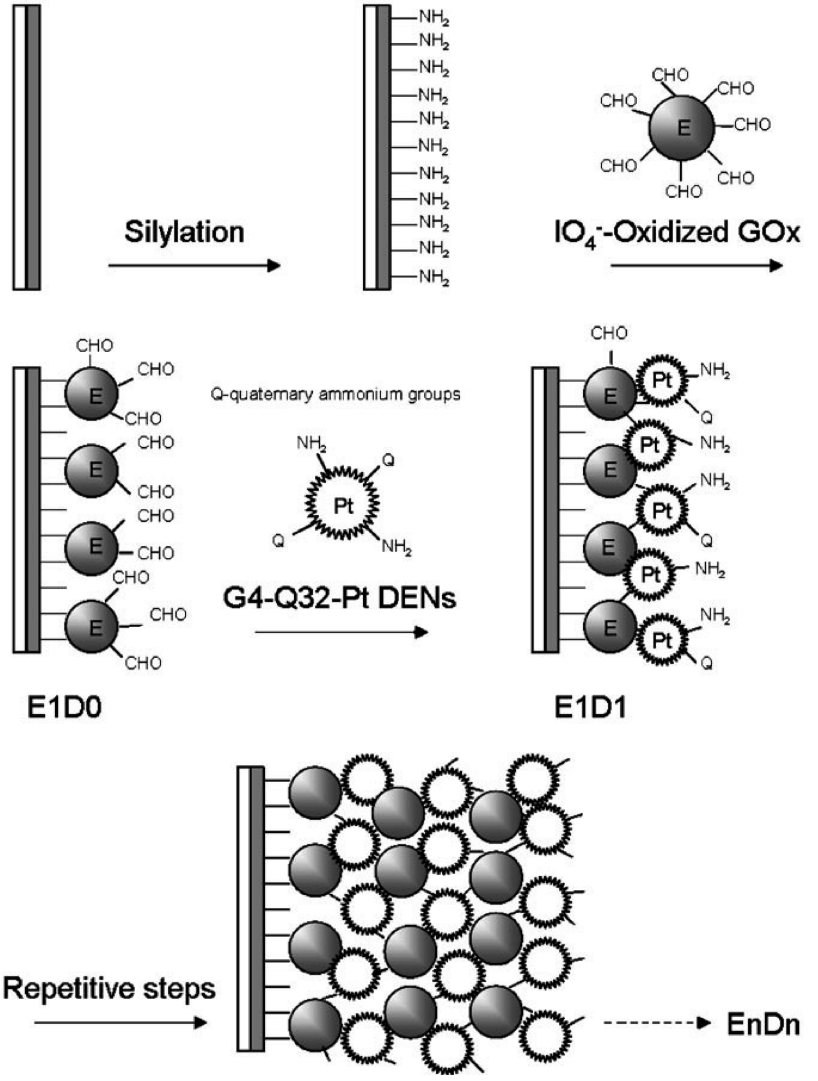

Figure 46. Schematic representation of the multilayered Pt-DENs/GOx network construction on the electrode using LbL approach. Reproduced with permission from ref 359. Copyright 2007 Wiley-VCH Verlag GmbH & Co. KGaA.

up to 0.5 μM.[203] In subsequent work, the same authors, however, abandoned carbon nanotubes and used a simple approach including direct LbL deposition of Pt NP-PAMAM and glucose oxidase (GOx) on Pt electrodes, also leading to significant enhancement of the glucose detection (Figure 46).[359] Besides, nanofibrous polyaniline[360] and titanium dioxide nanotubes (TNTs)[202] have been used as electrodes for deposition of Pt NP-PAMAM and glucose oxidase; however, our comparison of the data described in refs 202,359,360 does not show any advantage of the later systems.

Much lower glucose detection limit of 0.05 μM was reported for the hybrid nanocomposites synthesized under ultrasound irradiation resulting in 4 nm Au NPs stabilized by carboxyl-terminated G4 PAMAM dendrimers.[73] The authors believed that the high sensitivity, wide linear range, good reproducibility, and stability made this biosensor a promising candidate for a portable amperometric glucose biosensor.

A new approach was described to produce nanostructured electrocatalytic membranes via a combination of three methods. Using the LbL technique, PAMAM dendrimers with cobalt hexacyanoferrate-modified gold nanoparticles were alternated with poly(vinylsulfonic acid) layers on ITO electrodes.[185] This LbL film was used as substrate for immobilization of glucose oxidase in the presence of bovine serum albumin and glutaraldehyde as cross-linker. The modified electrode was successfully applied as a biosensor for the amperometric measurement of glucose, using glucose oxidase enzyme, at 0.0 V vs SCE (reference electrode).[184] This applied potential allowed minimization of interference effects when the biosensor is used in real and complex systems, such as biological media, food, and beverages. The authors believed that this new approach is promising for the construction of enzyme biosensors.

The complex nanohybrids (nanotubes) were formed by self-assembling of dendrons modified with long peripheral hydrocarbon chains and a pyrene molecule in the focal point and β-CD containing C6 hydrophobic tails.[361] These constructs and their assemblies with Au NPs formed by electrostatic interactions between the specific surface functionality of the tube and the precursors of Au NPs were suggested for sensing applications.[362] The placement of pyrene in the dendron focal point allowed one to use fluorescent properties for detecting biotin−avidin interactions (Figure 47).

dx.doi.org/10.1021/cr2000724 |*Chem. Rev.* 2011, 111, 5301–5344

Electrochemical behavior of laccase (copper-containing oxidaze enzyme) on Au NPs encapsulated in G3 PAMAM dendrimer was used to detect catechin.[363] To develop a sensor, the PAMAM/NP nanocomposite was attached to the electrode surface, modified with a terthiophene derivative, and then the enzyme was attached to a dendrimer. The catechin biosensor could be used in a wide range of concentrations (0.1−10 μM), had a low detection limit (0.05 ± 0.003 μM), and had a short response time (less than 10 s).

In other work, G2-OH PAMAM dendrimers were used for the formation of Au NPs, electrostatically conjugated to goat-derived antihuman IgG to be used as a human IgG sensor in solution over a broad range of concentrations.[364] The authors call these Au NPs QDs because they observed luminescence. However, it was well established that only gold nanoclusters with diameters ≤1 nm are luminescent, while in this work the NPs formed are much larger and broadly distributed. The authors believed that they observed Au NP/PAMAM conjugate and that is why it appeared larger; however, PAMAM is electron transparent and cannot be detected on TEM images. As for luminescence, it is possible that it was provided by a fraction of very small Au NPs which went undetected. The authors observed quenching of luminescence upon human IgG addition with no interference from BSA or β-casein, but a similar effect was found in the case of rabbit IgG, and thus no selectivity between these two was observed.

Recently,[365] a sensor to analyze insulin in human serum samples was developed on the basis of bifunctional hydroxyl/thiol-functionalized G4-PAMAM-encapsulated Au NPs. A NP/dendrimer composite was immobilized on a mixed self-assembled monolayer (SAM)-modified gold surface (Figure 48). This modified surface was resistant to nonspecific adsorption of proteins. Part of the dendrimer thiol groups were converted to hydrazide functionalities, providing further immobilization of receptors for immunoaffinity reaction. The surface plasmon resonance (SPR) detection of insulin was obtained by means of a competitive immunoassay principle. The resulting Au NP-dendrimer-surface sensor provided an assay with high stability, significantly enhanced sensitivity, and a detection limit for analyzing insulin of 0.5 pM. The results showed good correlation to the reference method. The authors suggested that the specificity and the improved sensitivity of this biosensing platform could have significant implications for the detection of a wide range of molecules and biomarkers in complex biological media.

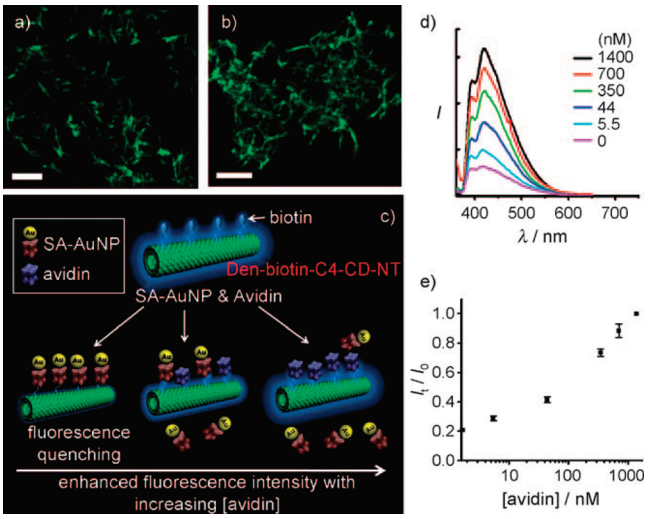

Figure 47. Detection of proteins using fluorescent Den-CD-NT templates. (a) SA-FITC/Den-biotin-CD-NTs and (b) SA-FITC/Den-biotin-C4-CD-NTs (scale bar: 5 μm). (c) Schematic representation of the inhibition assay on Den-biotin-C4-CD-NTs. (d) Fluorescence spectra of Den-biotin-C4-CD-NTs and SA-Au NP/Den-biotin-C4-CD-NTs. (e) I_t/I_0 ratio of SA-AuNP/Den-biotin-C4-CD-NTs as a function of avidin concentration. SA-FITC stands for fluorescein-labeled streptavidin. Reproduced with permission from ref 362. Copyright 2008 Wiley-VCH Verlag GmbH & Co. KGaA.

4.5. Catalytic Properties

Taking into consideration that a large number of recent reviews on catalytic properties of NP/dendrimer nanocomposites have been published,[18,20,22,23,25,26,366−369] in the present Review, we will outline only the major issues of catalysis with DENs, DSNs, and NCDs.

4.5.1. Homogeneous Catalysis with NP/Dendrimer Composites. A number of homogeneous catalytic reactions (or rather quasi-homogeneous or microheterogeneous as NP/dendrimer systems form colloidal solutions) such as hydrogenation, coupling (Mizoroki−Heck, Stille, and Suzuki), alcohol oxidation, etc., have been studied using DENs, DSNs, and NCDs as catalysts.[14,18,20,24,100,101,366,368−373]

There are several common key factors determining catalytic properties of NP/polymer systems including DENs, DSNs, and NCDs: the NP size, its surface properties, which, in turn, are determined by the conditions of NP formation, NP composition, polymer functional groups, polymer structure, etc. All of these parameters were actively discussed in numerous papers and reviews. We will focus on the aspects that are unique for DENs, DSNs, and NCDs and that might be crucial for their catalytic properties.

In general, the major parameters of catalytic reactions are selectivity, activity (which is often expressed as a turnover frequency, TOF), and stability. DENs, DSNs, and NCDs demonstrated enhanced stability, which is assigned to efficient stabilization of NPs by dendrimers/dendrons.[23,134,373]

Selectivity is an important feature that in various NP/polymer systems is provided by proper functionalization of the NP surface by polymer functional groups.[374] In the case of DENs, the size selectivity, that is, dependence of the catalytic reaction outcome on the size of a reacting molecule, was discovered.[132] For example, cyclohexadiene was selectively hydrogenated to cyclohexene, while osterol, which is a much larger molecule containing a cyclohexadiene ring, was not hydrogenated at all. Thus, the smaller molecules entered the DENs, while the larger ones did not.

It is commonly understood that in a DEN a catalytic NP is formed in a void and its surface is not fully covered by ligands, thus creating an advantage for reacting molecules to be adsorbed on the surface, which may facilitate a catalytic reaction. An elegant approach to determine the distance between the NP surface and a dendrimer was described in ref 14. The use of "molecular rulers" consisting of catalytically active allyl groups and cyclodextrin "stoppers" spanned by intervening alkyl chains with different lengths (0.5, 0.9, and 1.3 nm) allowed estimation of this distance. Using NMR to measure the relative hydrogenation rates of these rulers and making some structural and mechanistic assumptions, it was found that the surfaces of encapsulated NPs in G4-OH(Pd40) DENs are an average of 0.7 nm ± 0.2 nm from the surface of the dendrimer.

On the other hand, considering that the majority of dendrimers are quite flexible, the dendrimer functional groups may

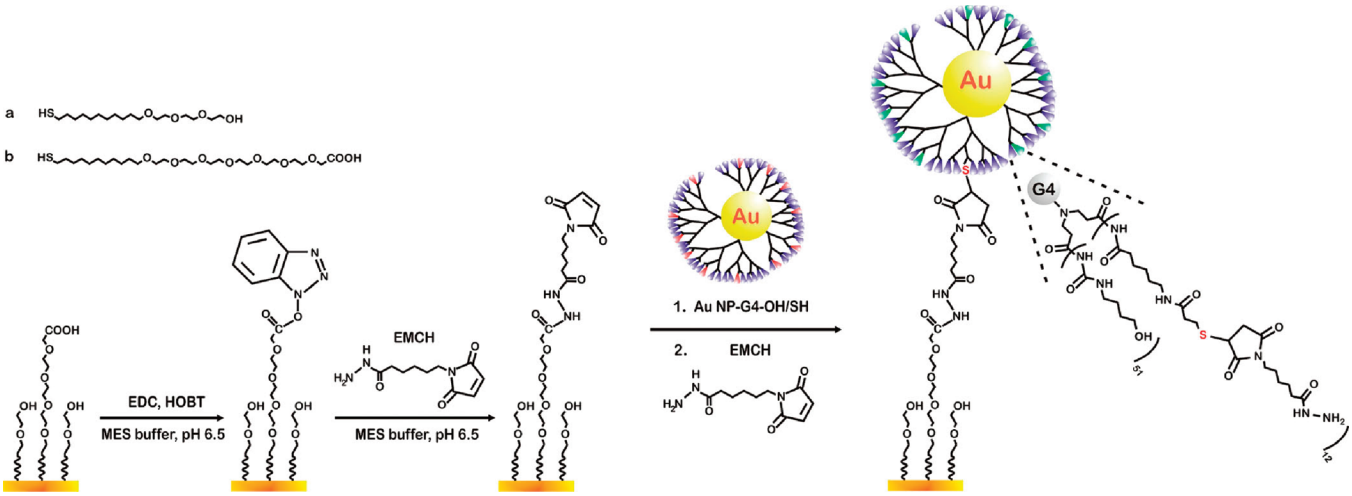

Figure 48. Immobilization of hydroxyl/LC-PDP-functionalized G4-PAMAM dendrimer-encapsulated Au nanoparticle onto mixed SAMs of alkanethiolates on gold derived from tri(ethylene glycol)-terminated thiol (a) and the hexa(ethylene glycol) carboxylic acid-terminated thiol (b). LC-PDP stands for succinimidyl 6-(3′-[2-pyridyldithio] propionamido)hexanoate; EDC is *N*-(3-dimethyl aminopropyl)-*N*′-ethyl carbodiimide hydrochloride; HOBT is 1-hydroxybenzotriazole hydrate; EMCH is heterobifunctional cross-linker *N*-(ε-maleimidocaproic acid)-hydrazide. Reprinted with permission from ref 365. Copyright 2010 American Chemical Society.

envelop the NPs surface. In the case of DSNs and NCDs, the dendrimer (dendron) density on the NP surface can be much lower than that of regular surfactants because of steric hindrances, thus creating a more "naked" surface. Despite numerous papers on catalytic properties of DENs and DSNs, only a few compared their catalytic activity. In ref 132, the catalytic activity of Pd NPs prepared as DSNs with a lower generation of triazole cycle-containing dendrimers and as DENs with higher generations of the same dendrimers were compared to Pd-DENs based on commercial PAMAM in hydrogenation of olefins. Although the authors observed the strongest increase in catalytic activity when $NaBH_4$ was replaced with methanol as a reducing agent (the effect assigned to the lack of residues on the NP surface), the higher activity was observed for DENs as compared to DSNs. It was explained by smaller NPs formed in DENs than those in DSNs. The higher catalytic activity for "click" DENs as compared to PAMAM DENs demonstrated the influence of a dendrimer structure on catalytic activity but did not explain the nature of this difference. On the other hand, in the Suzuki reaction, the same DENs and DSNs demonstrated a similar activity, which was difficult to explain. The authors believe deactivation of the catalyst took place, which made comparison invalid.[115] Thus, for now the lack of extensive comparative studies does not allow us to find distinction in catalytic activities between different types of NP/dendrimer nanocomposites.

A positive dendritic effect when catalytic activity and/or stability or reusability strongly improve with increasing a dendrimer generation is often observed for catalysts based on metal/dendrimer complexes as was shown in the Suzuki−Miyaura cross-coupling reaction,[375] dihydroxylation of olefins,[376] isomerization of allylic alcohols to ketones,[377] the Sonogashira reaction,[378] etc. However, to the best of our knowledge, no similar effects were reported for catalysis with DENs, DSNs, or NCDs.[379]

The advantages of bimetallic NPs formed in DENs and DSNs are similar to those observed in other systems.[380] For example, PdAu NPs with a gold core and Pd shell stabilized in a six-generation PAMAM dendrimer showed higher catalytic activity in hydrogenation of allyl alcohols than monometallic Pd NPs.[103] The authors believed that the gold core promotes catalytic activity due to electronic effects. A similar effect was reported in ref 230 for PtAu NPs stabilized by polyarylester dendrons in hydrogenation of nitrotoluenes to anilines. For DEN-based catalysts, it was demonstrated that the catalytic activity is higher for bimetallic NPs than for monometallic ones for such reactions as hydrogenation of *p*-nitrophenol,[99] selective hydrogenation of 1,3-cyclooctadiene,[103] and CO oxidation.[381] This effect is believed to be due to synergism of the influence of two metals located in the same NP.

4.5.2. Magnetically Separable Homogeneous Catalysts. Although numerous active and selective homogeneous catalysts are described in the literature, less than 20% of such processes are used in industry, while heterogeneous catalysis is clearly prevailing.[382] This should be ascribed to a complexity of separation of homogeneous catalysts from reaction solutions. The separation can be performed, as is thoroughly discussed in a recent review,[26] but it is time- and energy consuming. In recent years, a combination of catalytic species and magnetic NPs has been achieved, which allows robust and inexpensive magnetic separation of a catalyst. Along these lines, the PAMAM dendrons were formed on the NP consisting of a magnetic core and silica shell.[171] After dendron formation, their periphery was modified with diphenylphosphinomethanol and then phosphine groups complexed with $[Rh(COD)Cl]_2$. These homogeneous catalysts were tested in hydroformylation of various compounds and demonstrated high activity and selectivity along with easy recyclability.

In ref 383, the authors introduced the synthesis of dendron bearing diphosphinopalladium(II)-based complexes on the periphery and a primary amino group at the focal point for grafting onto core−shell γ-Fe_2O_3/polymer magnetic NPs. These functionalized magnetic NPs showed remarkable reactivity toward iodo- and bromoarenes under mild conditions, and unprecedented reactivity toward chloroarenes in the Suzuki reaction. The authors demonstrated that the chelating diphosphines on the dendron were necessary for the stability of these catalysts and their efficiency, while immobilization of complexes on magnetic

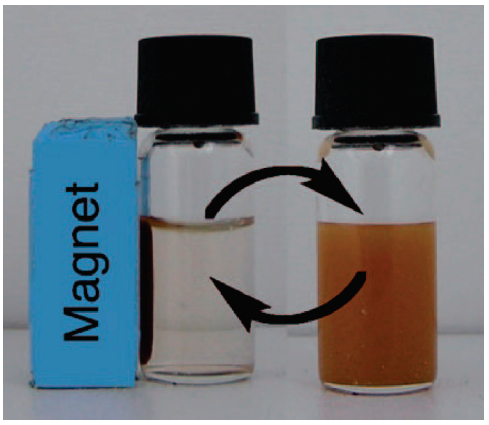

Figure 49. Magnetic separation of a grafted MNP catalyst in solution (THF/Tx 1/9) by an external magnet. Particles come close to the vial wall, and supernatant can be removed. Tx stands for triton X405. Reproduced with permission from ref 383. Copyright 2009 Wiley-VCH Verlag GmbH & Co. KGaA.

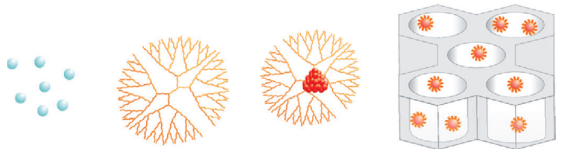

Figure 50. Depiction of the nanoparticle synthesis technique. Pt ions are loaded onto a PAMAM dendrimer and reduced to form a dendrimer-encapsulated NP. Sonication deposits the NPs on the mesoporous silica SBA-15 to generate the NP catalysts. Reprinted with permission from ref 392. Copyright 2009 Nature Publishing Group.

NPs allowed easy recovery and reuse of this grafted catalyst at least 25 times without any noticeable loss of reactivity (Figure 49).

4.5.3. Heterogeneous Catalysis with NP/Dendrimer Composites. Heterogenization of homogeneous catalysts is a traditional way for easy separation of a catalyst. Heterogenization of dendrimers or dendrons with NPs on different supports allows a combination of advantages of homogeneous and heterogeneous catalysis. Functional dendrimer groups permit a subtle control of catalytic center environment and normally do not prevent access of reagents to NPs.

Heterogenization can be carried out on both polymeric[384−386] and inorganic supports,[14,18,368,387−389] or a homogeneous catalyst can be merely precipitated or cross-linked and used in a heterogeneous state.[379,390] The last scenario seems to be disadvantageous, however, as it cannot provide high surface area and easy access to active sites as compared to specially designed catalytic supports. In a number of cases (for example, fuel cells), a conductive support is needed. This role can be played by carbon materials.[104,279,391] For example, the electrodes fabricated from carbon nanofibers with immobilized PAMAM dendrimers containing Pt NPs exhibited electrocatalytic activity in oxygen reduction.[391] The authors believed that such catalysts can be used in fuel cells because good catalytic activity can be achieved at lower Pt loadings than those currently used in conventional catalytic systems. Oxygen reduction was also studied with heterogeneous catalysts formed by adsorption of Pt-DENs on the nitrogen-doped carbon nanotubes.[279] The facile uptake of Pt-DENs was found to be influenced by the number of edge plane sites on the carbon

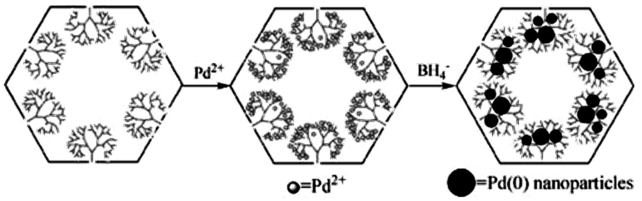

Figure 51. Depiction of the nanoparticle formation. Pd ions are loaded into dendrimers attached to the silica walls and reduced to form a DEN-SBA-15 catalyst. Reprinted with permission from ref 387. Copyright 2006 the American Chemical Society.

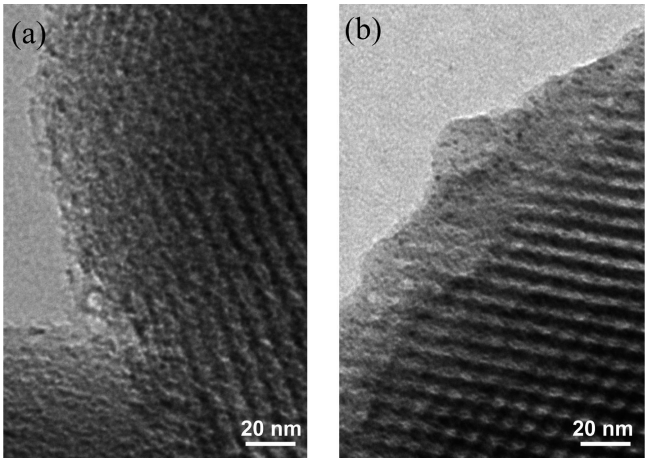

Figure 52. TEM images of dendrimer encapsulated (a) Rh_{30} and (b) Pt_{40} nanoparticle immobilized on SBA-15, denoted as Rh_{30}/SBA-15 and Pt_{40}/SBA-15, respectively. Reprinted with permission from ref 191. Copyright 2008 American Chemical Society.

nanotubes, with higher adsorption rates observed for those with increased nitrogen content.

An elegant way to heterogenize DENS, DSNs, or NCDs is their incorporation in the pores of mesoporous silica (SBA-15 or MCF-17).[191,387,392,393] This incorporation can be carried out either by noncovalent interactions (Figure 50)[191,392] or first by covalent attachment of dendrimers on the pore walls followed by NP formation in dendrimers (Figure 51).[387,393] It is noteworthy that with a heterogenized catalyst the dendritic effect was observed. For example, the higher generation dendrimers gave better defined NPs without agglomeration, and these particles showed better catalytic performance.[384]

The heterogeneous catalysts discussed in ref 191 were prepared by encapsulation of 1 nm Rh and Pt NPs in G4 PAMAM dendrimers immobilized in mesoposous silica SBA-15 (Figure 52). These catalysts were tested in hydrogenation of ethylene and pyrene. The highest catalytic activity was found when the catalysts were treated by hydrogen at 150 °C, that is, when dendrimers are not destroyed. The treatment at higher temperatures led to the decrease of activity, indicating that dendrimer environment of NPs is important for catalytic activity. Variation of Pt NP sizes in the same catalysts used in pyrene hydrogenation showed that the smallest NPs (0.8 nm) are the most active.[394] This is consistent with the increase of the surface area and the amount of accessible active centers when the NP size decreases.

The catalysts described in ref 387 showed high catalytic activity for the hydrogenation of allyl alcohol. The hydrogenation

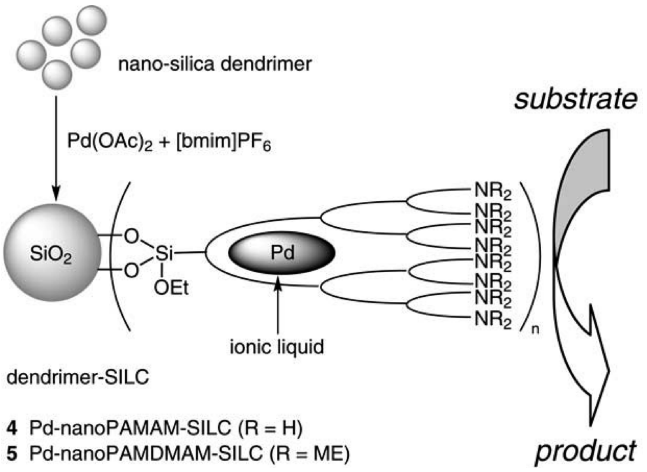

Figure 53. Pd-nanosilica dendrimer-SILC. Reprinted with permission from ref 388. Copyright 2010 Georg Thieme Verlag Stuttgart · New York.

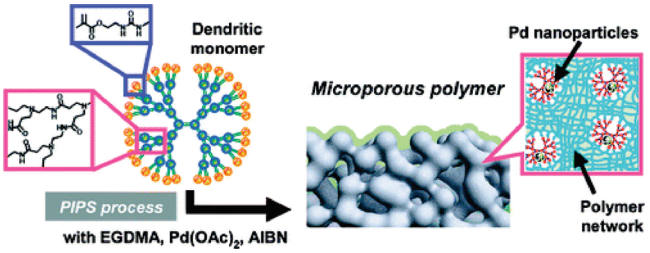

Figure 54. Schematic outline of the preparation of microporous network polymers that contain PdNPs. Reprinted with permission from ref 244. Copyright 2010 American Chemical Society.

rate and selectivity could be controlled by using different generation dendrimers, but no obvious (positive or negative) dendritic effect was observed. These catalysts demonstrated high stability to be recycled multiple times and were stored for 1 month under ambient conditions, while maintaining the catalytic activities. Pt PAMAM DENs embedded in mesoporous silica also demonstrated superior activity and recyclability as compared to larger, polymer-capped analogues in cyclization reactions of various molecules.

Silica NPs modified with PAMAM dendrons have been used for immobilization of Pd NPs by incorporation of Pd acetate assisted with the ionic liquid, butylmethylimidazolinium hexafluorophosphate ([bmim]PF_6) (Figure 53).[388] The authors believed that the ionic liquid molecules help with stabilization of NPs along with tertiary amines. This catalyst was effective for Suzuki−Miyaura reactions of ortho-substituted aryl bromides or aryl triflates without a ligand in 50% aqueous ethanol in air at room temperature. The catalyst could be reused up to five times in 93% average yield after simple centrifugation.

An interesting strategy based on polymerization-induced phase separation (PIPS) was proposed for fabricating Pd NPs immobilized in a microporous polymer.[244] For that, a Pd precursor was mixed with a monomer containing a PAMAM dendrimer, and a mixture was thermally polymerized with an excess amount of ethylene glycol dimethacrylate (solvent) under PIPS conditions (Figure 54). Despite that the authors called the polymer microporous, in fact, it is mesoporous with 9.9 nm pores, which are better suited for catalytic reactions than microporous materials (pore diameters ≤2 nm) due to improved mass transfer. The

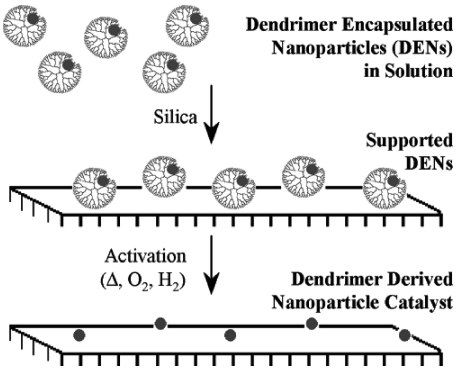

Figure 55. Schematic representation of using dendrimers as sacrificial templates for deposition of catalytic NPs on the support. Reprinted with permission from ref 395. Copyright 2005 American Chemical Society.

performance of this catalyst was investigated in a Suzuki−Miyaura reaction of 4′-bromoacetophenone and phenylboronic acid in water. The catalyst was successfully recovered by simple filtration and reused with only a minimal loss of activity (yield >90% even at the eighth run). Comparison of this catalyst with other analogues not containing dendrimers in their structure demonstrated that dendrimers significantly improved the stability of the catalysts.

In another recent article,[386] heterogenization was carried out by immobilization/stabilization of Au NPs on surface grafted G2 PPI dendrimer onto the cross-linked poly(4-vinylpyridine) (P4VP) beads. This catalyst was used in hydrogenation of 4-nitrophenol. However, the NPs formed demonstrated extremely high polydispersity (in both size and shape), revealing no control over NP formation. We believe no enhanced catalytic properties can be achieved with such a catalyst.

4.5.4. Removal of a Dendrimer Template after Deposition on Surfaces. In many cases, for preparation of heterogeneous catalysts, dendrimers are used as sacrificial templates for stabilization of NPs followed by deposition of DENs on supports and by dendrimer removal during a thermal treatment (Figure 55).[395] The dendrimer removal is performed to free the NP surface and to increase catalytic activity. To achieve a complete removal of dendrimers and products of their decomposition and to activate NPs, the thermal treatment can be carried out in O_2 and H_2,[395] O_2/He/H_2,[396] CO and O_2,[397] O_2/He and H_2/He,[398] and merely in O_2.[399] The choice of the atmosphere and the temperature for the template removal is dictated by the necessity of the complete template removal along with prevention of NP agglomeration and formation of catalytically active NP surface. For example, the presence of CO in O_2 was found to be especially advantageous as it allows full activation of Pt NPs at relatively low temperature (150 °C) and prevents fouling of NPs.[397]

PAMAM dendrimers were used to stabilize Pt, Au, Ir, Rh, Pt−Au, and Pt−Cu NPs.[261,395−403] After deposition on alumina, silica, zirconia, or titania surface, the dendrimers were burnt off, while NPs stayed partially embedded in the support, preventing their aggregation. Titania was shown to be a preferable support as compared to silica or alumina.[397,403] IR spectroscopy indicated that titania plays an active role in dendrimer adsorption and decomposition, while adsorption of DENs on silica is dominated by metal−support interactions. It was also demonstrated that the titania supported catalyst was resistant to deactivation during an extended treatment at 300 °C.[403] The catalysts formed after DEN removal were active in CO oxidation, hydrogenation of

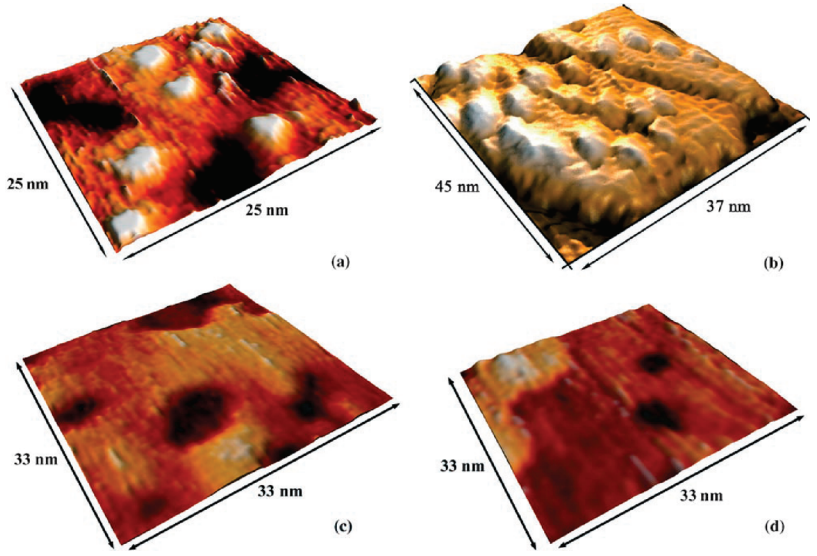

Figure 56. (a) STM image (recorded in UHV at room temperature) of dendrimer-encapsulated Au NPs immobilized at a β-CD SAM. Sample bias, −0.987 V; tunneling current, 0.08 nA. (b) STM image (recorded under ambient conditions at room temperature) of dendrimer-encapsulated Au NPs immobilized at a β-CD SAM. Tip bias, 1 V; tunneling current, 0.1 nA. (c) STM image (recorded in UHV at room temperature) of a β-CD SAM with a monolayer of the dendrimers. Sample bias, −0.987 V; tunneling current, 0.08 nA. (d) STM image of a β-CD SAM (recorded in UHV at room temperature). Sample bias, −0.987 V; tunneling current, 0.08 nA. Reproduced with permission from ref 214. Copyright 2006 Wiley-VCH Verlag GmbH & Co. KGaA.

toluene and benzonitrile, hydrodechlorination of 1,2-dichloroethane, and other reactions.[249,261,395−404]

Along these lines, carbon nanotubes were successfully synthesized using chemical vapor deposition in the presence of microwave plasma with the catalyst, prepared by burning off the G4-NH_2 PAMAM dendrimer with Fe_2O_3 NPs on the $Ti/SiO_2/Si$ support.[405] This approach often allows one to obtain more active and smaller NPs than by the conventional impregnation;[402] however, in a number of cases, NP agglomeration or growth due to calcination has been reported.[192,406,404]

On the other hand, in ref 396 the authors have demonstrated that even subnanometer Rh particles can be prepared on a ZrO_2 support via the dendrimer mediated synthetic route. EXAFS characterization of each step involved in this process indicated that Rh_3 clusters are formed within the dendrimer interior structure in aqueous solutions and the resulting Rh−dendrimer nanocomposites can be deposited onto the ZrO_2 support. Subsequent thermal treatments in O_2 and H_2 were performed to remove the dendrimer component and to form stable Rh nanoparticles. Very limited sintering of Rh was observed during these thermal treatments. The catalytic properties of these materials for ethane hydrogenolysis were substantially different from those of larger Rh particles.

4.6. Electronic and Other Properties

The interesting "bottom-up" approach was used to fabricate electronic devices that can work under ambient conditions.[214] In this approach, G5 PPI dendrimers (guest) with terminal adamantyl groups modified by β-CD were used first for the formation of 1.7 nm Au NPs and then to transfer Au NPs on the self-assembled monolayers (SAM) (a molecular printboard) with terminal β-CD groups. Because of replacement of free β-CD molecules for the β-CD anchored groups, Au NPs were fixed on the surface. The anchored Au NPs show Coulomb blockade and a Coulomb staircase, which is a sign that the Au

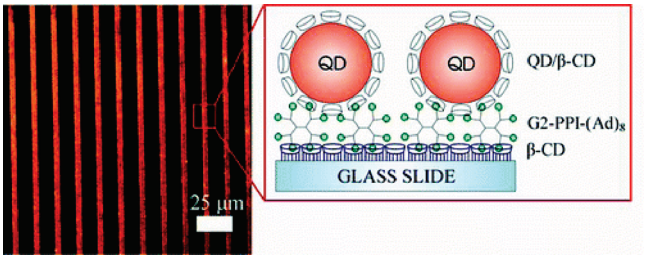

Figure 57. Fluorescence image by microcontact printing of the QDs onto a full G2-PPI-$(Ad)_8$ layer. The scale bar has a length of 25 μm. Reprinted with permission from ref 410. Copyright 2010 American Chemical Society.

NPs are effectively insulated by the dendrimers and that the β-CD SAM is an efficient tunnel barrier (Figure 56). The surface confinement of encapsulated Au NPs by self-assembly results in well-defined junctions with single-electron tunneling (SET) properties. The system is robust because the dendrimers are attached to the β-CD host surface by multiple specific host−guest interactions and the metal NPs are located inside the dendrimers. The authors believe that the observation of a Coulomb staircase at ambient conditions for metal NPs in a supramolecular system is a unique phenomenon. Analogous nanocomposites were further used for fabrication of 3D free-standing particle composites on topographically patterned substrates[407] and freestanding polystyrene particle bridges with controlled composition and macroscopic robustness.[408]

Further development of molecular printboards, that is, reversible attachment of nanostructures, was reported in ref 409. It was illustrated by the adsorption and desorption of β-CD-functionalized NPs onto and from stimuli-responsive preadsorbed ferrocenyl-functionalized PPI dendrimers at a β-CD SAM. A new function here is ferrocenyl end groups. Their electrochemical oxidation was

used to induce desorption of nanostructures from the β-CD SAMs. In a more recent paper of the same group, supramolecular microcontact printing was used to obtain controlled patterns consisting of CdSe/ZnS QDs instead of Au NPs with similar functionalization (Figure 57).[410] Here, the surface-immobilized QDs were able to form host−guest complexes with other molecules at binding cavities not occupied by adamantyl groups. Complex formation with ferrocene-functionalized molecules at these sites led to partial quenching of the luminescence emission of QDs, demonstrating the principle for sensing using the QD multilayer nanostructures. This series of papers demonstrated the extent of possibilities for molecular print boards with this kind of composite.

Passivation of Au NPs with an average diameter 2.1 ± 0.4 nm with rigid π-conjugated dendrons (21 per each NP) holds a promise of an interesting type of electronic device.[411] The fluorescence quenching of the Au NPs indicated an electron transfer interaction between the Au NP and the dendron wedge on the surface of the Au nanoparticle. The $I-V-R$ characteristics of the single layer device with these dendron-passivated NPs exhibited a clear electrical bistability, which is vital for memory applications.

It is worth noting that nanocomposites of dendrimers with NPs displayed tribological properties. In particular, the PAMAM dendrimers modified with fluorine-containing chains and containing Au NPs demonstrated a decreased friction coefficient after immobilization on the surface and formation of ultrathin films in supercritical CO_2.[412] The authors ascribed the improvement of tribological properties to suppression of Au NP aggregation in the presence of fluorinated chains. In later work,[413] the same authors studied the formation of bimetallic NPs in the PAMAM dendrimers and showed that nanocomposites with Fe−Ni NPs demonstrate improved tribological properties as compared to monometallic NPs; however, the authors did not explain the causes of this improvement. Moreover, this work showed no comparison with the previous paper where the decrease of the friction coefficient was observed for PAMAM dendrimers modified with fluorinated chains.

Nanocomposites based on CdS QDs and G4(3,5)-NH_2 PAMAM were used for fingerprint detection.[414] After the treatment with diimide, amino groups become reactive toward amino acids contained in fingerprints. Luminescence of NPs allowed significant signal enhancement (fingerprint labeling) as compared to other methods.

5. SUMMARY AND OUTLOOK

This Review demonstrates that dendrimers successfully stabilize NPs by playing the role of either a template (DENs) when a NP is located inside the dendrimer molecule or surfactants (DSNs) when NPs are formed between dendrimers. Dendrons with certain functionalities in a focal point can serve as surfactants either when NPs are formed or for a ligand exchange reaction leading to NCDs. Approaches described here for the NP/dendrimer composites take advantage of unique features of a dendrimer structure: (i) variable nature of terminal and interior groups and (ii) the three-dimensional structure and radial distribution function of a dendrimer density, allowing DEN formation.

It is worth noting that, from the synthetic point of view, unique dendrimer properties are fully realized when a dendrimer design or reaction conditions allow formation of very small NPs (for example, luminescent gold and silver nanoclusters, subnanometer catalytic NPs, etc), which would be difficult to make in the presence of regular surfactants or polymers. Another exclusive feature of dendrimers is control of NP size with increasing a dendrimer generation, allowing control over nanocomposite properties. On the other hand, when dendrimers serve as surfactants, because their structure differs significantly from the structure of conventional surfactants, this leads to opportunities of targeted control over solubility, functionality, and morphology of the NP/dendrimer nanocomposites. In any case, DENs, DSNs, and NCDs, or their complex structures, should be comprehensively characterized using a combination of physicochemical methods to assess and understand structure−property relationships for better exploration of these materials. NPs stabilized by dendrimers or nanostructures based on dendrimers, NPs, and other components possess fascinating optical, catalytic, magnetic, sensing, and biomedical properties, which make them highly promising for further use in nanotechnologies. We believe this area of science will be a fast developing field, bringing more surprises and novel applications in years to come. The time is ripe for transforming scientific findings into applications.

AUTHOR INFORMATION

Corresponding Author

*E-mail: lybronst@indiana.edu.

BIOGRAPHIES

Lyudmila M. Bronstein is a Senior Scientist at the Department of Chemistry, Indiana University. She received her M.S. degree cum laude from Tver Technical University (Tver, Russia) and her Ph.D. in polymer chemistry from the A.N. Nesmeyanov Institute of Organoelement Compounds (INEOS) of the Russian Academy of Sciences (Moscow, Russia). After two-years of postdoctoral research at the Institute of Synthetic Fibers (Tver, Russia), she started her research career at INEOS first as a junior researcher, then a research associate, a senior scientist, and as a leading scientist starting from 1997. In 1999, she moved to Indiana University. During her research career, she published over 160 papers, reviews, and book chapters. Dr. Bronstein's research program focuses on developing new materials with important applications in the fields of energy, catalysis, and life sciences. Her research group has been working on making solid polymer electrolytes and electrodes for Li ion batteries with

enhanced performance, efficient and selective catalytic systems based on nanostructured polymers, and multifunctional magnetic nanoparticles as bioprobes.

Dr. Zinaida Shifrina received a M.S. degree in polymer chemistry with honors from the D.I. Mendeleev Russian Chemical-Technological University, Moscow, Russia, in 1983. She was awarded her Ph.D. from the A.N. Nesmeyanov Institute of Organoelement Compounds, Russian Academy of Sciences (INEOS), Moscow, Russia, in 1988 under the guidance of Professor V. Korshak. She then was hired by the Helmholtz Moscow Research Institute of Eye Diseases where she held a position as a Research Fellow and was working on the development of new materials for contact lenses. Presently, she is a Head of the Group of Macromolecular Chemistry at the INEOS. Her current scientific interests include polymer chemistry and nanotechnology with a particular focus on dendrimer synthesis and nanocomposites for catalysis and medical applications.

ACKNOWLEDGMENT

This work has been supported, in part, by the NATO Science for Peace Program (grant SfP-981438) and the IU FRSP grant. Z. B.S. thanks the Federal Program "Scientists and Educators of Innovative Russia" 2009-20013, contract no. 14.740.11.0380 and the RFBR grant 11-03-00064. We are thankful for funding from the European Community's Seventh Framework Programme [FP7/2007-2013] under grant agreement no. CP-IP 24095.

LIST OF ABBREVIATIONS

AFM	atomic force microscopy
β-CD	β-cyclodextrin
BSA	bovine serum albumin
CT	X-ray computed tomography
DENs	dendrimer encapsulated nanoparticles
DLS	dynamic light scattering
DSNs	dendrimer stabilized nanoparticles
EDS	energy dispersive X-ray spectroscopy
EDX	energy dispersive X-ray analysis
EXAFS	extended X-ray absorption fine structure
FA	folic acid
FAR	FA receptors
FFT	fast Fourier transform
FI	fluorescein isothiocyanate
FTIR	Fourier transform infrared spectroscopy
GCE	glassy carbon electrode
HOPG	highly ordered pyrolytic graphite substrate
HRTEM	high resolution transmission electron microscopy
ITO	indium tin oxide
KB cells	a human epithelial carcinoma cell line
LbL	layer-by-layer
MALDI-TOF	matrix-assisted laser desorption/ionization time-of-flight mass spectrometry
MRI	magnetic resonance imaging
MWCNT	multiwall carbon nanotube
NCDs	nanoparticle-core dendrimers
NIL	top-down nanoimprint lithography
NMR	nuclear magnetic resonance spectroscopy
NP	nanoparticle
ODA	octadecylamine
P4VP	poly(4-vinylpyridine)
PAMAM	poly(amidoamine)
PEG	poly(ethylene glycol)
PDF	atomic pair distribution function analysis
PIPS	polymerization-induced phase separation
PPI	poly(propyleneimine)
PSA	prostate specific antigen
PSS	poly(sodium 4-styrenesulfonate)
QDs	quantum dots
RGD	Arg-Gly-Asp peptide
RSA	rice-shaped architecture
SAED	selected area electron diffraction
SAM	self-assembled monolayer
SANS	small-angle neutron scattering
SAXS	small-angle X-ray scattering
SET	single-electron tunneling
S-layer	surface-layer
SCIO	shell-cross-linked iron oxide
STEM	scanning transmission electron microscopy
STM	scanning tunneling microscopy
SWNTs	single-wall carbon nanotubes
TEM	transmission electron microscopy
TGA	thermogravimetric analysis
TOF	turnover frequency
TOPO	trioctylphosphine oxide
TNTs	titanium dioxide nanotubes
XANES	X-ray absorption near edge structure
XAS	X-ray absorption spectroscopy
XPS	X-ray photoelectron spectroscopy
XRD	X-ray powder diffraction
XRF	X-ray fluorescence

REFERENCES

(1) Newkome, G. R.; Moorefield, C. N.; Voegtle, F. *Dendrimers and Dendrons: Concepts, Syntheses, Applications*; Wiley-VCH: Weinheim, 2001.
(2) *Dendrimers and Other Dendritic Polymers*; Fréchet, J., Tomalia, D., Eds.; Wiley: Chichester, UK, 2001.
(3) Newkome, G. R.; He, E. F.; Moorefield, C. N. *Chem. Rev.* **1999**, *99*, 1689.
(4) Bosman, A. W.; Janssen, H. M.; Meijer, E. W. *Chem. Rev.* **1999**, *99*, 1665.
(5) Astruc, D.; Chardac, F. *Chem. Rev.* **2001**, *101*, 2991.
(6) Crooks, R. M.; Lemon, B. I.; Sun, L.; Yeung, L. K.; Zhao, M. Q. *Top. Curr. Chem.* **2001**, *212*, 81.
(7) Crooks, R. M.; Zhao, M. Q.; Sun, L.; Chechik, V.; Yeung, L. K. *Acc. Chem. Res.* **2001**, *34*, 181.
(8) Twyman, L. J.; King, A. S. H.; Martin, I. K. *Chem. Soc. Rev.* **2002**, *31*, 69.

(9) van Heerbeek, R.; Kamer, P. C. J.; van Leeuwen, P. W. N. M.; Reek, J. N. H. *Chem. Rev.* **2002**, *102*, 3717.
(10) Niu, Y. H.; Yeung, L. K.; Crooks, R. M. *J. Am. Chem. Soc.* **2001**, *123*, 6840.
(11) Esumi, K. *Top. Curr. Chem.* **2003**, *227*, 31.
(12) Goodson, T.; Varnavski, O.; Wang, Y. *Int. Rev. Phys. Chem.* **2004**, *23*, 109.
(13) Reek, J. N. H.; Arevalo, S.; Van Heerbeek, R.; Kamer, P. C. J.; Van Leeuwen, P. *Adv. Catal.* **2006**; Vol. *49*.
(14) Scott, R. W. J.; Wilson, O. M.; Crooks, R. M. *J. Phys. Chem. B* **2005**, *109*, 692.
(15) Shon, Y.-S.; Choi, D. *Curr. Nanosci.* **2007**, *7*, 245.
(16) Ozkan, M. *Drug Discovery Today* **2004**, *9*, 1065.
(17) Daniel, M. C.; Ruiz, J.; Nlate, S.; Astruc, D. *J. Inorg. Organomet. Polym. Mater.* **2005**, *15*, 107.
(18) Chandler, B. D.; Gilbertson, J. D. *Top. Organomet. Chem.* **2006**, *20*, 97.
(19) Vohs, J. K.; Fahlman, B. D. *New J. Chem.* **2007**, *31*, 1041.
(20) Andres, R.; De Jesus, E.; Flores, J. C. *New J. Chem.* **2007**, *31*, 1161.
(21) Tsuji, Y.; Fujihara, T. *Inorg. Chem.* **2007**, *46*, 1895.
(22) Peng, X.; Pan, Q.; Rempel, G. L. *Chem. Soc. Rev.* **2008**, *37*, 1619.
(23) Astruc, D.; Ornelas, C.; Ruiz, J. *Acc. Chem. Res.* **2008**, *41*, 841.
(24) Chandler, B. D.; Gilbertson, J. D. In *Nanoparticles and Catalysis*; Astruc, D., Ed.; Wiley-VCH: Weinheim, Germany, 2008.
(25) Bronstein, L. M. In *Encyclopedia of Nanoscience and Nanotechnology*; Nalwa, H. S., Ed.; American Scientific Publishers: Los Angeles, CA, 2004; Vol. 7.
(26) Astruc, D.; Boisselier, E.; Ornelas, C. *Chem. Rev.* **2010**, *110*, 1857.
(27) Tomalia, D. A.; Baker, H.; Dewald, J. R.; Hall, M.; Kallos, G.; Martin, S.; Roeck, J.; Ryder, J.; Smith, P. *Polym. J.* **1985**, *17*, 117.
(28) Tomalia, D. A.; Durst, H. D. *Top. Curr. Chem.* **1993**, *165*, 193.
(29) Tomalia, D. A.; Naylor, A. M.; Goddard, W. A. I. *Angew. Chem., Int. Ed. Engl.* **1990**, *29*, 138.
(30) Tomalia, D. A. *Prog. Polym. Sci.* **2005**, *30*, 294.
(31) Newkome, G. R.; Yao, Z. Q.; Baker, G. R.; Gupta, V. K. *J. Org. Chem.* **1985**, *50*, 2003.
(32) Newkome, G. R.; Shreiner, C. *Chem. Rev.* **2010**, *110*, 6338.
(33) Astruc, D.; Blais, J. C.; Cloutet, E.; Djakovitch, L.; Rigaut, S.; Ruiz, J.; Sartor, V.; Valerio, C. *Top. Curr. Chem.* **2000**, *210*, 229.
(34) Balzani, V.; Campagna, S.; Denti, G.; Juris, A.; Serroni, S.; Venturi, M. *Acc. Chem. Res.* **1998**, *31*, 26.
(35) Balzani, V.; Ceroni, P.; Juris, A.; Venturi, M.; Campagna, S.; Puntoriero, F.; Serroni, S. *Coord. Chem. Rev.* **2001**, *219*, 545.
(36) Balzani, V.; Ceroni, P.; Maestri, M.; Saudan, C.; Vicinelli, V. *Dendrimers V: Functional and Hyperbranched Building Blocks, Photophysical Properties, Applications in Materials and Life Sciences*; Springer-Verlag: Berlin, Heidelberg, New York; 2003; Vol. 228.
(37) Balzani, V.; Ceroni, P.; Maestri, M.; Vicinelli, V. *Curr. Opin. Chem. Biol.* **2003**, *7*, 657.
(38) Buhleier, E.; Wehner, W.; Voegtle, F. *Synthesis* **1978**, 155.
(39) Caminade, A. M.; Laurent, R.; Chaudret, B.; Majoral, J. P. *Coord. Chem. Rev.* **1998**, *180*, 793.
(40) Caminade, A. M.; Majoral, J. P. *Coord. Chem. Rev.* **2005**, *249*, 1917.
(41) Caminade, A. M.; Majoral, J. P.; Maraval, V.; Sebastian, R. M. *Phosphorus, Sulfur Silicon Relat. Elem.* **2002**, *177*, 1493.
(42) Caminade, A. M.; Maraval, V.; Laurent, R.; Turrin, C. O.; Sutra, P.; Leclaire, J.; Griffe, L.; Marchand, P.; Baudoin-Dehoux, C.; Rebout, C.; Majoral, J. P. *C. R. Chim.* **2003**, *6*, 791.
(43) Cuadrado, I.; Moran, M.; Casado, C. M.; Alonso, B.; Losada, J. *Coord. Chem. Rev.* **1999**, *195*, 395.
(44) Fisher, M.; Voegtle, F. *Angew. Chem., Int. Ed.* **1999**, *38*, 884.
(45) Gitsov, I.; Lin, C. *Curr. Org. Chem.* **2005**, *9*, 1025.
(46) Berresheim, A. J.; Muller, M.; Mullen, K. *Chem. Rev.* **1999**, *99*, 1747.
(47) Hawker, C. J.; Fréchet, J. M. J. *J. Am. Chem. Soc.* **1990**, *112*, 7638.
(48) Hirsch, A.; Vostrowsky, O. *Dendrimers IV*; Springer-Verlag: Berlin, Heidelberg, New York; 2001; Vol. 217.
(49) Inoue, K. *Prog. Polym. Sci.* **2000**, *25*, 453.
(50) Majoral, J. P.; Caminade, A. M. *Dendrimers* **1998**, *197*, 79.
(51) Majoral, J. P.; Caminade, A. M. *Chem. Rev.* **1999**, *99*, 845.
(52) Rajadurai, M. S.; Shifrina, Z. B.; Kuchkina, N. V.; Rusanov, A. L.; Muellen, K. *Russ. Chem. Rev.* **2007**, *76*, 767.
(53) Schlenk, C.; Frey, H. *Monatsh. Chem.* **1999**, *130*, 3.
(54) Ardoin, N.; Astruc, D. *Bull. Soc. Chim. Fr.* **1995**, *132*, 875.
(55) Grayson, S. M.; Fréchet, M. J. *Chem. Rev.* **2001**, *101*, 3819.
(56) Miller, T. M.; Neenan, T. X. *Chem. Mater.* **1990**, *2*, 346.
(57) Wiesler, U. M.; Weil, T.; Mullen, K. *Dendrimers III: Design, Dimension, Function*; Springer-Verlag: Berlin, Heidelberg, New York; 2001; Vol. 212.
(58) Newkome, G. R.; Moorefield, C. N.; Voegtle, F. *Dendritic Molecules-Concepts, Synthesis, Perspectives*; Wiley-VCH: Weinheim, Germany, 2002.
(59) Serroni, S.; Denti, G.; Campagna, S.; Juris, A.; Ciano, M.; Balzani, V. *Angew. Chem., Int. Ed.* **1992**, *31*, 1493.
(60) Balzani, V.; Juris, A.; Venturi, M.; Campagna, S.; Serroni, S. *Chem. Rev.* **1996**, *96*, 759.
(61) Vogtle, F.; Gestermann, S.; Hesse, R.; Schwierz, H.; Windisch, B. *Prog. Polym. Sci.* **2000**, *25*, 987.
(62) Caminade, A. M.; Maraval, V.; Laurent, R.; Majoral, J. P. *Curr. Org. Chem.* **2002**, *6*, 739.
(63) Antonietti, M.; Wenz, E.; Bronstein, L.; Seregina, M. *Adv. Mater.* **1995**, *7*, 1000.
(64) Seregina, M. V.; Bronstein, L. M.; Platonova, O. A.; Chernyshov, D. M.; Valetsky, P. M.; Hartmann, J.; Wenz, E.; Antonietti, M. *Chem. Mater.* **1997**, *9*, 923.
(65) Boisselier, E.; Diallo, A. K.; Salmon, L.; Ornelas, C. t.; Ruiz, J.; Astruc, D. *J. Am. Chem. Soc.* **2010**, *132*, 2729.
(66) Lopez-De Jesus, Y. M.; Williams, C. T. *Catal. Lett.* **2009**, *132*, 430.
(67) Wan, H.; Li, S.; Konovalova, T. A.; Zhou, Y.; Thrasher, J. S.; Dixon, D. A.; Street, S. C. *J. Phys. Chem. C* **2009**, *113*, 5358.
(68) Wan, H.; Li, S.; Konovalova, T. A.; Shuler, S. F.; Dixon, D. A.; Street, S. C. *J. Phys. Chem.* **2008**, *112*, 1335.
(69) Luo, X.; Imae, T. *J. Mater. Chem.* **2007**, *17*, 567.
(70) Luo, Y. L.; Sun, X. P. *Mater. Lett.* **2007**, *61*, 1622.
(71) Sun, X.; Luo, Y. *Mater. Lett.* **2005**, *59*, 4048.
(72) El Hamaoui, B.; Zhi, L.; Wu, J.; Kolb, U.; Muellen, K. *Adv. Mater.* **2005**, *17*, 2957.
(73) Wei, Y.; Li, Y.; Zhang, N.; Shi, G.; Jin, L. *Ultrason. Sonochem.* **2010**, *17*, 17.
(74) Juttukonda, V.; Paddock, R. L.; Raymond, J. E.; Denomme, D.; Richardson, A. E.; Slusher, L. E.; Fahlman, B. D. *J. Am. Chem. Soc.* **2006**, *128*, 420.
(75) Shi, X.; Wang, S.; Meshinchi, S.; Van Antwerp, M. E.; Bi, X.; Lee, I.; Baker, J. R., Jr. *Small* **2007**, *3*, 1245.
(76) Kuno, M.; Lee, J. K.; Dabbousi, B. O.; Mikulec, F. V.; Bawendi, M. G. *J. Phys. Chem.* **1997**, *106*, 9869.
(77) Hines, M. A.; Guyot-Sionnest, P. *J. Phys. Chem.* **1996**, *100*, 468.
(78) Peng, Z. A.; Peng, X. *J. Am. Chem. Soc.* **2001**, *123*, 183.
(79) Lemon, B. I., III; Crooks, R. M. *J. Am. Chem. Soc.* **2000**, *122*, 12886.
(80) Fahmi, A.; Pietsch, T.; Appelhans, D.; Gindy, N.; Voit, B. *New J. Chem.* **2009**, *33*, 703.
(81) Priyam, A.; Blumling, D. E.; Knappenberger, K. L. *Langmuir* **2010**, *26*, 10636.
(82) Ghosh, S.; Priyam, A.; Chatterjee, A.; Saha, A. *J. Nanosci. Nanotechnol.* **2008**, *8*, 5952.
(83) Wisher, A. C.; Bronstein, I.; Chechik, V. *Chem. Commun.* **2006**, 1637.
(84) Liu, J. a.; Li, H.; Wang, W.; Xu, H.; Yang, X.; Liang, J.; He, Z. *Small* **2006**, *2*, 999.
(85) Spatz, J. P.; Roescher, A.; Moeller, M. *Adv. Mater.* **1996**, *8*, 337.
(86) Foerster, S.; Antonietti, M. *Adv. Mater.* **1998**, *10*, 195.

(87) Underhill, R. S.; Liu, G. *Chem. Mater.* **2000**, *12*, 2082.
(88) Cao, L.; Manners, I.; Winnik, M. A. *Macromolecules* **2001**, *34*, 3353.
(89) Xu, J.; Sun, G.; Rossin, R.; Hagooly, A.; Li, Z.; Fukukawa, K.-i.; Messmore, B. W.; Moore, D. A.; Welch, M. J.; Hawker, C. J.; Wooley, K. L. *Macromolecules* **2997**, *40*, 2971.
(90) Zhao, M. Q.; Sun, L.; Crooks, R. M. *J. Am. Chem. Soc.* **1998**, *120*, 4877.
(91) Balogh, L.; Tomalia, D. A. *J. Am. Chem. Soc.* **1998**, *120*, 7355.
(92) Garcia-Martinez, J. C.; Crooks, R. M. *J. Am. Chem. Soc.* **2004**, *126*, 16170.
(93) Zhao, M. Q.; Crooks, R. M. *Angew. Chem., Int. Ed.* **1999**, *38*, 364.
(94) Zhao, M. Q.; Crooks, R. M. *Adv. Mater.* **1999**, *11*, 217.
(95) Lang, H.; May, R. A.; Iversen, B. L.; Chandler, B. D. *J. Am. Chem. Soc.* **2003**, *125*, 14832.
(96) Yamamoto, D.; Watanabe, S.; Miyahara, M. T. *Langmuir* **2010**, *26*, 2339.
(97) Zhao, M. Q.; Crooks, R. M. *Chem. Mater.* **1999**, *11*, 3379.
(98) Kim, Y. G.; Oh, S. K.; Crooks, R. M. *Chem. Mater.* **2004**, *16*, 167.
(99) Scott, R. W. J.; Datye, A. K.; Crooks, R. M. *J. Am. Chem. Soc.* **2003**, *125*, 3708.
(100) Chung, Y. M.; Rhee, H. K. *Catal. Lett.* **2003**, *85*, 159.
(101) Chung, Y.-M.; Rhee, H.-K. *J. Mol. Catal. A: Chem.* **2003**, *206*, 291.
(102) Wilson, O. M.; Scott, R. W. J.; Garcia-Martinez, J. C.; Crooks, R. M. *J. Am. Chem. Soc.* **2005**, *127*, 1015.
(103) Scott, R. W. J.; Wilson, O. M.; Oh, S. K.; Kenik, E. A.; Crooks, R. M. *J. Am. Chem. Soc.* **2004**, *126*, 15583.
(104) Yancey, D. F.; Carino, E. V.; Crooks, R. M. *J. Am. Chem. Soc.* **2010**, *132*, 10988.
(105) Zheng, J.; Petty, J. T.; Dickson, R. M. *J. Am. Chem. Soc.* **2003**, *125*, 7780.
(106) Alvarez, M. M.; Khoury, J. T.; Schaaff, T. G.; Shafigullin, M. N.; Vezmar, I.; Whetten, R. L. J. o. P. C. B. *J. Phys. Chem. B* **1997**, *101*, 3706.
(107) Zheng, J.; Dickson, R. M. *J. Am. Chem. Soc.* **2002**, *124*, 13982.
(108) Oh, S. K.; Niu, Y. H.; Crooks, R. M. *Langmuir* **2005**, *21*, 10209.
(109) Deng, S.; Locklin, J.; Patton, D.; Baba, A.; Advincula, R. C. *J. Am. Chem. Soc.* **2005**, *127*, 1744.
(110) Groehn, F.; Bauer, B. J.; Akpalu, Y. A.; Jackson, C. L.; Amis, E. J. *Macromolecules* **2000**, *33*, 6042.
(111) Michels, J. J.; Huskens, J.; Reinhoudt, D. N. *J. Chem. Soc., Perkin Trans. 2* **2002**, 102.
(112) Yamamoto, M.; Sato, S.; Hemmi, H.; Sanjo, H.; Uematsu, S.; Kaisho, T.; Hoshino, K.; Takeuchi, O.; Kobayashi, M.; Fujita, T.; Takeda, K.; Akira, S. *Nature* **2002**, *420*, 324.
(113) Nakamula, I.; Yamanoi, Y.; Yonezawa, T.; Imaoka, T.; Yamamoto, K.; Nishihara, H. *Chem. Commun.* **2008**, 5716.
(114) Ornelas, C.; Ruiz, J.; Cloutet, E.; Alves, S.; Astruc, D. *Angew. Chem., Int. Ed.* **2007**, *46*, 872.
(115) Diallo, A. K.; Ornelas, C.; Salmon, L.; Ruiz, J.; Astruc, D. *Angew. Chem., Int. Ed.* **2007**, *46*, 8644.
(116) Esumi, K.; Hosoya, T.; Suzuki, A.; Torigoe, K. *Langmuir* **2000**, *16*, 2978.
(117) Esumi, K.; Hosoya, T.; Suzuki, A.; Torigoe, K. *J. Colloid Interface Sci.* **2000**, *229*, 303.
(118) Oh, S. K.; Kim, Y. G.; Ye, H. C.; Crooks, R. M. *Langmuir* **2003**, *19*, 10420.
(119) Ye, H. C.; Scott, R. W. J.; Crooks, R. M. *Langmuir* **2004**, *20*, 2915.
(120) Templeton, A. C.; Wuelfing, W. P.; Murray, R. W. *Acc. Chem. Res.* **2000**, *33*, 27.
(121) Peng, X. H.; Pan, Q. M.; Rempel, G. L.; Wu, S. *Catal. Commun.* **2009**, *11*, 62.
(122) Yeung, L. K.; Crooks, R. M. *Nano Lett.* **2001**, *1*, 14.
(123) Knecht, M. R.; Garcia-Martinez, J. C.; Crooks, R. M. *Chem. Mater.* **2006**, *18*, 5039.
(124) Gates, A. T.; Nettleton, E. G.; Myers, V. S.; Crooks, R. M. *Langmuir* **2010**, *26*, 12994.
(125) Esumi, K.; Suzuki, A.; Aihara, N.; Usui, K.; Torigoe, K. *Langmuir* **1998**, *14*, 3157.
(126) Garcia, M. E.; Baker, L. A.; Crooks, R. M. *Anal. Chem.* **1999**, *71*, 256.
(127) Lakowicz, J. R.; Gryczynski, I.; Gryczynski, Z.; Murphy, C. J. *J. Phys. Chem. B* **1999**, *103*, 7613.
(128) Shi, X. Y.; Ganser, T. R.; Sun, K.; Balogh, L. P.; Baker, J. R. *Nanotechnology* **2006**, *17*, 1072.
(129) Sooklal, K.; Hanus, L. H.; Ploehn, H. J.; Murphy, C. J. *Adv. Mater.* **1998**, *10*, 1083.
(130) Chandra, S.; Lang, H. *Mater. Chem. Phys.* **2009**, *114*, 926.
(131) Li, C.; Li, D.; Zhao, Z.-S.; Duan, X.-M.; Hou, W. *Colloids Surf,. A* **2010**, *366*, 45.
(132) Ornelas, C.; Ruiz, J.; Salmon, L.; Astruc, D. *Chem.-Eur. J.* **2008**, *14*, 50.
(133) Ornelas, C.; Salmon, L.; Ruiz, J.; Astruc, D. *Chem. Commun.* **2007**, 4946.
(134) Ornelas, C.; Ruiz, J.; Salmon, L.; Astruc, D. *Adv. Synth. Catal.* **2008**, *350*, 837.
(135) Shifrina, Z. B.; Rajadurai, M. S.; Firsova, N. V.; Bronstein, L. M.; Huang, X.; Rusanov, A. L.; Muellen, K. *Macromolecules* **2005**, *38*, 9920.
(136) Kuchkina, N. V.; Bronstein, L. M.; Rusanov, A. L.; Shifrina, Z. B. *Russ. Chem. Bull.* **2009**, *58*, 862.
(137) Shi, X. Y.; Lee, I.; Baker, J. R. *J. Mater. Chem.* **2008**, *18*, 586.
(138) D'Aleo, A.; Williams, R. M.; Osswald, F.; Edamana, P.; Hahn, U.; van Heyst, J.; Tichelaar, F. D.; Voegtle, F.; De Cola, L. *Adv. Funct. Mater.* **2004**, *14*, 1167.
(139) Gopidas, K. R.; Whitesell, J. K.; Fox, M. A. *Nano Lett.* **2003**, *3*, 1757.
(140) Cutler, E. C.; Lundin, E.; Garabato, B. D.; Choi, D.; Shon, Y.-S. *Mater. Res. Bull.* **2007**, *42*, 1178.
(141) Gopidas, K. R.; Whitesell, J. K.; Fox, M. A. *J. Am. Chem. Soc.* **2003**, *125*, 14168.
(142) Gopidas, K. R.; Whitesell, J. K.; Fox, M. A. *J. Am. Chem. Soc.* **2003**, *125*, 6491.
(143) Kumar, V. K. R.; Gopidas, K. R. *Chem. Asian J.* **2010**, *5*, 887.
(144) Astruc, D.; Daniel, M. C.; Ruiz, J. *Chem. Commun.* **2004**, 2637.
(145) Daniel, M.-C.; Ruiz, J.; Nlate, S.; Blais, J.-C.; Astruc, D. *J. Am. Chem. Soc.* **2003**, *125*, 2617.
(146) Love, C. S.; Chechik, V.; Smith, D. K.; Brennan, C. *J. Mater. Chem.* **2004**, *14*, 919.
(147) Komine, Y.; Ueda, I.; Goto, T.; Fujihara, H. *Chem. Commun.* **2006**, 302.
(148) Wang, Y. A.; Li, J. J.; Chen, H. Y.; Peng, X. G. *J. Am. Chem. Soc.* **2002**, *124*, 2293.
(149) Guo, W. H.; Li, J. J.; Wang, Y. A.; Peng, X. G. *J. Am. Chem. Soc.* **2003**, *125*, 3901.
(150) Wang, R. Y.; Yang, J.; Zheng, Z. P.; Carducci, M. D.; Jiao, J.; Seraphin, S. *Angew. Chem., Int. Ed.* **2001**, *40*, 549.
(151) Shon, Y.-S.; Choi, D.; Dare, J.; Dinh, T. *Langmuir* **2008**, *24*, 6924.
(152) Shon, Y. S.; Choi, D. *Chem. Lett.* **2006**, *35*, 644.
(153) Yang, P.; Zhang, W.; Du, Y.; Wang, X. *J. Mol. Catal. A: Chem.* **2006**, *260*, 4.
(154) Hirano, C.; Imae, T.; Tamura, M.; Takaguchi, Y. *Chem. Lett.* **2005**, *34*, 862.
(155) Hwang, S.-H.; Moorefield, C. N.; Wang, P.; Jeong, K.-U.; Cheng, S. Z. D.; Kotta, K. K.; Newkome, G. R. *J. Am. Chem. Soc.* **2006**, *128*, 7505.
(156) Tao, L.; Chen, G. J.; Mantovani, G.; York, S.; Haddleton, D. M. *Chem. Commun.* **2006**, 4949.
(157) Park, Y.; Taranekar, P.; Park, J. Y.; Baba, A.; Fulghum, T.; Ponnapati, R.; Advincula, R. C. *Adv. Funct. Mater.* **2008**, *18*, 2071.
(158) Wu, L.; Li, B.-L.; Huang, Y.-Y.; Zhou, H.-F.; He, Y.-M.; Fan, Q.-H. *Org. Lett.* **2006**, *8*, 3605.

(159) Kim, M.-K.; Jeon, Y.-M.; Jeon, W. S.; Kim, H.-J.; Kim, K.; Hong, S. G.; Park, C. G. *Chem. Commun.* **2001**, *7*, 667.
(160) Li, D.; Li, J. *Colloids Surf., A* **2005**, *257−258*, 255.
(161) Brust, M.; Walker, M.; Bethell, D.; Schiffrin, D. J.; Whyman, R. *J. Chem. Soc., Chem. Commun.* **1994**, 801.
(162) Huang, B.; Tomalia, D. A. *J. Lumin.* **2005**, *111*, 215.
(163) Kim, M.; Chen, Y. F.; Liu, Y. C.; Peng, X. G. *Adv. Mater.* **2005**, *17*, 1429.
(164) Duanmu, C.; Saha, I.; Zheng, Y.; Goodson, B. M.; Gao, Y. *Chem. Mater.* **2006**, *18*, 5973.
(165) Advincula, R. C. *Dalton Trans.* **2006**, 2778.
(166) Men, Y.; Higuchi, M.; Yamamoto, K. *Sci. Technol. Adv. Mater.* **2006**, *7*, 139.
(167) Zhao, Y. L.; Li, Y. P.; Song, Y. T.; Jiang, W.; Wu, Z. Y.; Wang, Y. A.; Sun, J. H.; Wang, J. Y. *J. Colloid Interface Sci.* **2009**, *339*, 336.
(168) Wu, M. L.; O'Neill, S. A.; Brousseau, L. C.; McConnell, W. P.; Shultz, D. A.; Linderman, R. J.; Feldheim, D. L. *Chem. Commun.* **2000**, 775.
(169) Gopidas, K. R.; Whitesell, J. K.; Fox, M. A. *J. Am. Chem. Soc.* **2003**, *125*, 14168.
(170) Gopidas, K. R.; Whitesell, J. K.; Fox, M. A. *J. Am. Chem. Soc.* **2003**, *125*, 6491.
(171) Abu-Reziq, R.; Alper, H.; Wang, D. S.; Post, M. L. *J. Am. Chem. Soc.* **2006**, *128*, 5279.
(172) Schmid, G.; Emmrich, E.; Majoral, J. P.; Caminade, A. M. *Small* **2005**, *1*, 73.
(173) Gu, Y.; Xie, H.; Gao, J.; Liu, D.; Williams, C. T.; Murphy, C. J.; Ploehn, H. J. *Langmuir* **2005**, *21*, 3122.
(174) Mark, S. S.; Bergkvist, M.; Yang, X.; Angert, E. R.; Batt, C. A. *Biomacromolecules* **2006**, *7*, 1884.
(175) Lukkari, J.; Salomaki, M.; Viinikanoja, A.; Aaritalo, T.; Paukkunen, J.; Kocharova, N.; Kankare, J. *J. Am. Chem. Soc.* **2001**, *123*, 6083.
(176) Ott, P.; Gensel, J.; Roesler, S.; Trenkenschuh, K.; Andreeva, D.; Laschewsky, A.; Fery, A. *Chem. Mater.* **2010**, *22*, 3323.
(177) Kotov, N. A.; Dekany, I.; Fendler, J. H. *J. Phys. Chem.* **1995**, *99*, 13065.
(178) Caruso, F.; Trau, D.; Moehwald, H.; Renneberg, R. *Langmuir* **2000**, *16*, 1485.
(179) Radtchenko, I. L.; Giersig, M.; Sukhorukov, G. B. *Langmuir* **2002**, *18*, 8204.
(180) Lvov, Y.; Decher, G.; Moehwald, H. *Langmuir* **1993**, *9*, 481.
(181) Puniredd, S. R.; Yin, C. M.; Hooi, Y. S.; Lee, P. S.; Srinivasan, M. P. *J. Colloid Interface Sci.* **2009**, *332*, 505.
(182) Won, J.; Ihn, K. J.; Kang, Y. S. *Langmuir* **2002**, *18*, 8246.
(183) He, J. A.; Valluzzi, R.; Yang, K.; Dolukhanyan, T.; Sung, C. M.; Kumar, J.; Tripathy, S. K.; Samuelson, L.; Balogh, L.; Tomalia, D. A. *Chem. Mater.* **1999**, *11*, 3268.
(184) Crespilho, F. N.; Ghica, M. E.; Zucolotto, V.; Nart, F. C.; Oliveira, O. N., Jr.; Brett, C. M. A. *Electroanalysis* **2007**, *19*, 805.
(185) Crespilho, F. N.; Ghica, M. E.; Florescu, M.; Nart, F. C.; Oliveira, O. N.; Brett, C. M. A. *Electrochem. Commun.* **2006**, *8*, 1665.
(186) Knecht, M. R.; Wright, D. W. *Chem. Mater.* **2004**, *16*, 4890.
(187) Shaffer, A. W.; Worden, J. G.; Huo, Q. *Langmuir* **2004**, *20*, 8343.
(188) Worden, J. G.; Dai, Q.; Shaffer, A. W.; Huo, Q. *Chem. Mater.* **2004**, *16*, 3746.
(189) Worden, J. G.; Shaffer, A. W.; Huo, Q. *Chem. Commun.* **2004**, 518.
(190) Worden, J. G.; Dai, Q.; Huo, Q. *Chem. Commun.* **2006**, 1536.
(191) Huang, W.; Kuhn, J. N.; Tsung, C. K.; Zhang, Y.; Habas, S. E.; Yang, P.; Somorjai, G. A. *Nano Lett.* **2008**, *8*, 2027.
(192) Sun, L.; Crooks, R. M. *Langmuir* **2002**, *18*, 8231.
(193) Ling, X. Y.; Huskens, J. *Chem. Commun.* **2009**, 5521.
(194) Qi, X.; Xue, C.; Huang, X.; Huang, Y.; Zhou, X.; Li, H.; Liu, D.; Boey, F.; Yan, Q.; Huang, W.; De Feyter, S.; Mullen, K.; Zhang, H. *Adv. Funct. Mater.* **2010**, *20*, 43.
(195) Qi, X.; Huang, Y.; Klapper, M.; Boey, F.; Huang, W.; De Feyter, S.; Mullen, K.; Zhang, H. *J. Phys. Chem. C* **2010**, *114*, 13465.
(196) Ascencio, J. A.; Gutierrez-Wing, C.; Espinosa, M. E.; Marin, M.; Tehuacanero, S.; Zorrilla, C.; Jose-Yacaman, M. *Surf. Sci.* **1998**, *396*, 349.
(197) Tang, Q.; Cheng, F.; Lou, X. L.; Liu, H. J.; Chen, Y. *J. Colloid Interface Sci.* **2009**, *337*, 485.
(198) Xu, D. M.; Zhang, K. D.; Zhu, X. L. *J. Appl. Polym. Sci.* **2007**, *104*, 422.
(199) Umeda, Y.; Kojima, C.; Harada, A.; Horinaka, H.; Kono, K. *Bioconjugate Chem.* **2010**, *21*, 1559.
(200) Lu, X.; Imae, T. *J. Phys. Chem. C* **2007**, *111*, 2416.
(201) Zhu, H.; Zhu, Y.; Yang, X.; Li, C. *Chem. Lett.* **2006**, *35*, 326.
(202) Han, X.; Zhu, Y.; Yang, X.; Li, C. *J. Alloys Compd.* **2010**, *500*, 247.
(203) Xu, L.; Zhu, Y.; Yang, X.; Li, C. *Mater. Sci. Eng., C* **2009**, *29*, 1306.
(204) Li, J.; Piehler, L. T.; Qin, D.; Baker, J. R.; Tomalia, D. A.; Meier, D. J. *Langmuir* **2000**, *16*, 5613.
(205) Hierlemann, A.; Campbell, J. K.; Baker, L. A.; Crooks, R. M.; Ricco, A. J. *J. Am. Chem. Soc.* **1998**, *120*, 5323.
(206) Tsukruk, V. V. *Adv. Mater.* **1998**, *10*, 253.
(207) Betley, T. A.; Hessler, J. A.; Mecke, A.; Holl, M. M. B.; Orr, B. G.; Uppuluri, S.; Tomalia, D. A.; Baker, J. R. *Langmuir* **2002**, *18*, 3127.
(208) Muller, T.; Yablon, D. G.; Karchner, R.; Knapp, D.; Kleinman, M. H.; Fang, H. B.; Durning, C. J.; Tomalia, D. A.; Turro, N. J.; Flynn, G. W. *Langmuir* **2002**, *18*, 7452.
(209) Zhang, H.; Grim, P. C. M.; Vosch, T.; Wiesler, U. M.; Berresheim, A. J.; Mullen, K.; De Schryver, F. C. *Langmuir* **2000**, *16*, 9294.
(210) Coen, M. C.; Lorenz, K.; Kressler, J.; Frey, H.; Mulhaupt, R. *Macromolecules* **1996**, *29*, 8069.
(211) Pellechia, P. J.; Gao, J. X.; Gu, Y. L.; Ploehn, H. J.; Murphy, C. J. *Inorg. Chem.* **2004**, *43*, 1421.
(212) Gu, Y. L.; Xie, H.; Gao, J. X.; Liu, D. X.; Williams, C. T.; Murphy, C. J.; Ploehn, H. J. *Langmuir* **2005**, *21*, 3122.
(213) Li, W. S.; Kim, K. S.; Jiang, D. L.; Tanaka, H.; Kawai, T.; Kwon, J. H.; Kim, D.; Aida, T. *J. Am. Chem. Soc.* **2006**, *128*, 10527.
(214) Nijhuis, C. A.; Oncel, N.; Huskens, J.; Zandvliet, H. J. W.; Ravoo, B. J.; Poelsema, B.; Reinhoudt, D. N. *Small* **2006**, *2*, 1422.
(215) Esumi, K.; Matsumoto, T.; Seto, Y.; Yoshimura, T. *J. Colloid Interface Sci.* **2005**, *284*, 199.
(216) Okugaichi, A.; Torigoe, K.; Yoshimura, T.; Esumi, K. *Colloids Surf., A* **2006**, *273*, 154.
(217) Wu, J.; Mao, Y.; Xu, J.; Li, L.; Guo, Q.; Yu, X.; Yan, G.; Guo, D. *J. Nanosci. Nanotechnol.* **2010**, *10*, 2181.
(218) Hashimoto, T.; Saijo, K. *J. Chem. Phys.* **1998**, *109*, 5627.
(219) Sakamoto, N.; Harada, M.; Hashimoto, T. *Macromolecules* **2006**, *39*, 1116.
(220) Tan, N. C. B.; Balogh, L.; Trevino, S. F.; Tomalia, D. A.; Lin, J. S. *Polymer* **1999**, *40*, 2537.
(221) Hashimoto, T.; Harada, M.; Sakamoto, N. *Macromolecules* **1999**, *32*, 6867.
(222) Tanaka, H.; Koizumi, S.; Hashimoto, T.; Itoh, H.; Satoh, M.; Naka, K.; Chujo, Y. *Macromolecules* **2007**, *40*, 4327.
(223) Srivastava, S.; Frankamp, B. L.; Rotello, V. M. *Chem. Mater.* **2005**, *17*, 487.
(224) Groehn, F.; Kim, G.; Bauer, A. J.; Amis, E. J. *Macromolecules* **2001**, *34*, 2179.
(225) Shtykova, E. V.; Gao, X.; Huang, X.; Dyke, J. C.; Schmucker, A. L.; Remmes, N.; Baxter, D. V.; Stein, B.; Dragnea, B.; Konarev, P. V.; Svergun, D. I.; Bronstein, L. M. *J. Phys. Chem. C* **2008**, *112*, 16809.
(226) Shtykova, E. V.; Malyutin, A.; Dyke, J.; Stein, B.; Konarev, P. V.; Dragnea, B.; Svergun, D. I.; Bronstein, L. M. *J. Phys. Chem. C* **2010**, *114*, 21908.
(227) Bronstein, L. M.; Shtykova, E. V.; Malyutin, A.; Dyke, J. C.; Gunn, E.; Gao, X.; Stein, B.; Konarev, P. V.; Dragnea, B.; Svergun, D. I. *J. Phys. Chem. C* **2010**, *114*, 21900.
(228) Ozerin, A. N.; Svergun, D. I.; Volkov, V. V.; Kuklin, A. I.; Gordelyi, V. I.; Islamov, A. K.; Ozerina, L. A.; Zavorotnyuk, D. S. *J. Appl. Crystallogr.* **2005**, *38*, 996.

(229) Redecke, L.; von Bergen, M.; Clos, J.; Konarev, P. V.; Svergun, D. I.; Fittschen, U. E. A.; Broekaert, J. A. C.; Bruns, O.; Georgieva, D.; Mandelkow, E.; Genov, N.; Betzel, C. *J. Struct. Biol.* **2007**, *157*, 308.
(230) Zhang, W.; Li, L.; Du, Y.; Wang, X.; Yang, P. *Catal. Lett.* **2009**, *127*, 429.
(231) Ledesma-Garcia, J.; Escalante-Garcia, I. L.; Chapman, T. W.; Arriaga, L. G.; Baglio, V.; Antonucci, V.; Arico, A. S.; Ornelas, R.; Godinez, L. A. *J. Solid State Electrochem.* **2010**, *14*, 835.
(232) Petkov, V.; Bedford, N.; Knecht, M. R.; Weir, M. G.; Crooks, R. M.; Tang, W.; Henkelman, G.; Frenkel, A. *J. Phys. Chem. C* **2008**, *112*, 8907.
(233) Petkov, V.; Parvanov, V.; Tomalia, D.; Swanson, D.; Bergstrom, D.; Vogt, T. *Solid State Commun.* **2005**, *134*, 671.
(234) Bedford, N. M. *Solid State Commun.* **2010**, *150*, 1505.
(235) Gu, Y.; Wu, G.; Hu, X. F.; Chen, D. A.; Hansen, T.; Loye, H.-C. z.; Ploehn, H. J. *J. Power Sources* **2010**, *195*, 425.
(236) Long, J. W.; Logan, M. S.; Rhodes, C. P.; Carpenter, E. E.; Stroud, R. M.; Rolison, D. R. *J. Am. Chem. Soc.* **2004**, *126*, 16879.
(237) Rebodos, R. L.; Vikesland, P. J. *Langmuir* **2010**, *26*, 16745.
(238) Wei, X.; Wei, Z.; Zhang, L.; Liu, Y.; He, D. *J. Colloid Interface Sci.* **2011**, *354*, 76.
(239) Mitran, E.; Dellinger, B.; McCarley, R. L. *Chem. Mater.* **2010**, *22*, 6555.
(240) Ghosh, S.; Datta, A.; Saha, A. *Colloids Surf., A* **2010**, *355*, 130.
(241) Raghu, S.; Nirmal, R. G.; Mathiyarasu, J.; Berchmans, S.; Phani, K. L. N.; Yegnaraman, V. *Catal. Lett.* **2007**, *119*, 40.
(242) Brice-Profeta, S.; Arrio, M. A.; Tronc, E.; Menguy, N.; Letard, I.; Moulin, C. C. D.; Nogues, M.; Chaneac, C.; Jolivet, J. P.; Sainctavit, P. *J. Magn. Magn. Mater.* **2005**, *288*, 354.
(243) Serna, C. J.; Bodker, F.; Morup, S.; Morales, M. P.; Sandiumenge, F.; Veintemillas-Verdaguer, S. *Solid State Commun.* **2001**, *118*, 437.
(244) Ogasawara, S.; Kato, S. *J. Am. Chem. Soc.* **2010**, *132*, 4608.
(245) Magno, L. M.; Sigle, W.; van Aken, P. A.; Angelescu, D. G.; Stubenrauch, C. *Chem. Mater.* **2010**, *22*, 6263.
(246) Stavila, V.; Whitmire, K. H.; Rusakova, I. *Chem. Mater.* **2009**, *21*, 5456.
(247) Tang, L.; Zhu, Y.; Yang, X.; Li, C. *Anal. Chim. Acta* **2007**, *597*, 145.
(248) Li, G. P.; Luo, Y. J. *Inorg. Chem.* **2008**, *47*, 360.
(249) Lang, H.; Maldonado, S.; Stevenson, K. J.; Chandler, B. D. *J. Am. Chem. Soc.* **2004**, *126*, 12949.
(250) Scott, R. W. J.; Ye, H. C.; Henriquez, R. R.; Crooks, R. M. *Chem. Mater.* **2003**, *15*, 3873.
(251) Qian, L.; Yang, X. R. *J. Phys. Chem. B* **2006**, *110*, 16672.
(252) Xu, J.; Dozier, A.; Bhattacharyya, D. *J. Nanopart. Res.* **2005**, 7.
(253) Wagner, C.; Riggs, W.; Davis, L.; Mullenberg, G. *Handbook of X-ray Photoelectron Spectroscopy*; Perkin-Elmer Corp.: MN, 1978.
(254) Tielsch, B. J.; Fulghum, J. E. *Surf. Interface Anal.* **1996**, *24*, 422.
(255) Ozturk, O.; Black, T. J.; Perrine, K.; Pizzolato, K.; Williams, C. T.; Parsons, F. W.; Ratliff, J. S.; Gao, J.; Murphy, C. J.; Xie, H.; Ploehn, H. J.; Chen, D. A. *Langmuir* **2005**, *21*, 3998.
(256) Alexeev, O. S.; Siani, A.; Lafaye, G.; Williams, C. T.; Ploehn, H. J.; Amiridis, M. D. *J. Phys. Chem. B* **2006**, *110*, 24903.
(257) Harada, M.; Asakura, K.; Ueki, Y.; Toshima, N. *J. Phys. Chem.* **1993**, *97*, 10742.
(258) Beakley, L. W.; Yost, S. E.; Cheng, R.; Chandler, B. D. *Appl. Catal., A* **2005**, *292*, 124.
(259) Esumi, K.; Isono, R.; Yoshimura, T. *Langmuir* **2004**, *20*, 237.
(260) Xie, H.; Gu, Y. L.; Ploehn, H. J. *Nanotechnology* **2005**, *16*, S492.
(261) Lopez-De Jesus, Y. M.; Vicente, A.; Lafaye, G.; Marecot, P.; Williams, C. T. *J. Phys. Chem. C* **2008**, *112*, 13837.
(262) Floriano, P. N.; Noble, C. O.; Schoonmaker, J. M.; Poliakoff, E. D.; McCarley, R. L. *J. Am. Chem. Soc.* **2001**, *123*, 10545.
(263) Weir, M. G.; Knecht, M. R.; Frenkel, A. I.; Crooks, R. M. *Langmuir* **2010**, *26*, 1137.
(264) Knecht, M. R.; Weir, M. G.; Frenkel, A. I.; Crooks, R. M. *Chem. Mater.* **2008**, *20*, 1019.
(265) Myers, S. V.; Frenkel, A. I.; Crooks, R. M. *Chem. Mater.* **2009**, *21*, 4824.
(266) Niu, Y. H.; Crooks, R. M. *Chem. Mater.* **2003**, *15*, 3463.
(267) Henglein, A. *Chem. Rev.* **1989**, *89*, 1861.
(268) Moffitt, M.; Eisenberg, A. *Chem. Mater.* **1995**, *7*, 1178.
(269) Qu, L.; Yu, W. W.; Peng, X. *Nano Lett.* **2004**, *4*, 465.
(270) Yu, W. W.; Qu, L.; Guo, W.; Peng, X. *Chem. Mater.* **2003**, *15*, 2854.
(271) Yu, W. W.; Falkner, J. C.; Shih, B. S.; Colvin, V. L. *Chem. Mater.* **2004**, *16*, 3318.
(272) Dai, Q.; Li, D.; Chang, J.; Song, Y.; Kan, S.; Chen, H.; Zou, B.; Xu, W.; Xu, S.; Liu, B.; Zou, G. *Nanotechnology* **2007**, *18*, 405603/1.
(273) El-Sayed, M. A. *Acc. Chem. Res.* **2001**, *34*, 257.
(274) Zhang, W.-L.; Li, N.; Huang, J.; Yu, J.-H.; Wang, D.-X.; Li, Y.-P.; Liu, S.-Y. *J. Appl. Polym. Sci.* **2010**, *118*, 1805.
(275) Kaewtong, C.; Jiang, G.; Ponnapati, R.; Pulpoka, B.; Advincula, R. *Soft. Matter* **2010**, *6*, 5316.
(276) Wu, H.-X.; Zhang, C.-X.; Jin, L.; Yang, H.; Yang, S.-P. *Mater. Chem. Phys.* **2010**, *121*, 342.
(277) Guo, Z.-X.; Yu, J. *J. Mater. Chem.* **2001**, *12*, 468.
(278) Gopidas, K. R.; Whitesell, J. K.; Fox, M. A. *Nano Lett.* **2003**, *3*, 1757.
(279) Vijayaraghavan, G.; Stevenson, K. J. *Langmuir* **2007**, *23*, 5279.
(280) Yuan, W.; Jiang, G.; Che, J.; Qi, X.; Xu, R.; Chang, M. W.; Chen, Y.; Lim, S. Y.; Dai, J.; Chan-Park, M. B. *J. Phys. Chem. C* **2008**, *112*, 18754.
(281) Yu, J.; Zhao, H.; Ye, L.; Yang, H.; Ku, S.; Yang, N.; Xiao, N. *J. Mater. Chem.* **2009**, *19*, 1265.
(282) Lu, X.; Imae, T. *J. Phys. Chem. C* **2007**, *111*, 2416.
(283) Liu, H.; Wang, H.; Guo, R.; Cao, X.; Zhao, J.; Luo, Y.; Shen, M.; Zhang, G.; Shi, X. P. C. *Polym. Chem.* **2010**, *1*, 1677.
(284) Ramirez, E.; Erades, L.; Philippot, K.; Lecante, P.; Chaudret, B. *Adv. Funct. Mater.* **2007**, *17*, 2219.
(285) Gomez, M. V.; Guerra, J.; Myers, V. S.; Crooks, R. M.; Velders, A. H. *J. Am. Chem. Soc.* **2009**, *131*, 14634.
(286) Gomez, M. V.; Giuerra, J.; Velders, A. H.; Crooks, R. M. *J. Am. Chem. Soc.* **2009**, *131*, 341.
(287) Martin, A. L.; Bernas, L. M.; Rutt, B. K.; Foster, P. J.; Gillies, E. R. *Bioconjugate Chem.* **2008**, *19*, 2375.
(288) Bronstein, L. M.; Chernyshov, D. M.; Karlinsey, R.; Zwanziger, J. W.; Matveeva, V. G.; Sulman, E. M.; Demidenko, G. N.; Hentze, H.-P.; Antonietti, M. *Chem. Mater.* **2003**, *15*, 2623.
(289) Gayen, S. K.; Brito, M.; Das, B. B.; Comanescu, G.; Liang, X. C.; Alrubaiee, M.; Alfano, R. R.; Gonzalez, C.; Byro, A. H.; Bauer, D. L. V.; Balogh-Nair, V. *J. Opt. Soc. Am. B* **2007**, *24*, 3064.
(290) Liu, Y.; Kim, M.; Wang, Y.; Wang, Y. A.; Peng, X. *Langmuir* **2006**, *22*, 6341.
(291) Bruchez, M.; Moronne, M.; Gin, P.; Weiss, S.; Alivisatos, A. P. *Science* **1998**, *281*, 2013.
(292) Link, S.; Beeby, A.; FitzGerald, S.; El-Sayed, M. A.; Schaaff, T. G.; Whetten, R. L. *J. Phys. Chem. B* **2002**, *106*, 3410.
(293) Huang, T.; Murray, R. W. *J. Phys. Chem. B* **2001**, *105*, 12498.
(294) Imamura, M.; Miyashita, T.; Tanaka, A.; Yasuda, H.; Negishi, Y.; Tsukuda, T. *Eur. Phys. J. D* **2007**, *43*, 233.
(295) Lee, W. I.; Bae, Y.; Bard, A. J. *J. Am. Chem. Soc.* **2004**, *126*, 8358.
(296) Tran, M. L.; Zvyagin, A. V.; Plakhotnik, T. *Chem. Commun.* **2006**, 2400.
(297) Jin, R. C.; Egusa, S.; Scherer, N. F. *J. Am. Chem. Soc.* **2004**, *126*, 9900.
(298) Zheng, J.; Nicovich, P. R.; Dickson, R. M. *Annu. Rev. Phys. Chem.* **2007**, *58*, 409.
(299) Zheng, J.; Zhang, C.; Dickson, R. M. *Phys. Rev. Lett.* **2004**, *93*, 077402/1.
(300) Capadona, L. P.; Zheng, J.; Gonzalez, J. I.; Lee, T.-H.; Patel, S. A.; Dickson, R. M. *Phys. Rev. Lett.* **2005**, *94*, 058301/1.
(301) Sato, T.; Jiang, D.-L.; Aida, T. *J. Am. Chem. Soc.* **1999**, *121*, 10658.

(302) Tozawa, T. *Chem. Commun.* **2004**, 1904.
(303) Chou, C.-H.; Wang, H.-S.; Wei, K.-H.; Huang, J. Y. *Adv. Funct. Mater.* **2006**, *16*, 909.
(304) Locklin, J.; Patton, D.; Deng, S.; Baba, A.; Millan, M.; Advincula, R. C. *Chem. Mater.* **2004**, *16*, 5187.
(305) Advincula, R. C. *Eur. Coat. J.* **2008**, 29.
(306) West, R.; Wang, Y.; Goodson, T. *J. Phys. Chem. B* **2003**, *107*, 3419.
(307) Wang, Y.; Xie, X.; Goodson, T., III. *Nano Lett.* **2005**, *5*, 2379.
(308) Hellstern, D.; Schulze, K.; Schopf, B.; Petri-Fink, A.; Steitz, B.; Kamau, S.; Hilbe, M.; Koch-Schneidemann, S.; Vaughan, L.; Hottiger, M.; Hofmann, M.; Hofmann, H.; von Rechenberg, B. *J. Nanosci. Nanotechnol.* **2006**, *6*, 3261.
(309) Briley-Saebo, K.; Bjornerud, A.; Grant, D.; Ahlstrom, H.; Berg, T.; Kindberg, G. M. *Cell Tissue Res.* **2004**, *316*, 315.
(310) Strable, E.; Bulte, J. W. M.; Moskowitz, B.; Vivekanandan, K.; Allen, M.; Douglas, T. *Chem. Mater.* **2001**, *13*, 2201.
(311) Frankamp, B. L.; Boal, A. K.; Tuominen, M. T.; Rotello, V. M. *J. Am. Chem. Soc.* **2005**, *127*, 9731.
(312) Knecht, M. R.; Crooks, R. M. *New J. Chem.* **2007**, *31*, 1349.
(313) Auten, B. J.; Hahn, B. P.; Vijayaraghavan, G.; Stevenson, K. J.; Chandler, B. D. *J. Phys. Chem. C* **2008**, *112*, 5365.
(314) Wan, H.; Shi, S.; Bai, L.; Shamsuzzoha, M.; Harrell, J. W.; Street, S. C. *J. Nanosci. Nanotechnol.* **2010**, *10*, 5089.
(315) Donnio, B.; Garcia-Vazquez, P.; Gallani, J.-L.; Guillon, D.; Terazzi, E. *Adv. Mater.* **2007**, *19*, 3534.
(316) Majoros, I. J.; Thomas, T. P.; Mehta, C. B.; Baker, J. R., Jr. *J. Med. Chem.* **2005**, *48*, 5892.
(317) Majoros, I. J.; Myc, A.; Thomas, T.; Mehta, C. B.; Baker, J. R., Jr. *Biomacromolecules* **2006**, *7*, 572.
(318) Kukowska-Latallo, J. F.; Candido, K. A.; Cao, Z. Y.; Nigavekar, S. S.; Majoros, I. J.; Thomas, T. P.; Balogh, L. P.; Khan, M. K.; Baker, J. R. *Cancer Res.* **2005**, *65*, 5317.
(319) Thomas, T. P.; Majoros, I. J.; Kotlyar, A.; Kukowska-Latallo, J. F.; Bielinska, A.; Myc, A.; Baker, J. R. *J. Med. Chem.* **2005**, *48*, 3729.
(320) Talanov, V. S.; Regino, C. A. S.; Kobayashi, H.; Bernardo, M.; Choyke, P. L.; Brechbiel, M. W. *Nano Lett.* **2006**, *6*, 1459.
(321) Debbage, P.; Jaschke, W. *Histochem. Cell Biol.* **2008**, *130*, 845.
(322) Shi, X.; Thomas, T. P.; Myc, L. A.; Kotlyar, A.; Baker, J. R., Jr. *Phys. Chem. Chem. Phys.* **2007**, *9*, 5712.
(323) Shi, X.; Wang, S. H.; Swanson, S. D.; Ge, S.; Cao, Z.; Van Antwerp, M. E.; Landmark, K. J.; Baker, J. R., Jr. *Adv. Mater.* **2008**, *20*, 1671.
(324) Wang, S. H.; Shi, X.; Van Antwerp, M.; Cao, Z.; Swanson, S. D.; Bi, X.; Baker, J. R., Jr. *Adv. Funct. Mater.* **2007**, *17*, 3043.
(325) Shi, X.; Wang, S. H.; Lee, I.; Shen, M.; Baker, J. R. *Biopolymers* **2009**, *91*, 936.
(326) Shi, X. Y.; Wang, S. H.; Sun, H. P.; Baker, J. R. *Soft Matter* **2007**, *3*, 71.
(327) Bielinska, A.; Eichman, J. D.; Lee, I.; Baker, J.; Balogh, L. *J. Nanopart. Res.* **2002**, *4*, 395.
(328) Shukla, R.; Hill, E.; Shi, X.; Kim, J.; Muniz, M. C.; Sun, K.; Baker, J. R., Jr. *Soft Matter* **2008**, *4*, 2160.
(329) Hussain, N.; Singh, B.; Sakthivel, T.; Florence, A. T. *Int. J. Pharm.* **2003**, *254*, 27.
(330) Ghosh, P. S.; Kim, C.-K.; Han, G.; Forbes, N. S.; Rotello, V. M. *ACS Nano* **2008**, *2*, 2213.
(331) Chen, C.-T.; Munot, Y. S.; Salunke, S. B.; Wang, Y.-C.; Lin, R.-K.; Lin, C.-C.; Chen, C.-C.; Liu, Y.-H. *Adv. Funct. Mater.* **2008**, *18*, 527.
(332) Link, S.; El-Sayed, M. A. *Int. Rev. Phys. Chem.* **2000**, *19*, 409.
(333) Everts, M.; Saini, V.; Leddon, J. L.; Kok, R. J.; Stoff-Khalili, M.; Preuss, M. A.; Millican, C. L.; Perkins, G.; Brown, J. M.; Bagaria, H.; Nikles, D. E.; Johnson, D. T.; Zharov, V. P.; Curiel, D. T. *Nano Lett.* **2006**, *6*, 587.
(334) Haba, Y.; Kojima, C.; Harada, A.; Ura, T.; Horinaka, H.; Kono, K. *Langmuir* **2007**, *23*, 5243.
(335) Nam, J.; Won, N.; Jin, H.; Chung, H.; Kim, S. *J. Am. Chem. Soc.* **2009**, *131*, 13639.
(336) Li, Z.; Huang, P.; Zhang, X.; Lin, J. Y.; Sen; Liu, B.; Gao, F. X.; Peng; Ren, Q.; Cui, D. *Mol. Pharm.* **2010**, *7*, 94.
(337) Kojima, C.; Umeda, Y.; Ogawa, M.; Harada, A.; Magata, Y.; Kono, K. *Nanotechnology* **2010**, *21*, 245104/1.
(338) Gao, F.; Pan, B.-F.; Zheng, W.-M.; Ao, L.-M.; Gu, H.-C. *J. Magn. Magn. Mater.* **2005**, *293*, 48.
(339) Pan, B.-f.; Gao, F.; Gu, H.-C. *J. Colloid Interface Sci.* **2005**, *284*, 1.
(340) Pan, B.-F.; Gao, F.; Ao, L.-M. *J. Magn. Magn. Mater.* **2005**, *293*, 252.
(341) Pan, B.; Cui, D.; Sheng, Y.; Ozkan, C.; Gao, F.; He, R.; Li, Q.; Xu, P.; Huang, T. *Cancer Res.* **2007**, *67*, 8156.
(342) Landmark, K. J.; DiMaggio, S.; Ward, J.; Kelly, C.; Vogt, S.; Hong, S.; Kotlyar, A.; Myc, A.; Thomas, T. P.; Penner-Hahn, J. E.; Baker, J. R.; Banaszak Holl, M. M.; Orr, B. G. *ACS Nano* **2008**, *2*, 773.
(343) Kunzmann, A.; Andersson, B.; Thurnherr, T.; Krug, H.; Scheynius, A.; Fadeel, B. *Biochim. Biophys. Acta, Gen. Subj.* **2011**, *1810*, 361.
(344) Aillon, K. L.; Xie, Y.; El-Gendy, N.; Berkland, C. J.; Forrest, M. L. *Adv. Drug Delivery Rev.* **2009**, *61*, 457.
(345) Pan, Y.; Leifert, A.; Ruau, D.; Neuss, S.; Bornemann, J.; Schmid, G.; Brandau, W.; Simon, U.; Jahnen-Dechent, W. *Small* **2009**, *5*, 2067.
(346) Gu, Y. J.; Cheng, J.; Lin, C. C.; Lam, Y. W.; Cheng, S. H.; Wong, W. T. *Toxicol. Appl. Pharmacol.* **2009**, *237*, 196.
(347) Longmire, M.; Choyke, P. L.; Kobayashi, H. *Nanomedicine* **2008**, *3*, 703.
(348) Daniel, M.-C.; Ruiz, J.; Nlate, S.; Palumbo, J.; Blais, J.-C.; Astruc, D. *Chem. Commun.* **2001**, 2000.
(349) Krasteva, N.; Fogel, Y.; Bauer, R. E.; Mullen, K.; Joseph, Y.; Matsuzawa, N.; Yasuda, A.; Vossmeyer, T. *Adv. Funct. Mater.* **2007**, *17*, 881.
(350) Vossmeyer, T.; Guse, B.; Besnard, I.; Bauer, R.; Muellen, K.; Yasuda, A. *Adv. Mater.* **2002**, *14*, 238.
(351) Krasteva, N.; Besnard, I.; Guse, B.; Bauer, R. E.; Mullen, K.; Yasuda, A.; Vossmeyer, T. *Nano Lett.* **2002**, *2*, 551.
(352) Krasteva, N.; Guse, B.; Besnard, I.; Yasuda, A.; Vossmeyer, T. *Sens. Actuators, B* **2003**, *92*, 137.
(353) Das, J.; Aziz, M. A.; Yang, H. *J. Am. Chem. Soc.* **2006**, *128*, 16022.
(354) Selvaraju, T.; Das, J.; Jo, K.; Kwon, K.; Huh, C.-H.; Kim, T. K.; Yang, H. *Langmuir* **2008**, *24*, 9883.
(355) Shiddiky, M. J. A.; Rahman, M. A.; Shim, Y.-B. *Anal. Chem.* **2007**, *79*, 6886.
(356) Shiddiky, M. J. A.; Rahman, M. A.; Cheol, C. S.; Shim, Y.-B. *Anal. Biochem.* **2008**, *379*, 170.
(357) Stofik, M.; Stryhal, Z.; Maly, J. *Biosens. Bioelectron.* **2009**, *24*, 1918.
(358) Chandra, S.; Lokesh, K. S.; Nicolai, A.; Lang, H. *Anal. Chim. Acta* **2009**, *632*, 63.
(359) Zhu, Y.; Zhu, H.; Yang, X.; Xu, L.; Li, C. *Electroanalysis* **2007**, *19*, 698.
(360) Xu, L.; Zhu, Y.; Tang, L.; Yang, X.; Li, C. *J. Appl. Polym. Sci.* **2008**, *109*, 1802.
(361) Park, C.; Lee, I. H.; Lee, S.; Song, Y.; Rhue, M.; Kim, C. *Proc. Natl. Acad. Sci. U.S.A.* **2006**, *103*, 1199.
(362) Park, C.; Im, M. S.; Lee, S.; Lim, J.; Kim, C. *Angew. Chem., Int. Ed.* **2008**, *47*, 9922.
(363) Rahman, M. A.; Noh, H.-B.; Shim, Y.-B. *Anal. Chem.* **2008**, *80*, 8020.
(364) Triulzi, R. C.; Micic, M.; Orbulescu, J.; Giordani, S.; Mueller, B.; Leblanc, R. M. *Analyst* **2008**, *133*, 667.
(365) Frasconi, M.; Tortolini, C.; Botre, F.; Mazzei, F. *Anal. Chem.* **2010**, *82*, 7335.
(366) Chung, Y.-M.; Rhee, H.-K. *Catal. Surv. Asia* **2004**, *8*, 211.
(367) Bronstein, L. M.; Sidorov, S. N.; Valetsky, P. M. *Russ. Chem. Rev.* **2004**, *73*, 501.
(368) Chung, Y.-M.; Rhee, H.-K. *Korean J. Chem. Eng.* **2004**, *21*, 81.

(369) Astruc, D. *Tetrahedron: Asymmetry* **2010**, *21*, 1041.
(370) Wu, L.; Li, Z.-W.; Zhang, F.; He, Y.-M.; Fan, Q.-H. *Adv. Synth. Catal.* **2008**, *350*, 846.
(371) Garcia-Martinez, J. C.; Lezutekong, R.; Crooks, R. M. *J. Am. Chem. Soc.* **2005**, *127*, 5097.
(372) Mizugaki, T.; Murata, M.; Fukubayashi, S.; Mitsudome, T.; Jitsukawa, K.; Kaneda, K. *Chem. Commun.* **2008**, 241.
(373) Keilitz, J.; Nowag, S.; Marty, J. D.; Haag, R. *Adv. Synth. Catal.* **2010**, *352*, 1503.
(374) Bronstein, L. M.; Matveeva, V. G.; Sulman, E. M. In *Nanoparticles and Catalysis*; Astruc, D., Ed.; Wiley-VCH: Weinheim, Germany, 2008.
(375) Snelders, D. J. M.; van Koten, G.; Gebbink, R. J. M. K. *J. Am. Chem. Soc.* **2009**, *131*, 11407.
(376) Fujita, K.-i.; Yamazaki, M.; Ainoya, T.; Tsuchimoto, T.; Yasuda, H. *Tetrahedron* **2010**, *66*, 8536.
(377) Servin, P.; Laurent, R.; Gonsalvi, L.; Tristany, M.; Peruzzini, M.; Majoral, J.-P.; Caminade, A.-M. *Dalton Trans.* **2009**, 4432.
(378) Servin, P.; Laurent, R.; Romerosa, A.; Peruzzini, M.; Majoral, J.-P.; Caminade, A.-M. *Organometallics* **2008**, *27*, 2066.
(379) Badetti, E.; Caminade, A.-M.; Majoral, J.-P.; Moreno-Manas, M.; Sebastian, R. *Langmuir* **2008**, *24*, 2090.
(380) Bronstein, L. M.; Chernyshov, D. M.; Volkov, I. O.; Ezernitskaya, M. G.; Valetsky, P. M.; Matveeva, V. G.; Sulman, E. M. *J. Catal.* **2000**, *196*, 302.
(381) Bernechea, M.; Garcia-Rodriguez, S.; Terreros, P.; de Jesus, E.; Fierro, J. L. G.; Rojas, S. *J. Phys. Chem. C* **2011**, *115*, 1287.
(382) Hagen, J. *Industrial Catalysis: A Practical Approach*; Wiley-VCH: Weinheim, Germany, 1999.
(383) Rosario-Amorin, D.; Wang, X.; Gaboyard, M.; Clerac, R.; Nlate, S.; Heuze, K. *Chem.-Eur. J.* **2009**, *15*, 12636.
(384) Krishnan, G. R.; Sreekumar, K. *Soft Mater.* **2010**, *8*, 114.
(385) Ogasawara, S.; Kato, S. *J. Am. Chem. Soc.* **2010**, *132*, 4608.
(386) Murugan, E.; Rangasamy, R. *J. Polym. Sci., Part A: Polym. Chem.* **2010**, *48*, 2525.
(387) Jiang, Y.; Gao, Q. *J. Am. Chem. Soc.* **2006**, *128*, 716.
(388) Hagiwara, H.; Sasaki, H.; Tsubokawa, N.; Hoshi, T.; Suzuki, T.; Tsuda, T.; Kuwabata, S. *Synlett* **2010**, 1990.
(389) Kumar, P. A.; Ha, H. P. *Catal. Lett.* **2010**, *136*, 177.
(390) Karakhanov, E. A.; Maximov, A. L.; Skorkin, V. A.; Zolotukhina, A. V.; Smerdov, A. S.; Tereshchenko, A. Y. *Pure Appl. Chem.* **2009**, *81*, 2013.
(391) Ledesma-Garcia, J.; Escalante Garcia, I. L.; Rodriguez, F. J.; Chapman, T. W.; Godinez, L. A. *J. Appl. Electrochem.* **2008**, *38*, 515.
(392) Witham, C. A.; Huang, W.; Tsung, C.-K.; Kuhn, J. N.; Somorjai, G. A.; Toste, F. D. *Nat. Chem.* **2010**, *2*, 36.
(393) Zheng, Z.; Li, H.; Liu, T.; Cao, R. *J. Catal.* **2010**, *270*, 268.
(394) Kuhn, J. N.; Huang, W.; Tsung, C.-K.; Zhang, Y.; Somorjai, G. A. *J. Am. Chem. Soc.* **2008**, *130*, 14026.
(395) Singh, A.; Chandler, B. D. *Langmuir* **2005**, *21*, 10776.
(396) Siani, A.; Alexeev, O. S.; Deutsch, D. S.; Monnier, J. R.; Fanson, P. T.; Hirata, H.; Matsumoto, S.; Williams, C. T.; Amiridis, M. D. *J. Catal.* **2009**, *266*, 331.
(397) Auten, B. J.; Crump, C. J.; Singh, A. R.; Chandler, B. D. *Chem. Ind.* **2007**, *115*, 315.
(398) Lang, H.; May, R. A.; Iversen, B. L.; Chandler, B. D. *Chem. Ind.* **2005**, 243.
(399) Hoover, N. N.; Auten, B. J.; Chandler, B. D. *J. Phys. Chem. B* **2006**, *110*, 8606.
(400) Korkosz, R. J.; Gilbertson, J. D.; Prasifka, K. S.; Chandler, B. D. *Catal. Today* **2007**, *122*, 370.
(401) Crump, C. J.; Gilbertson, J. D.; Chandler, B. *Top. Catal.* **2008**, *49*, 233.
(402) Xie, H.; Howe, J. Y.; Schwartz, V.; Monnier, J. R.; Williams, C. T.; Ploehn, H. J. *J. Catal.* **2008**, *259*, 111.
(403) Auten, B. J.; Lang, H.; Chandler, B. D. *Appl. Catal., B* **2008**, *81*, 225.
(404) Scott, R. W. J.; Sivadinarayana, C.; Wilson, O. M.; Yan, Z.; Goodman, D. W.; Crooks, R. M. *J. Am. Chem. Soc.* **2005**, *127*, 1380.
(405) Amama, P. B.; Cola, B. A.; Sands, T. D.; Xu, X.; Fisher, T. S. *Nanotechnology* **2007**, *18*, 385303/1.
(406) Scott, R. W. J.; Wilson, O. M.; Crooks, R. M. *Chem. Mater.* **2004**, *16*, 5682.
(407) Ling, X. Y.; Phang, I. Y.; Maijehburg, W.; Schoenherr, H.; Reinhoudt, D. N.; Vancso, G. J.; Huskens, J. *Angew. Chem., Int. Ed.* **2009**, *48*, 983.
(408) Ling, X. Y.; Phang, I. Y.; Schoenherr, H.; Reinhoudt, D. N.; Vancso, G. J.; Huskens, J. *Small* **2009**, *5*, 1428.
(409) Ling, X. Y.; Reinhoudt, D. N.; Huskens, J. *Chem. Mater.* **2008**, *20*, 3574.
(410) Dorokhin, D.; Hsu, S.-H.; Tomczak, N.; Reinhoudt, D. N.; Huskens, J.; Velders, A. H.; Vancso, G. J. *ACS Nano* **2010**, *4*, 137.
(411) Kim, C. K.; Joo, W.-J.; Kim, H. J.; Song, E. S.; Kim, J.; Lee, S.; Park, C.; Kim, C. *Synth. Met.* **2008**, *158*, 359.
(412) Puniredd, S. R.; Wai, Y. K.; Satyanarayana, N.; Sinha, S. K.; Srinivasan, M. P. *Langmuir* **2007**, *23*, 8299.
(413) Puniredd, S. R.; Weiyi, S.; Srinivasan, M. P. *J. Colloid Interface Sci.* **2008**, *320*, 333.
(414) Bouldin, K. K.; Menzel, E. R.; Takatsu, M.; Murdock, R. H. *J. Forensic Sci.* **2000**, *45*, 1239.